SAFE DISPOSAL OF COAL BOTTOM ASH USING CEMENT-BASED SOLIDIFICATION AND STABILIZATION TECHNIQUES

SAJEDEH SADAT GHAZIZADEH HASHEMI

FACULTY OF ENGINEERING
UNIVERSITY OF MALAYA
KUALA LUMPUR

2018

SAFE DISPOSAL OF COAL BOTTOM ASH USING CEMENT-BASED SOLIDIFICATION AND STABILIZATION TECHNIQUES

SAJEDEH SADAT GHAZIZADEH HASHEMI

THESIS SUBMITTED IN FULFILMENT OF THE REQUIREMENTS FOR THE DEGREE OF DOCTOR OF PHILOSOPHY

FACULTY OF ENGINEERING
UNIVERSITY OF MALAYA
KUALA LUMPUR

2018

UNIVERSITY OF MALAYA
ORIGINAL LITERARY WORK DECLARATION

Name of Candidate: SAJEDEH SADAT GHAZIZADEH HASHEMI

Matric No: KHA140035

Name of Degree: Doctor of Philosophy (Thesis)

Title of Thesis ("this Work"):

SAFE DISPOSAL OF COAL BOTTOM ASH USING CEMENT-BASED SOLIDIFICATION AND STABILIZATION TECHNIQUES

Field of Study: Environmental-Civil Engineering

I do solemnly and sincerely declare that:

(1) I am the sole author/writer of this Work;
(2) This Work is original;
(3) Any use of any work in which copyright exists was done by way of fair dealing and for permitted purposes and any excerpt or extract from, or reference to or reproduction of any copyright work has been disclosed expressly and sufficiently and the title of the Work and its authorship have been acknowledged in this Work;
(4) I do not have any actual knowledge nor do I ought reasonably to know that the making of this work constitutes an infringement of any copyright work;
(5) I hereby assign all and every right in the copyright to this Work to the University of Malaya ("UM"), who henceforth shall be the owner of the copyright in this Work and that any reproduction or use in any form or by any means whatsoever is prohibited without the written consent of UM having been first had and obtained;
(6) I am fully aware that if in the course of making this Work, I have infringed any copyright whether intentionally or otherwise, I may be subject to legal action or any other action as may be determined by UM.

Candidate's Signature   Date:

Subscribed and solemnly declared before,

Witness's Signature   Date:

Name:

Designation:

SAFE DISPOSAL OF COAL BOTTOM ASH USING CEMENT-BASED SOLIDIFICATION AND STABILIZATION TECHNIQUES

ABSTRACT

Coal Bottom Ash (CBA) is one of the widely-produced residues of coal incineration in electric power plants. It is categorized as scheduled waste that must be disposed at a licensed treatment plant in the Malaysia. The annual extraction of such a huge amount of waste needs a massive transfer field, which constitutes a threat to the environment. However, the utilization of such residue as a fine aggregate in concrete can be an environmentally-friendly opportunity. Moreover, contaminated heavy metals contained in the CBA such as nickel, copper, cadmium and lead can be immobilized using Solidification/Stabilization technique to reduce toxic solubility and leachability. As observed in this study, CBA has a reactive fraction with pozzolanic characteristics. This provides stronger mortar mixture when a medium volume of the CBA (up to 40%) is substituted with silica sand. The compressive strength value of the specimen using 40% CBA with W/C ratio of 0.55 at 56 days was 55 MPa, which reached the same strength limit of control mortar mixture. However, the reduction of compressive strength in high-volume CBA replacement is attributed to the porous structure of CBA, which causes absorption of the mixing water as well as an increase in the total pore volume of the mortar mixtures. OPC-based immobilization and encapsulation of contaminated heavy metals was effective for prevention of metals leaching, were below the applicable Malaysian Environmental Quality Act and highly decreased to zero leaching, further high enough strength property and acceptable permeable porosity value attained by OPC/CBA ratio of 2 which was more than sufficient to be disposed safely in landfills. Besides, the solidified/stabilized samples exhibited ettringite and amorphous C-S-H. Inclusion of CBA has changed the surface of the solidified sample into more C-S-H and less ettringite. The main crystal in the solidified samples was calcite, which were formed by carbonation

reaction of C-S-H and C-H with CO_2 in the cement hydration product. Thermogravimetry analysis of solidified samples exhibited the active pozzolanic reaction at temperature of 400 to 750 ˚C, shown by the weight loss of $Ca(OH)_2$ and decomposition of carbonation product. The optimum mixture of 40% CBA replacement at constant W/C ratio of 0.55 achieved applicable value in terms of compressive strength, abrasion resistance and water absorption to fabricate Portland cement paving blocks. Moreover, it is observed that the degree of shrinkage of CBA/ silica sand paving blocks decreased with increase in the CBA content. This reduction might be attributed to pore texture of the CBA that also resulted in reducing compressive strength.

Keywords: Solidification, Coal Bottom Ash, Stabilization, Microstructure Cement.

SAFE DISPOSAL OF COAL BOTTOM ASH USING CEMENT-BASED SOLIDIFICATION AND STABILIZATION TECHNIQUES

ABSTRAK

Abu bawahan arang (CBA) adalah salah satu daripada residu pembakaran arang di loji janakuasa elektrik. Ia dikategorikan sebagai sisa berjadual yang mesti dilupuskan di loji rawatan berlesen di Malaysia. Pengekstrakan tahunan bagi jumlah sisa yang besar ini memerlukan lapangan pemuggahan yang besar, yang menjadi ancaman kepada alam sekitar. Walau bagaimanapun, penggunaan sisa tersebut sebagai agregat halus dalam konkrit boleh menjadi peluang yang mesra alam. Selain itu, logam berat yang tercemar yang terkandung di dalam CBA seperti nikel, tembaga, kadmium dan plumbum boleh dialihkan menggunakan teknik Pengukuhan / Penstabilan untuk mengurangkan keterlarutan dan kebolehtelapan racun. Seperti yang diperhatikan dalam kajian ini, CBA mempunyai bahagian reaktif dengan ciri-ciri pozzolanic. Ini memberikan campuran mortar yang lebih kuat apabila jumlah medium CBA (sehingga 40%) digantikan dengan pasir silika. Nilai kekuatan mampatan spesimen menggunakan 40% CBA dengan nisbah W / C 0.55 pada 56 hari adalah 55 MPa, yang mencapai had kekuatan campuran mortar yang sama. Walau bagaimanapun, pengurangan kekuatan mampatan dalam penggantian CBA pada nilai yang tinggi dikaitkan dengan struktur poros CBA, yang menyebabkan penyerapan air pencampuran serta peningkatan jumlah liang campuran mortar. Imobilisasi berasaskan OPC dan enkapsulasi bagi logam berat yang tercemar adalah berkesan untuk pencegahan pelepasan logam, adalah di bawah Akta Kualiti Alam Sekitar Malaysia yang berkuatkuasa dan sangat berkurangan kepada larutan sifar, sifat kekuatan yang lebih tinggi lagi dan nilai porositi telap yang dapat diterima oleh nisbah OPC/CBA bersamaan 2 yang lebih daripada cukup untuk dilupuskan dengan selamat di tapak pelupusan sampah. Selain itu, sampel yang dikukuhkan / stabil mempunyai ettringite dan amorfus C-S-H. Penggunaan CBA telah mengubah permukaan sampel padu kepada lebih

banyak C-S-H dan pengurangan ettringit. Kristal utama dalam sampel pepejal adalah kalsit, yang dibentuk oleh reaksi karbonasi C-S-H dan C-H dengan CO2 dalam produk penghidratan simen. Analisis thermmogravimetry bagi sampel padat menunjukkan reaksi pozzolanic aktif pada suhu 400 hingga 750 ˚C, berpabdukan kepada penurunan berat Ca (OH) 2 dan penguraian produk karbonasi. Campuran optimum 40% penggantian CBA pada nisbah tetap W/C pada 0.55 memberikan nilai yang boleh digunakan dari segi kekuatan mampatan, rintangan lelasan dan penyerapan air untuk menghasilkan blok paving simen Portland. Selain itu, diperhatikan bahawa tahap pengecutan blok paving pasir CBA / silika menurun dengan peningkatan dalam kandungan CBA. Pengurangan ini mungkin dikaitkan dengan tekstur liang CBA yang juga mengakibatkan mengurangkan kekuatan mampatan.

Kata kunci: Pengukuhan, Abu bawahan arang, Penstabilan, Mikrostruktur, Semen.

ACKNOWLEDGEMENTS

TABLE OF CONTENTS

LIST OF FIGURES

LIST OF TABLES

LIST OF SYMBOLS AND ABBREVIATIONS

ACAA   American Coal Ash Association

ASTM   :   American Standard of Test Material

BJH   :   Barrett-Joyner-Halenda

BET   :   Brunauer Emmett and Teller

BSI   :   British standard institution

CBA   :   Coal bottom ash

CCPs   :   Coal combustion products

CH   :   Calcium hydroxide, $Ca(OH)_2$

C_3A :   Tri calcium aluminate

C_4AF :   Tetra calcium aluminate ferric

C_2A :   Dicalcium aluminate

C_3A :   Tricalcium aluminate

CBL   :   Crushed block leaching

C_3S :   Tricalcium silicate, $3CaOSiO_2$

C_2S :   Dicalcium silicate, $2CaOSiO$

C-S-H   :   Hydrated calcium silicate

DIW   :   Deionized water

EPA   :   Environmental Protection Agency

EQA   :   Environmental quality order

FA   :   Fly ash

HF   :   Hydrofluoric acid

ICP-OES   :   Inductively couple plasma atomic electronic spectrophotometer

LDPE   :   Low-density polyethylene

LOI   :   Loss on ignition

MESV	:	Malaysia Electricity Supply & Voltage
MS	:	Malaysian standard
OPC	:	Ordinary Portland cement
PCBs	:	Polychlorinated biphenyls
PCPB	:	Portland cement paving block
PSD	:	Particle size distribution
SEM	:	Scanning electron microscope
S/S	:	Solidification/Stabilization
SP	:	Superplasticizer
SPLP	:	Synthetic Precipitation Leaching Procedure
SVOCs	:	Semi volatile organic compounds
TCLP	:	Toxicity Characteristic Leaching Procedure
TGA	:	Thermogravimetric analysis
USEPA	:	United States Environmental Protection Agency
VOCs	:	Volatile organic compounds
XRD	:	X-Ray Diffraction
XRF	:	X-Ray Fluorescence
WBL	:	Whole block leaching
W/C	:	Water to cement ratio

LIST OF APPENDICES

CHAPTER 1: INTRODUCTION

1.1 Background

Globally, numerous waste materials are produced by various industries such as electric power plants, metal manufacturing and metal recovery plant. Moreover, disposal of these durable wastes is a significant risk for the surrounding living people (Torkittikul et al., 2015). Likewise, due to high consumption of natural resources of aggregate in construction they are depleting rapidly. At present condition, as aggregate resources are becoming scarce, it is vital to identify a suitable substitute for natural aggregate (Khan & Ganesh, 2016).

In view of expanding ecological concerns and practical issues, efficient usage of durable waste materials is needed of great importance. The benefits of utilization of waste materials is the most ideal approach to reduce the issues that are caused by their disposal. The construction industries have huge potential for the utilization of durable waste materials as sustainable construction material. Subject to their properties, the durable waste materials can either be utilized as complementary cementitious materials or substitution of fine aggregate in concrete mixtures (Rafieizonooz et al., 2016; Singh & Siddique, 2014). In view of some research reports, many waste materials, for instance, silica fume, fly ash and grounded blast furnace slag have been used in the production of concrete and cement paste (Cachim et al., 2014).

Malaysia with its developing economy and growing population is undergoing a nonstop, intensification in its electricity expenditure (Raju et al., 2014). Besides that, with high demand for electricity, the Malaysian rule has permitted private financier to construct numerous huge coal-fired power plants. Jimah power station is one of the main coal-fired power plants in Malaysia which has an electricity generating capacity of 1400 MW (2 units $\times$ 700 MW) that started its operation in 2003 (Abubakar & Baharudin, 2012).

It is the first and largest private coal-fired power plant in Malaysia and Asia which is utilizing pure coal in the production of electricity.

The production of electricity has been identified as the main industrial performance which used the coal as one of the important sources of fuel (Ramzi et al., 2016; Tiwari et al., 2014). Abubakar and Baharudin (2012) observed that coal is rapidly accepted by the electricity industry. The total consumption in the fuel mix to produce electricity has been increasing from 14% in 2008 to 24% in 2011 (MESV, 2014). Besides that, it causes disposal of tremendous amounts of CBA (coal bottom ash) for decades, which has some impacts on the environment and human health (Singh & Siddique, 2015). Coal is a composite amalgamation of mostly inorganic heavy metals concentrations and organic contents. Coal can be classified as bituminous or sub-bituminous. However, Jimah coal-fired power plant burned up to 30% of sub-bituminous coal which is imported from South-East Asia and South Africa (Oka & Embi, 2007).

The higher demand for electricity generation has led to a higher consumption of coal ash and hence higher amount of coal waste formed as by product of electricity generations. Cheriaf et al. (1999) reported that the incineration of 2.9 million metric tons of coal produced about 1.2 million metric tons of coal ash wastes. Tiwari et al. (2014) concluded that there are various types of coal ash wastes that are produced from coal combustion during the electricity generation process such as fly ash (FA), coal bottom ash (CBA), boiler slag, clinker etc. As shown in Figure 1.1, the major coal ash waste products that have been produced are FA and CBA (Bajare et al., 2013). Recently, the most well-known coal ash combustion product is fly ash. It is known as supplementary cementitious material that is usually used in concrete mixtures (Han et al., 2015; Singh & Siddique, 2016). Meanwhile, coal ash accumulated at the bottom of a furnace is known as CBA, because it is heavier and stiffer to be passed by flue gas in comparison with fly ash (Menéndez et al., 2014). However, the application of CBA as a sustainable

construction material in the building industry plays an important role to decrease the volume of residual waste and conserving existing natural fine aggregates.
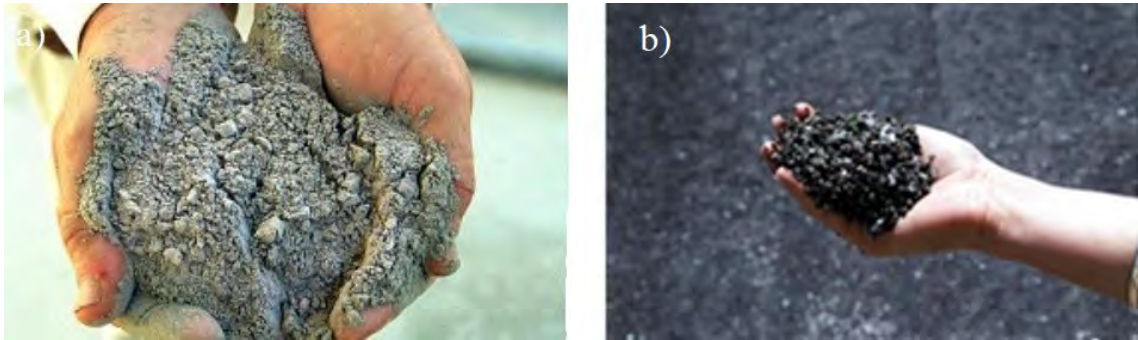
Figure 1.1: Coal Ash Wastes (a) FA, (b) CBA

CBA has contributed to the environmental problems such as contaminating the surface and ground water due to heavy metals concentrations toxicity. It is essential to pre-treat the CBA before discharging to ash ponds or landfill sites. According to the Environmental Protection Agency (EPA), the surrounding area to a coal ash pond sites are subjected to higher possibility of human health risk of cancer and other diseases. It can also affect the drinking water from a well where humans may get cancer from drinking water contaminated with metals such as arsenic, copper and cadmium (ACAA, 2016).

On the other hand, large volumes of sand are extracted for the use of construction material as aggregate in the manufacture of concrete. In addition, the natural resources like sand are dwindling gradually. Moreover, exploitation of natural resources has resulted in unbalance to the ecological system. Therefore, the detection of replacement material of sand becomes vital and important to save the non-renewable natural resources (Singh & Siddique, 2016).

Recently, many researchers have shown an interest in exploring CBA as a sustainable fine aggregate in concrete mixture which has brought many interests to the construction

and manufacturing sectors due to its low cost, low mass filler and its appropriateness to be applied as substitution of aggregates (Bajare et al., 2013).

CBA can be usefully applied in various sustainable construction utilizations. Figure 1.2 illustrates the common usage of CBA according to American Coal Ash Association (ACAA, 2016) . The CBA is mostly applied as structural fills (46.51%) in the United States. While, high portions of CBA are used in bridges and structural stones in most European countries. In Germany, 50% of CBA is recycled in sound filling walls along highways and for sub paddings of city roads. Similarly, about 60% of the CBA is utilized for the structure of asphalt and for sublayer of roads in the Netherlands. In Denmark, over 72% of CBA is utilized to produce parking lots, cycling tracks and other roads (Reijnders, 2005). Despite the high potential of CBA in infrastructures, its application is not common in Malaysia (Anastasiadou et al., 2012).
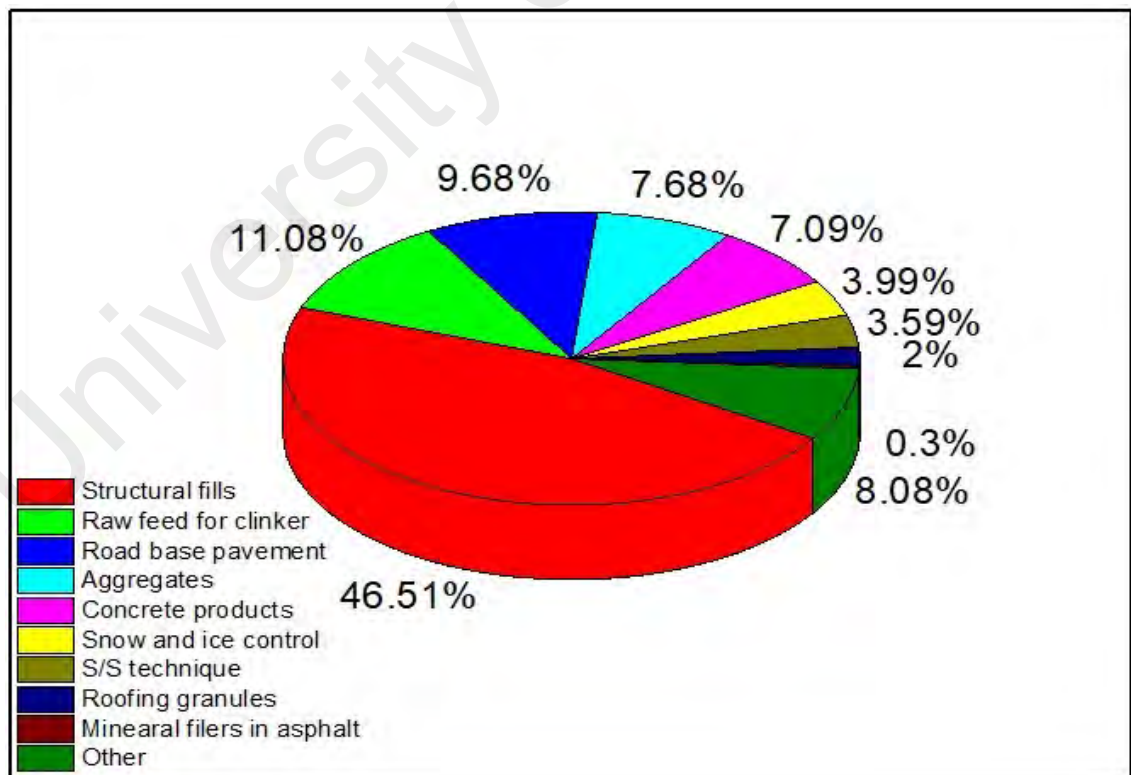
Figure 1.2: Applications of CBA in the United State (ACAA, 2016)

Overall, the ash pond sites have overtaken a shocking quantity. Therefore, CBA utilization in structural applications is an obligation in order to economize the building cost and diminishing the amount of ash disposed to landfill sites (Abubakar & Baharudin, 2012). CBA can be used as fine aggregate replacement in mortar mixture to decrease the depletion of natural fine aggregate like sand (Kim & Lee, 2011; Singh & Siddique, 2014). However, CBA contains significant amounts of various heavy metals such as lead, cadmium, copper and nickel that are categorized as toxic waste (Aggarwal et al., 2007). The Portland cement may have the chemical bonding capabilities of solidified/stabilize CBA as less or non- contaminated material.

1.2   Problem statements

The expansive amounts of hazardous wastes delivered by many industries can cause genuine natural harm when they are discarded in the environment without treatment. The environmentally friendly solution is to reuse and recycle these low-cost industrial residues. In addition, the decrease in the amount of these wastes sent to landfills and the impact of severe environmental hazards, the positive advance in sustainable development would open new market opportunities. Besides, these wastes may contain major amounts of various heavy metals such as copper, cadmium, nickel, lead, arsenic which may cause environmental contamination and health problems when migrate to the water sources. Therefore, a segment of these wastes is unsafe and requires cost-effective leachate treatment.

The waste ash is generated in huge amounts at coal-fired power plants in Malaysia (4.3 million tons, each year). It must be treated before being dumped to sanitary landfill. The capacity for dumping of tremendous amount of CBA is inadequate due to lack of available disposal sites. Currently, ash pond sites are an inappropriate way of dumping ash wastes, as the formation of underground water pollution caused by the ash residues containing

contaminated heavy metals cumulated in the ash ponds. The most significant environmental problem is caused by CBA leachate discharging. The leaching problem requires the adoption of pre-treatment systems. To reduce the quantity of CBA waste in the landfills and its effects on environmental pollution, one of the most important environmentally-friendly solution is to recycle or reuse such low-cost industrial residue as sustainable substitution of aggregate in concrete mixtures. However, the leaching problem in CBA in terms of heavy metals concentrations need to be treated. Moreover, not much study has been reported on the crystalline phases of Portland cement mixtures containing CBA.

1.3   Objectives of study

The present research embraces the safe disposal of the CBA using cement-based solidification/stabilization as well as the potential reuse of the end-product as construction application. The leachability of heavy metals, compressive strength of CBA mixtures and the effects of the heavy metals on the hydration of the cement-based CBA mixtures are reported.

This research work is broken down into the following specific sub-objectives:

1. To ascertain the optimal cement-based mortar mixture containing CBA as fine aggregate substitution that contribute to high strength property.

2. To study the compressive strength, porosity and heavy metals leachability properties of cement-based CBA mixtures according to the solidification and stabilization techniques.

3. To investigate the microstructure properties of cement-based CBA mortar mixtures that contribute to high strength and low leachability monolithic.

4. To determine the ideal CBA mortar mixture as complying to paving block requirements in terms of compressive strength, abrasion resistance and water absorption.

1.4 Significance of study

Large amounts of CBA are discharged from electricity power stations, especially to ash ponds. However, CBA is not being used in any form in Malaysia. Ash wastes produced are classified as scheduled waste under the Malaysian Environmental Quality Act and must be treated and disposed properly (EQA, 1979). Solidification/stabilization (S/S) technique is generically defined as a technique of reducing the mobility as well as solubility of contaminated heavy metals present in waste to convert that waste into chemically inert form. However, limited aspects of the S/S technique and microstructure analysis of mixtures containing CBA were studied. Also, there is a lack of research on the leachability properties of CBA. Therefore, in this study cement-based S/S technique of CBA may result in application of paving block product of high strength and low leachability. Moreover, the effect of cementation crystalline phases on heavy metals concentration is necessary to evaluate in certain construction aspects such as paving blocks.

1.5 Outline of thesis

The study is organized into five chapters. The first chapter highlights the background of the study, the problem statements existing in this area which provide the motivation for this research, objectives and significance of research. The second chapter provides literature reviews of the previous works which covered the related evidence of toxic waste handling in Malaysia and previous studies on the characteristics of CBA as fine aggregate in concrete mixtures. The properties of substitution CBA as aggregate in concrete mixtures, performance parameters of S/S technique and production of paving block are also discussed in this chapter. The third chapter presents the fundamental procedure for laboratory tests performed to evaluate the cementation process in mortar mixtures, mechanisms involved in S/S technique, micro-structural investigations and parameters in

production paving blocks. Explanation of the results and scientific analysis of the outcomes of this research are discussed in the fourth chapter. The fifth chapter presents comprehensive conclusions together with recommendations for further work on CBA that would take this material to industrial sustainable construction application.

CHAPTER 2: LITERATURE REVIEW

2.1   Introduction

This chapter covers literature reviews of the previous works which based on related evidence of toxic waste handling in Malaysia and previous studies on the characteristics of CBA as fine aggregate in concrete mixtures. The properties of substitution CBA as aggregate in concrete mixtures, performance parameters of S/S technique in accourdance with standards and production of paving block requirments are also discussed in this chapter.

2.2   Toxic waste handling

In recent years, the huge amounts of hazardous waste have made with growing in industrialization and fast economic development. Due to the inappropriately treated and disposal of the hazardous waste, they may migrate to the underground water and pollute drinking water. Department of Environment Malaysia has announced Scheduled Wastes Regulation to qualify the dumping of toxic wastes by accepting cradle to the grave following framework under waste organizations to prevent environmental degradation. The three-main strategies used as in-plant possibilities system for handling toxic wastes in Malaysia are presented in Figure 2.1.

Developing countries like Malaysia have rapid industrialization which resulted in an increase in the production of waste materials. Various industries generate numerous waste materials and the disposal of these waste materials is a major environmental issue. Disposal of waste materials should be managed in such a way that it should pose minimum environmental problems. The productive use of these waste materials is the best way to mitigate the issues associated with their disposal. The use of industrial by-products is an important factor in the economics of many industries. The waste materials

can be put in numerous uses depending upon their physical and chemical properties. The building manufacturing has huge potential for use of waste materials as a sustainable construction material. Based upon their properties, these waste materials can either be used as supplementary cementitious materials or as replacement of aggregate in concrete. Governments should create economic incentives for managing the waste materials in a more environmentally-friendly beneficial manner (Han et al., 2015; Singh & Siddique, 2013).

In-plant possibilities			
1. Reuse or modification			

2. Transformation of toxic wastes to less or non-toxic composits		
Physical Treatments	Chemical Alternatives	Land Alternatives

3. Permanent Storage				
Landfill Sites	Underground Infusions	Mine Storage Waste Piles	Surface Impoundments	Salt Foundations
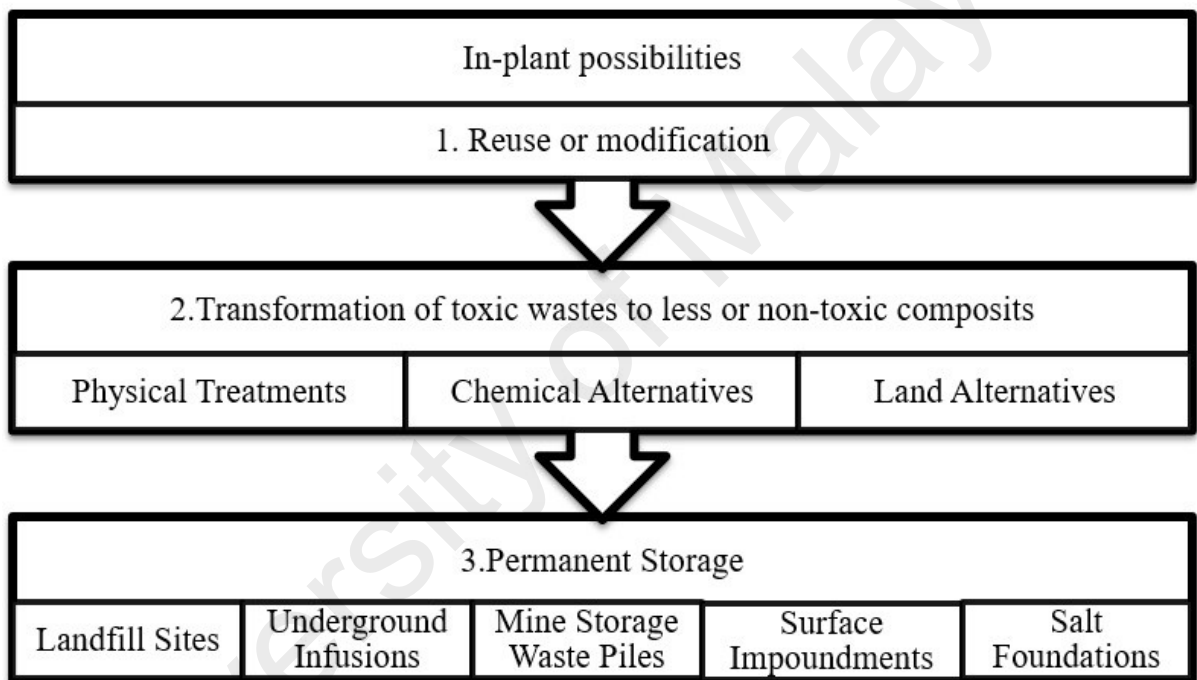
Figure 2.1: Hazardous waste handling in Malaysia (Shaaban, 1993)

2.3   Coal combustion power plant

A coal fired power plant is an energy conversion center that burns fossil fuels to produce electricity. As shown in Figure 2.2, a coal is ground in a coal mill to enhance the efficiency and accelerate the transformation of minerals at high temperatures. Then,the ground coal is fed into combustion furnace. Basically, organogenous, crystalline and amorphous are three types of substances available in coal. When the ground coal is subjected to the high temperatures, the organic compositions such as carbone are burnt and the temperature is increased subsequently.

As a result, the transition of cations from the bound state to an activated state in primary layers of silicates and carbonates leads to a decomposition, dehydration, dehydroxilation and decarbonatization in softened and partially melted materials which have a lower melting point. At this stage, the product consists mainly of amorphous glass phase of essentially an aluminosilicate composition (from 29 to 90 wt.%) and some crystalline phases (Ranjbar & Kuenzel, 2017a; Vassilev & Vassileva, 1996). In addition, these coarser particles, which settle down at the base of the furnace are CBA. Depending on the mineralogy source of the feed coal, the micro-crystalline admixtures consist of quartz, lime, periclase, anhydrite, sodalite, feldspars and ferrite spinel ($FeAl_2O_4$), mullite, hematite, aluminates and calcium iron. Following heating up of the remaining component, with higher melting points, results in further phase formation because of solid-liquid interaction in the presence of fuel wastes including mainly quartz and feldspars. The products at this stage are dense and vesicular spheres that originate from fully and partially degasificated melts of various minerals (Ranjbar & Kuenzel, 2017a; Vassilev & Vassileva, 1996). At a temperature of about 1000–1200 ˚C, high-ferrous silicate and ferritic melts under reduction conditions due to the presence of Fe^{2+} (Sokol et al., 2000). Further increase of the temperature causes that nonmolten quartz particles to be captured

by the molten glass phase and partially dissolved leading to an increase of the SiO_2/Al_2O_3 ratio (Goodarzi, 2006; Sokol et al., 2000). Swirling air carries the ash particles out of the hot zone where it cools down. The boiler flue gas carries away the finer and lighter particles of coal ash. The boiler flue gases pass through the electrostatic precipitators before discharging the dumping area. In the electrostatic precipitators, ash particles are extracted from the boiler flue gases (Ranjbar & Kuenzel, 2017a).
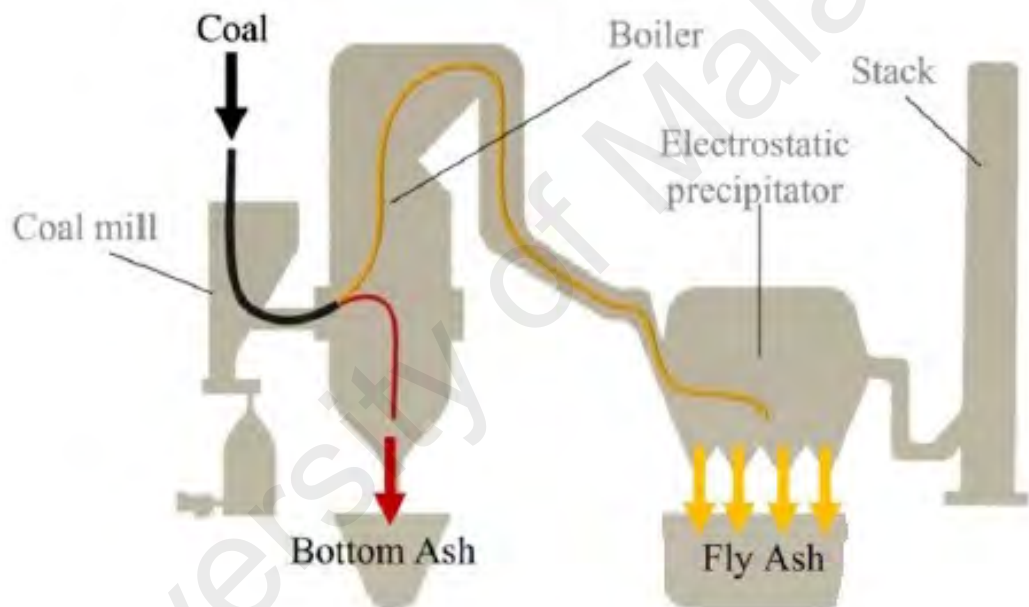
Figure 2.2: Coal combustion wastes production (Ranjbar & Kuenzel, 2017a)

Chemical energy that is stored in coal is converted successively into thermal energy, mechanical energy and at last converted into electrical energy. Basically, the electrical energy is generated based on heat from the burning coal that is used to generate steam that is used to spin one or more turbines to generate electricity. About 23% of the electricity consumed worldwide is generated by coal-fired power plants. When coal is burnt, it produces side waste residues like CBA (30%) and Fly Ash (FA 70%) with the flue gases and volatilized minerals (Michelle Christine, 2008). In Malaysia, coal-fired electricity production leads to estimate 6.8 million tons of coal fly ash (CFA) and 1.7 million tons coal bottom ash (CBA) each year. Wet disposal method known as ash pond is a disposed site which the CBA in a slurry form is dumped (Susie, 2008). Ash ponds are a surface impoundment used to dispose of ash, primarily from the combustion of coal. Coal ashes are stored for disposal as a slurry or sludge. A large ash pond is referred to as surface impoundment, ash reservoir in Malaysia (Figure 2.3).

Figure 2.3: Coal ash waste disposal area

2.3.1 Specific heavy metals in coal combustion wastes

The main heavy metals lead (Pb), nickel (Ni), arsenic (As), zinc (Zn), cadmium (Cd), copper (Cu), chromium (Cr), barium (Ba) are the trace elements in coal combustion residue which are an important concern for land disposal due to their environmental significance (Jayaranjan et al., 2014; Lee et al., 2017; Rozumová et al., 2015). The ultimate impact and type of each trace element will depend upon its state in coal sources and toxicity, mobility and availability in the ecosystem. The leaching of heavy metals to surface and underground water source is one of the major concerns with coal combustion residue disposal. The leaching of heavy metal may contaminate the ground water quality around the ash disposal area.

2.4 Physical characterizations of CBA

The CBA is primarily due to the existence of rock detritus in the fissures of the coal seams. The variability in the rock detritus from one source to another therefore causes differences in the characteristics of CBA as well. The aspects that affect the positions of CBA are: degree of pulverization of coal, firing temperature in the furnace, and type of furnace (Lee et al., 2017; Singh & Siddique, 2014).

CBA is an angular, irregular, with rough surface textured particles. The particles size of CBA is ranges from fine sand to fine gravel (63 μm - 9.5 mm). Moreover, it is normally a well-graded material, although fluctuations in particle size distribution can be encountered from the same power plant. Its particles have interlocking features that enhance the lighter and more brittle as compared to natural sand. CBA contains higher proportions of particles finer than 75 μm as compared to the natural sand. While, natural sand particles are dense, smooth textured and regular shaped (Lee et al., 2017; Singh & Siddique, 2014). The specific gravity of CBA is ranges from 1.2 to 2.47 depending upon the source and type of coal. The lower specific gravity in the CBA with a porous texture

causes the CBA to degrade easily under compression (Jayaranjan et al., 2014; Singh & Siddique, 2014). The CBA which derived from high sulphur coal and low rank coal is normally less porous and dense (Singh & Siddique, 2014). In literature a wide range in CBA physical properties is found in Table 2.1 (Kim & Lee, 2011; Lee et al., 2017).

It appears that contradicting results have been found by various researchers, which could have been due to non-Optimal use of CBA in mortar/concrete, for instance sufficient water content to smear CBA particles for appropriate lubrication towards flow ability and compatibility. This may be Ascribed to significant variation in the CBA physical properties including water absorption capacity.

Table 2.1: Physical specifications of CBA

Physical specifications	CBA in the literature (ranges)	References
Specific gravity	1.39-2.19	(Singh & Siddique, 2014)
Water Absorption (%)	5.45-31.58	(Jayaranjan et al., 2014)
Specific surface area (m^2/g)	1.01-1.06	(Lee et al., 2017; Kim & Lee, 2011)

2.5 Chemical properties of CBA

Chemical properties of CBA produced on burning of lignite or sub bituminous coal contain high calcium oxide content. Anthracite or bituminous coals on burning result in low-calcium coal ash, which has pozzolanic properties and very small fraction of calcium oxide (Lee et al., 2017). Principally, CBA constituted of silica, alumina and iron with small amounts of calcium, magnesium, sulphate etc. Basically, the source of coal determines its chemical structure. The data reported in literature shows variation in chemical composition of CBA.

Table 2.2 shows the chemical composition of CBA (Kou & Poon, 2009; Lee et al., 2017; Singh & Siddique, 2014).

Table 2.2: Chemical compositions of CBA (Singh & Siddique, 2014)

Chemical mixture (wt.%)	CBA in the literature (%)
SiO_2	20-70
K_2O	0-4
Fe_2O_3	2-15
CaO	0-15
MgO	0-5
Al_2O_3	15-30
Na_2O	0-2
LOI	0-12

2.6 Mineralogy characteristics of CBA

X-ray diffraction (XRD) analysis of pure CBA was investigated by Marto et al. (2010) and the results presented that mullite ($Al_6Si_2O_{13}$), silicon oxide (SiO_2) and silicon phosphate are the major crystalline form constituents. They found that silica exists partly in the crystalline forms of quartz (SiO_2) and moderately in combination with the alumina as mullite ($Al_6Si_2O_{13}$). The iron appears partly as the oxide forms, magnetite (Fe_3O_4) and hematite (Fe_2O_3). The conformation of CBA depends on the source of coal and furnace condition (Lee et al., 2017; Singh & Siddique, 2013). Alumina silicates such as clays melt or decompose to form glass or mullite ($Al_6Si_2O_{13}$). Carbonates including calcite ($CaCO_3$), dolomite [$CaMg(CO_3)_2$], ankerite [$CaMgxFe_{(1-x)} (CO3)_2$] and siderite ($FeCO_3$) decompose, release CO_2 and form lime (CaO), calcium ferrite ($CaFe_2O_4$), hematite (Fe_2O_3), magnetite (Fe_3O_4) and periclase (MgO). Sulphides such as pyrite (FeS_2) oxidize, loose SO_2 and form sulfates (SO_3). Iron oxides such as hematite (Fe_2O_3) and magnetite (Fe_3O_4), chlorides volatilize as NaCl and KCl. Quartz (SiO_2) generally remains unaltered.

2.7 CBA as a fine aggregate replacement

Based on the research reports, waste ash such as fly ash is reused in production of concrete as sustainable construction materials. Mortar mixture is the most widely procedure which cement, fine aggregate and sand are its core component materials. Natural resources of sand are getting depleted regularly by usage as fine aggregate in the concrete mixtures. The lack of sand has caused growth in the cost of production of concrete.

Hussain et al. (2013) reported that the use of CBA as a partial replacement of fine aggregate, decreased the curing susceptible of concrete exclusively at a lower water to binder ratio because of its inner curing effect. While, the substitution of sand with CBA appears to result in the drop of compressive strength due to a growth in porous structures in concretes (Cheng, 2012; Singh & Siddique, 2014).

The research carried out by Cyr and Ludmann (2006) observed that the CBA can be used as replacement of sand in mortar mixtures. Compressive strength of mortar incorporating up to 17% CBA as replacement of sand did not change.

The coarse, and glassy texture of CBA causes it to become an ideal substitute for natural aggregates (Cheriaf et al., 1999; Lee et al., 2017). The particle size distribution of CBA motivated researchers to investigate its replacement as aggregate in the manufacture of concrete (Lee et al., 2017; Singh & Siddique, 2014). Experimental study carried out by Rafieizonooz et al. (2016) investigated concrete specimens with 0, 20, 50, 75 and 100% of CBA replacing the sand. They concluded that workability of concrete mixture reduced when CBA content increased in the mixtures. On the other hand, at the early age of 28 days no significant outcome was detected in compressive strength of all concrete specimens. After curing, at 91 and 180 days, compressive strength of both the

experimental and control concrete samples increased significantly but remained almost similar.

In Malaysia, construction is significantly hampered by the shortage and high cost of sand. On the other hand, coal-fired thermal power plants have produced significant volumes of CBA for decades. Dumping of CBA is becoming an environmental threat to the nearby community. Raising the environmental complications posed by CBA, many researchers have targeted CBA as aggregate replacement in concrete. Recently, there are few reports on using CBA in mortar mixture who they reported the use of CBA either as partial or as total replacement of sand in concrete. However, the micro-chemical bonding of CBA in cement paste is not well explored (Rafieizonooz et al., 2016).

2.8   Fresh properties of CBA concrete

2.8.1   Flowability

The requirement of water for desired flowability of concrete principally depends on textures of aggregates (Lee et al., 2017). The following independent records which show a reduction in flowability on use of CBA as partial or full replacement aggregate in concrete mixture:

Ghafoori and Bucholc (1997) investigated fresh properties of concrete mixtures incorporating high-calcium CBA as a fine aggregate replacement. In their study, the control mixtures were designed to progress 28-day compressive strength of 41 MPa. They observed that in comparison to control concrete, for CBA concrete mixtures, the requirement of water raised to achieve the same workability on incorporation of CBA to replace sand. Water absorption of CBA used in their study was 7.0%. While, for 50% mixture (CBA + sand) water requirement decreased significantly but still was more than that of normal mixture. It further improved on use of water reducing admixture but was

still more than that of normal concrete just in case of 41 MPa mixture. In case of CBA concrete mixture which contains cement amount of 474 kg/m^3, the requirement of water was 189.6 kg/m^3 against 194.3 kg/m^3 for control concrete on use of higher quantity of water reducing admixtures. They observed that for the same workability, the difference in requirement of water of CBA concrete mixtures and the control concrete mixture tightens down with the growth in cement proportions.

Ghafoori and Bucholc (1996) reported the impact of using chemical admixtures like Superplasticizer (SP) on fresh mixtures combining lignite-based CBA as fine aggregate replacement. In their study, four control concrete mixtures with fluctuating cement volume of 297, 356, 424, and 474 kg/m^3 were designed to develop 28-day strength of 41 MPa. Water absorption of CBA used in their study was 7.0%. They resulted that for stable water cement ratio mixture comprising CBA showed far less flowability than the control mixture. The CBA concrete mixtures were stiff. They concluded that for the similar workability, CBA concrete was desperate for 269.6 kg/m^3 of mixing water against 183.7 kg/m^3 for control concrete containing 297 kg/m^3 cement. However, the water requirement reduced, but was still more than control mixture. CBA concrete mixtures formed in median of 7.0% higher water capacity in the mixture. With the applying chemical admixture like SP, the increase in water volume released to 4.0%. However, on the utilization of high dosage of superplasticizer, in comparison to control concrete, for CBA concrete mixtures the requirement of water reduced to achieve same workability value.

Aramraks (2006) studied the water demand of mortar mixtures incorporating 50 and 100% CBA as substitution of fine aggregate. CBA based lignite grains (passing through No. 4 sieve) were utilized as fine aggregate in concrete mixture. Water absorption of CBA used in their study was 5.45%. He concluded that the mixtures by means of CBA required almost 25 to 50% more quantity of free water than conventional mixture to acquire

appropriate flowability. Chun et al. (2008) also investigated that workability of mixture incorporating sludge ash diminished with the increase in quantity of sludge ash. Water absorption of sludge ash used in their study was 5.45% which caused reduction in flowability of fresh mixture.

Bai et al. (2005) resulted that when natural sand was substituted with CBA, for stable water to cement (W/C) ratios of 0.45 and 0.55, the workability of CBA concrete mixtures containing 382 kg/m^3 cement contents raised to increase in CBA volume. For the controlled workability value was in the range of 0-10 mm and 30-60 mm, respectively. The requirement of free water decreased with the increase in quantity of CBA as partial aggregate in concrete. Consequently, there was lessening in the free W/C ratio since the cement content was kept the equal for all the mixtures. Water absorption of CBA used in their study was 30.4%. They observed that a sphere attitude effect of the interlocked form of CBA particles as equated to a typical sand particle resulted in a growth in workability.

Yuksel and Genç (2007) studied the properties of concrete comprising different percentage range of 10 to 50% CBA as sand substitution, 35 kg/m^3 of fly ash, 350 kg/m^3 of cement and 167 liters of mixing water. The slump values of fresh CBA concrete increased up to 40% replacement level and thereafter decreased marginally. Water absorption of CBA used in their study was 6.10%. The slump of CBA 50% mixture replacement of sand, was 50 mm as against 60 mm of control mixture concrete. However, when the CBA was used in the amalgamation of natural sand, there was an enhancement in the flowability at all sand replacement levels as to control mixture. Kou and Poon (2009) carried out the effect of CBA as a sand substitution at ranges of 0, 25, 50, 75 and 100% by volume at constant W/C ratio. Water absorption of CBA used in their study was 28.9%. They used saturated surface dried CBA in all concrete mixtures. They resulted that the workability values enlarged in quantity of CBA in the concrete. This was because

of higher water absorbency and lower water retention values of CBA than natural sand. As such, CBA kept more available water to upsurge the flowability of fresh mixture. Kim and Lee (2011) investigated the flow characteristics of concrete incorporating CBA as the substitution of sand. Water absorption of CBA used in their study was 5.45%. They observed that the workability of concrete decreased marginally on utilization of fine CBA as sand replacement. The reduction in slump flow values with the use of fine CBA can be neglected.

The most of the research reports show that in comparison to conventional concrete, the requirement of water to achieve same workability rises 50% on use of CBA content as fine aggregate in concrete mixtures (Lee et al., 2017). It is challenging to define the exact water to cement ratio due to the extremely porous structure of CBA which capable to uptake more water (Andrade et al., 2009), then there is water caught inside the CBA through slender maintenance, which does not add to the development of cementitious gel (Andrade et al., 2009; Cheriaf et al., 1999).

2.8.2 Bleeding

The amount of bleeding water in concrete is mainly depends on the water to cement (W/C) ratio, physical properties of fine aggregate and cement such as water absorption, particles size distributions, etc.

Andrade et al. (2007) found that the existence of CBA as substitution of sand in concrete enlarged the amount of bleeding water, the bleeding period and the water release percentage. The sophisticated quantity of CBA in the fresh mixtures caused the superior effect in bleeding. The total amount of bleeding water of 25% and 50% CBA replacement with sand mixtures was very near to the conventional concrete. For concrete mixtures containing 75% and 100% CBA, amount of bleeding water was more than control

concrete. This may be due to the higher quantity of water added in CBA concrete mixtures as compared to control concrete. The amount of water added in CBA concrete mixtures containing 75% and 100% CBA was 373 kg/m^3 and 378 kg/m^3, respectively, contracted to 219 kg/m^3 for control concrete.

Ghafoori and Bucholc (1996) proved that the CBA fresh mixtures displayed more bleeding than the conventional concrete. The amount of water surcharged in CBA fresh mixtures was much higher than adding in control concrete. The dosage of water added in CBA mixtures varied from 251.2 kg/m^3 to 269.6 kg/m^3 as compared to 182.7 kg/m^3 to 194.3 kg/m^3 added to control concrete. The CBA concrete mixtures displayed about 84% higher total amount of bleeding water in low cement content mixtures.

Ghafoori and Bucholc (1997) reported that for concrete mixture containing 297 kg/m^3 cement, bleeding percentage increased from 2.2 to 4.0 and 2.79 for use of 50% and 100% CBA as substitution of sand in concrete mixtures, respectively. With higher amount of cement in concrete mixtures, the bleeding percentage in fully CBA concrete mixtures decreased from 4.0 to 0.84 as compared from 2.2 to 0.08 decreases in normal concrete. With the use of water-reducing chemical compound, bleeding percentage of CBA mixtures were approximately identical to that of a respective control concrete mixture. This may be due to fact that the W/C ratio of CBA mixtures with water-reducing admixtures was lower than respective control concrete mixtures.

As a result, the utilization of CBA as substitution of sand in the mortar mixture affects the bleeding property of fresh mixture. It is believed that, the CBA's texture absorbs portion of water inside through the mixing process as well as water taken into texture voids present in the fresh mixture. Moreover, CBA textures have a minor water preservation volume in comparison with the natural sand. CBA particles release the internally absorbed water to the concrete mixture during curing days. The water released

by CBA texture outcomes in advanced loss of water via bleeding in CBA mixture in comparison with that in normal concrete (Lee et al., 2017; Singh & Siddique, 2016).

2.8.3 Setting Time

The level of stiffness characteristics can be defined as the initial setting time of concrete mixture. Ghafoori and Bucholc (1996) found that, setting times of CBA concrete mixtures slightly decreased with a high proportion of cement used. For fresh CBA mixtures having cement proportion of 474 kg/m^3, compared with the mixtures of low cement content of 297 kg/m^3, the initial setting times reduced from 3.3 to 2.5 h. Moreover, the final setting times of CBA concrete mixture decreased from 4.4 to 3.7 h.

Ghafoori and Bucholc (1997) concluded that setting times of fresh mortar mixtures with partial substitution of sand with CBA were identical to control concrete. This is due to the application of chemical admixtures, the initial and final setting times of concrete mixtures incorporating 50% CBA as replacement of sand dropped approximately by 9% and 13.5%, respectively.

Andrade et al. (2009) investigated the effect of CBA as substitution of sand in concrete on its setting times. They observed that initial setting times of CBA fresh mixtures were higher than control concrete. According to the moisture content, initial setting time enlarged with growth in CBA content. Maximum to 75% substitution of sand with CBA, initial setting time increased from 230 min to 350 min. The initial setting time of concrete mixture incorporating 100% CBA was 270 min. Final setting time of the CBA concrete enlarged with the growth in quantity of CBA in concrete. For fresh concrete in which quantities of the CBA were not reformed according to moisture content, the setting times of CBA concrete mixtures except mixture containing 25% CBA were lower than control concrete. The setting times (initial and final) of CBA fresh concrete containing 25% CBA

were 240 min and 340 min as compared to 230 min and 330 min of control concrete, respectively.

The research reports published reveals that the replacement of sand with CBA in concrete mixtures increases the setting time of concrete. It is believed that the higher demand of mixture water for use of CBA is the possible reason for higher setting times (Lee et al., 2017). The higher amount of mixing water in the concrete mixtures drops the pH value of the extraction and growths the interval between cement hydration process. The above factors result in postponement or reduction in hydration function of the cement pastes, and thus increase in setting times of concrete incorporating CBA as replacement of sand. The water-reducing admixtures has little impact on setting times of CBA concrete with low percentage of cement. For CBA concrete mixtures with higher proportions of cement, the setting times decline with the intensification in dosage of chemical admixtures like SP.

2.9   Harden properties of CBA concrete

2.9.1   Bulk density

The available studies present noticeable reduction in bulk density of concrete mixture on utilization of CBA as a substitution of natural sand in concrete.

Andrade et al. (2007) showed that the utilization of CBA with characterization of specific gravity 1.67 g/cm^3 as substitution of sand in concrete eventuated in reduction the unit weight of concrete by 25% from 2070 kg/m^3 to 1625 kg/m^3.

Kim and Lee (2011) studied the outcome of fine CBA on the unit weight of concrete. The mixture design of concrete applied in their researches comprised 143 kg/m^3 of silica fume, 14 kg/m^3 of superplasticizer, 187 kg/m^3 of water and 607 kg/m^3 of cement in all the samples with varying proportions of CBA as replacement of sand aggregate

replacement. They concluded that the superior CBA contents in concrete linearly results in the inferior density of hardened concrete. The density of high strength concrete was less than 2000 kg/m^3 when 100% fine CBA were utilized. The reduction in bulk density was 109 kg/m^3 (4.6%) and 228 kg/m^3 (9.6%) when sand was substituted with CBA as fine aggregate in concrete mixture.

Topçu and Bilir (2010) investigated the effect of CBA as a substitution of sand in 7 and 28 days density of mortar mixture. The mix proportions of mortar consisted 500 kg/m^3 cement and varying proportions of CBA with specific gravity 1.39 g/cm^3 as replacement of natural sand. They showed that the bulk density of specimens reduced with increase in CBA proportions used. The air-dried density at the curing age of 7 and 28 days fluctuated by 1.23 kg/dm^3 and 2.23 kg/dm^3; and 1.35 and 2.28 kg/dm^3, respectively.

Ghafoori and Bucholc (1996) reported that CBA concretes exhibited a lower air-dried density in comparison with conventional concrete. Bulk density of CBA mixture was 2263.4 kg/m^3 as compared to 2343.5 kg/m^3 of control concrete. Air-dried density of CBA concrete increased with applying of chemical admixtures to reduce water mixing in concrete. The mass amplified by a mean of 0.8% on the use of low dosage of 369.7 ml per 45.36 kg of cement and an extra 0.25% when more admixture amount of 739.3 ml each 45.36 kg of Portland cement was used. Arumugam et al. (2011) found out that the average air-dried density of CBA concrete mixture diminished linearly with advanced in quantity of CBA in concrete.

The density of CBA in comparison with natural sand is moderately low. Moreover, the utilization of CBA caused a growth in demand of mixing water in concrete mixture, which it eventuates in a growth in the amount and extent of pores and thus causes the porous compound of concrete (Lee et al., 2017; Singh & Siddique, 2016). Moreover, the higher

substitution of sand with CBA as fine aggregate in concrete subscribe the reduction in its bulk density.

2.9.2 Compressive strength

Ghafoori and Bucholc (1996) studied the effect of high-calcium CBA on compaction strength of concrete. Their study found that the compressive strength pattern of CBA concrete was like the conventional concrete. At early curing days, the strength of CBA concrete was lesser than that of normal concrete, but at 180 days of curing age, it was almost comparable for all the concrete mixtures. At the age of 7 days, CBA concrete mixtures having cement content of 297 kg/m^3, 356 kg/m^3, 424 kg/m^3 and 474 kg/m^3 achieved 67, 81, 78 and 86% of 28 days compressive strength, respectively. The mean compressive strengths of CBA mixtures were 30% and 25% lesser than normal concrete at age 7 and 14 days, respectively. This difference is resulted in 17% and 7% at 28 and 180 days, respectively. Compaction strength of CBA concrete at all proportions of cement are increased with the applying of low quantity of chemical admixture. Compressive strength of CBA concrete improved by approximately 20% at the age of 28 days. Compressive strength of composing a combination of 50% CBA and 50% natural sand exceeded those of conventional concrete mixture on the use of high range water reducing chemical admixture.

Ghafoori and Bucholc (1997) reported that the strength of CBA concrete mixture containing 50% CBA as substitution of sand was lesser than conventional concrete. The mean variations in strength property were 12% and 14.5%, at the age of 3 and 7 days, respectively. With age, the difference in compressive strength of CBA concrete and that of control concrete decreased. Compressive strength of CBA concrete mixtures was lower by 10 and 1.5% at 28 and 180 days, respectively. The utilization of high range water-reducing admixture, compressive strength of CBA concrete mixture containing 50% CBA

as substitution of natural sand exceeded that of normal concrete at all levels of age. At the age of 7, 28, 90 and 180 days, the compressive strength increased by 30, 24, 21.4 and 19%, respectively.

Andrade et al. (2007) reported that mixtures made with CBA as an equivalent percentage replacement consistent with the humidity quantity displayed high substantial adverse effect on compressive strength. However, in terms of mixtures made with the replacement of CBA as 70%, and 100% with natural sand without the wetness content the compressive strength of CBA mixture was same that of normal concrete.

Kou and Poon (2009) concluded the compressive strength of CBA mixtures at a constant W/C ratio, diminished by the growth in the CBA proportions at all the ages. However, at constant workability range the compressive strength of CBA mixtures was superior than that of control concrete at all the ages. The enhancement in compressive strength could be credited to the decrease in the free W/C ratio.

Kim and Lee (2011) reported that CBA as a substitution of sand in concrete was not powerfully adverse effect on compressive strength at the age 7 and 28 days. They observed that the usage of CBA has insignificant effect on compressive strength due to higher cement paste content in concrete.

Sani et al. (2011) found that, the compressive strength of CBA concrete mixtures containing 30% washed CBA replacement are the highest at 3 days curing age compared to other proportion of washed CBA concrete mixtures. CBA concrete mixture containing 30% washed CBA is verified has the highest compressive strength at early and late curing ages. They found that a 30% replacement of natural sand with washed CBA in concrete is the ideal proportion to get satisfactory compaction.

Topçu and Bilir (2010) resulted that compressive strength of cement and CBA mixture concrete diminished with the higher percentage of CBA. The reduction rate of compressive strength in early age days was same to the age 28 days. Overall, compressive strength results of the mixture incorporating CBA were minor comparing to the normal mixture.

Ghafoori and Cai (1998) investigated the effect of CBA on the properties of roller compacted concrete. They observed that pressing strength development of CBA roller compressed mixture was resembling to that of control concrete. In 7 days, CBA concrete mixtures achieved approximately 75% of the 28 days compressive strength.

Yuksel and Genç (2007) discussed usage of coal ash as replacement fine aggregate in concrete. They eventuated that 28 days compressive strength of CBA concrete mixtures decreased with increase in CBA content. Compressive strength of CBA concrete mixture containing 50% CBA as a sand replacement was lower by 31.8% than that of control concrete. This demonstrates that CBA retards the improvement in strength property of CBA concrete mixtures.

Aramraks (2006) demonstrated that the compressive strength of CBA concrete mixtures including 100% CBA as a sand replacement was approximately 40% lesser than that of conventional concrete mixtures.

Aggarwal et al. (2007) resulted that, the using CBA as fluctuating stages from 20 to 50% as a sand substitution made resulted in reduction compressive strength of CBA concrete mixtures comparing to conventional concrete mixture at early and late curing days. Compressive strength of CBA concrete mixtures kept increasing with the age.

Bai et al. (2005) resulted that using CBA as fine aggregate in concrete mixture at constant W/C ratio, the growth in CBA content in the concrete mixture, results in

decreasing compressive strength. The constant workability range of 30-60 mm, eventuated an enhancement in compressive strength in comparison with normal concrete at all the ages. This could be accredited to reduction in water requirement on utilization of CBA in mixtures.

Arumugam et al. (2011) discussed the compressive results of amalgamation 20% sludge ash as a sand replacement in mixture concrete. It showed improvement in compressive strength over the normal concrete at all the curing aging. However, compressive strength of concrete mixtures decreased with additional of sludge ash as sand substitution level from 20%. Also similar results was detected by Yuksel and Genç (2007) that compressive strength decreased slightly on substitution of CBA as aggregate in concrete.

2.9.3 Drying shrinkage

The published literature on drying shrinkage specifications of CBA mixtures is limited. It is assumed that the permeable texture of CBA is useful for dropping the drying shrinkage effect of concrete mixtures. The porous particles of CBA act as reservoirs. It is believed that the porous CBA particles gradually liberate the humidity through the drying stage of mixture and thus the outcome in condensed shrinkage.

Bai et al. (2005) resulted that at a constant W/C ratio of 0.45 and 0.55, drying shrinkage amounts of all CBA mixtures were lesser than that of conventional mixture, while at constant flowability, the shrinkage values were advanced. In constant W/C ratio, the amount of permeable structure of mixture concrete increased with higher CBA proportion. It gradually released the water throughout freshening of mixture and therefore lead to reduction shrinkage. At constant slump values, the higher CBA content resulted

in higher drying shrinkage. This is conflicting to the reduction in drying shrinkage on lessening of available water dosage.

Ghafoori and Bucholc (1997) resulted concrete mixture in corporation with CBA displayed better dimensional stability as compared to the normal concrete. They believed that higher bleeding resulted in lower drying shrinkage tension value of CBA concrete. Drying shrinkage strain values of CBA concrete mixture comprising 50% CBA was lower than that of normal concrete, but higher than 100% CBA concrete mixture.

Kou and Poon (2009) detected that the constant slump value for all the CBA mixtures, the drying shrinkage values were minor than that of normal concrete. This was because with the growth in CBA proportion, the needed free water dosage in CBA concrete mixtures decreased.

Singh and Siddique (2015) resulted that the drying shrinkage decreased with the increase in coal bottom ash content in concrete. The drying shrinkage of concrete mixtures contained 30, 40, 50, 75 and 100% CBA experienced 14.10, 10.25, 21.79, 34.62, and 37.17%, respectively, less shrinkage strain as compared to control concrete (Figure 2.4). However, the bottom ash concrete mixture containing 20% coal bottom ash as fine aggregate experienced 6.40% higher drying shrinkage strain than the control concrete.
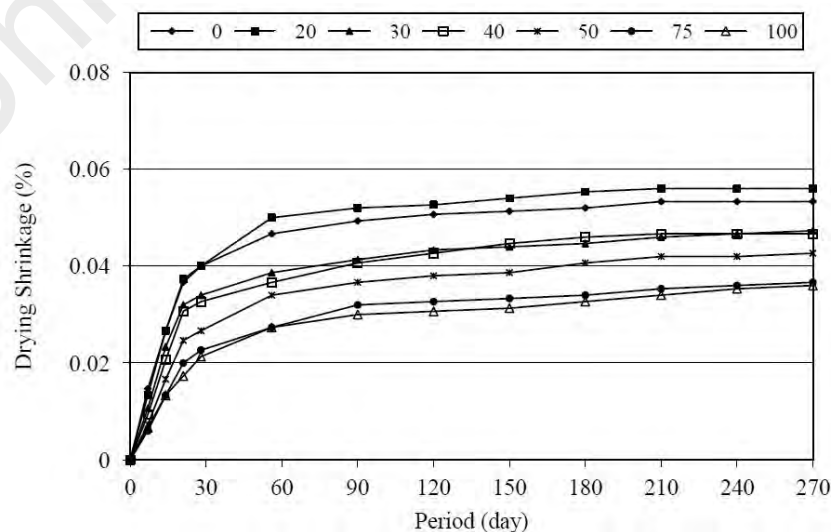
Figure 2.4 : Effect of coal bottom ash on drying shrinkage of concrete mixture

2.10   Solidification and stabilization (S/S) technique

Basically, S/S technique defines as a method which contains some specific binders mixing with waste to diminish the level of toxin leachability. It has been extensively used in toxin waste pre-treatment for manufacturing solid waste that based on reduction hazardous waste migration to groundwater and soil prior to land disposal (Conner, 1990; Hunce et al., 2012; Malviya & Chaudhary, 2006b; USEPA, 2000).

Stabilization is referred as the procedures that lessen the solubility, mobility, and chemical reactions of contaminated heavy metals by altering its chemical nature. While, solidification refers to encapsulating the waste into easily applied blocks with zero or less toxin leaching rate. Worldly, the amalgamation of S/S is regularly considered as "waste fixation" or "encapsulation" by many researchers. The encapsulation may include fine waste elements or large mass of waste which attempts to mechanically bind the waste into the monolith integrity structure. S/S is physiochemical process which has been experienced significantly in four parts: (1) development of alleviated foundation methods for road construction, (2) mine structural filling, (3) soil balance and handling, and (4) radioactive hazardous maintenance and removal (Conner et al., 1994; Erdem & Özverdi, 2011; Hunce et al., 2012).

Recently, treated waste material must accomplish firm values for safe site remediation by detoxifying the toxin specifications, particularly in developing country like Malaysia at disposal areas. This typically needs to pass concentration-based level using the Environmental Quality Act Malaysia for evaluation disposal hazardous harden compositions. The S/S technique is based on a nature binder is frequently applied to alleviate the contaminations in the waste and to eliminate the rate of leaching, where suitable binder choice must be proof as the way to success application. To achieve this rate, a diversity of policies may be considered to avoid toxins leaching, comprised of

oxidation, neutralization, and physiochemical properties of the toxin (Cerbo et al., 2017; John et al., 2011; Paria & Yuet, 2006).

Generally, cement-based S/S technique is broader appeal for contaminated heavy metals wastes. The industrial wastes (defined by source and type) that have been treated by S/S techniques are summarized as shown in Table 2.3. Most systems in use include varying mixtures of hydraulic cements, gypsum and silicates. In opinion, they rely upon the form of a silicate or alumina-silicate matrix within which the waste constituents are incorporated. In some cases, the toxic material will not only be encapsulated (solidified) but also chemically bound (stabilized) within the silicate-aluminosilicate matrixes. Frequently, S/S technique is applied to diminish the leaching rate of the inorganic heavy metal constituents from the hazardous waste. After this technique, the toxic constituent properties of the waste are removal and can be dumped as less or non-hazardous waste in the disposal site (Cerbo et al., 2017; Sollars & Perry, 1989).

Table 2.3: Industrial wastes treated with S/S technique (Sollars & Perry, 1989)

Manufacturing	Sort of wastes	Pollutants
Electrocoating	Sludges/filter	Cu, Cd, Pb, Cr, Ni, Zn, cyanide
Electrical manufacture	Filter cakes/sludges	Carbone, cyanide, Sn, Pb,
Heavy metal treatments	Liquids	Cyanide, Acids, alkalis, Zn, Mg, Ba
Heavy metal recovery plant	Solids	Cu, Ni, Zn
Combustion wastes	Solids	Mn, Fe, Pb, Zn, v

2.10.1 Portland cement as main binder

Portland cement is a popular binder, mainly utilized in production of concrete for building and other construction applications. It is also known as an adaptable binding

component for solidified/stabilized waste products with the skill to both fixed and immobilized toxin heavy metals (Chen et al., 2009; Du et al., 2014; Harbottle et al., 2007; Kogbara et al., 2012). Portland cement binding combination have been used to a widespread diversity of hazardous wastes comparing with any other binding mixture (Conner, 1990; Malviya & Chaudhary, 2006b).

Cement is often nominated for the reagent's capacity to (a) compresses waste elements adjacent them with a resistant covering, (b) decrease the porousness of the harden waste, (c) chemically fix free liquids, (d) chemically alternated hazardous constituents, and (e) ease the decrease of the toxicity of some metal contaminations. Moreover, physicochemical changes to the solidified/stabilized waste products are accomplished by using Portland cement binding mixture to treat wastes which have inorganic hazardous elements before disposed them in sites (Conner et al., 1994; Lee et al., 2017).

Ordinary Portland cement (OPC) is categorized as hydraulic cement. It is the ability to setting, hardening, lasting, and stable under water. The main constituent of OPC is tricalcium silicate (C_3S), di calcium silicate (C_2S), tri calcium aluminate (C_3A) and tetra calcium aluminate ferric (C_4AF) as shown in Table 2.4. As shown in Table 2.5 and Figure 2.5, OPC reactivated with mixing water by creating calcium hydroxide (CH), calcium sulfur-aluminate hydrate (ettringite of $C_6AS_3H_{32}$ or C_4ASH_{18}), calcium silicate hydrate (C-S-H), and anhydrite clinker granule in dense forms. When an OPC mixed with water is totally dissolved and precipitated and produce heat of hydration before toughens to uniform mass.

Table 2.4: OPC constitutes and formations (Mehta & Monteiro, 2006)

Cement constitutes	formation	Percentage	influence
C_3S	$3CaOSiO_2$	50%	Reactive, high heat and high early strength
C_2S	$2CaOSiO$	25%	Strength
C_3A	$3CaOAl_2O_3$	10%	Low heat and slow process
C_4AF	$4CaOAl_2O_3Fe_2O_3$	10%	High heat and high early strength
Gypsum, CSH_2	$CaSO_4.2H_2O$	5%	High early strength, set of cement

The chemical reactions of OPC and heat of hydration can be shown in Equations 2.1 to 2.4:

$$2C_3S + 6H \rightarrow C_3S_2H_3 + 3CH + 120 \text{ cal/g} \tag{2.1}$$

$$2C_2S + 4H \rightarrow C_3S_2H_3 + CH + 62 \text{ cal/g} \tag{2.2}$$

$$C_3A + CSH_2 \rightarrow \text{Ettringite} + 300 \text{ cal/g} \tag{2.3}$$

$$C_4AF + CSH_2 \rightarrow \text{Ettringite} + \text{monosulphate} + 100 \text{ cal/g} \tag{2.4}$$
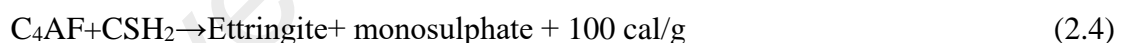
Table 2.5: Hydrated outcomes by OPC (Mehta & Monteiro, 2006)

Hydrated products	Structure	Percent (%)	Significant property
C-S-H	Tobermorite gel	50-60	100-700 m^2/g surface area, high strength
CH, portandite	Large hexagonal prism	20-25	Limited strength
Ettringite, $C_6AS_3H_{32}$	Needle shape crystal	15-20	Focus to sulphate reactivity, high early strength
Monosulfate hydrate, C_4ASH_{18}	Hexagonal plate crystal	-	Final sample of cement hydration comprising>5%C_3A
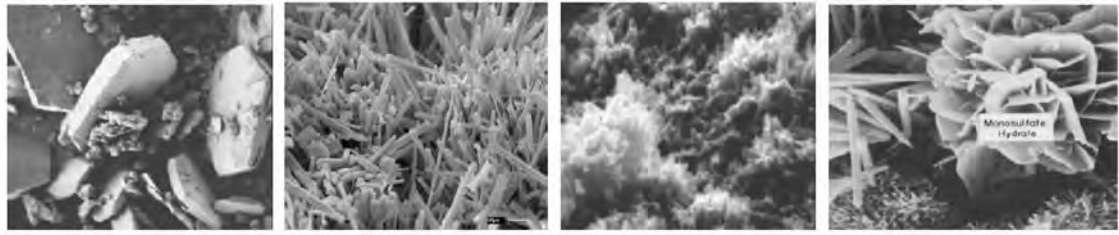
(a) Portlandite   (b) Ettringite   (c) C-S-H   (d) Monosulfate hydrate

Figure 2.5 : Hydration products of Portland Cement (Mehta & Monteiro, 2006)

2.10.2   OPC- based solidification/stabilization technique

Basically, cement-based S/S technique is widely put in for production final treated waste concrete mixture which could be applicable in construction. Schematic illustration of cement hydration is as shown in Figure 2.6. It presents the formation unsolvable hydrates with capsulation of heavy metal component into chalk content existing in cement mixture. When the waste is composed mainly inorganic contaminated metals, the OPC cement-based S/S technique is mostly effective due to transformation of most metal composites into unsolvable metal hydroxides in high pH conditions. These unsolvable components trapped by lattice amalgamation into crystalline groups of set OPC cement (Glasser, 1993; Lee et al., 2017). In some cases, in terms of strength property of solidified/stabilized harden samples, OPC structures with C-S-H gel has high specific surface area is accountable for achieve highest compaction of harden paste (Shi, 2004). OPC as binder using has numerous benefits which are low price, long-term firmness, dense structure and high strength properties (Spence & Shi, 2004). Fundamentally, OPC-based solidified/stabilized of harden waste is satisfactorily and cost-effective feasible for manufacturing waste originators (Cerbo et al., 2017; Silva et al., 2007).
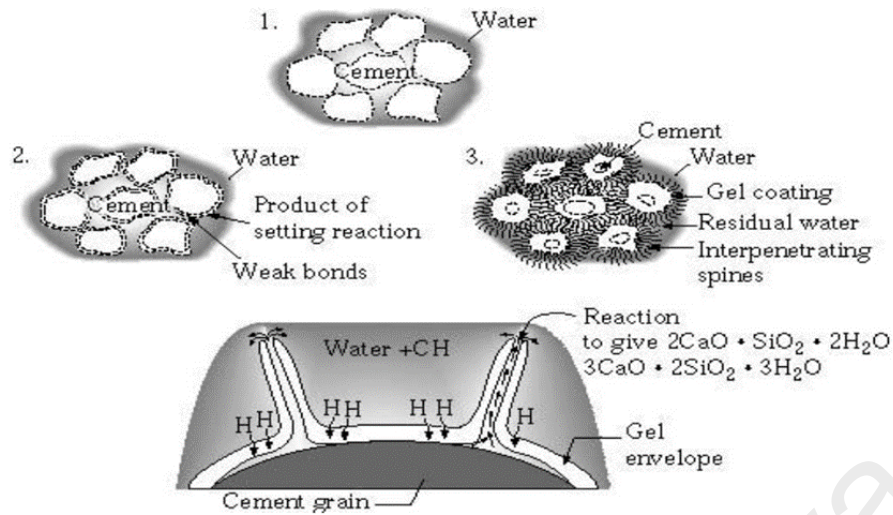
Figure 2.6: Diagram of Portland Cement hydration process (Glasser, 1993)

2.10.3 Features of OPC- based metal immobilization

There are six main factors affecting immobilization of waste in Portland cement based S/S technique (Cerbo et al., 2017; Conner, 1990; Du et al., 2014). The stabilization process is depends on pH, precipitation, chemical reactions, adsorption, chemisorption, ion exchange, diadochy, encapsulation and alteration of physical modification as following sections:

2.10.3.1 pH

The pH is directly control the leachability of the inorganic metals of the encapsulate of waste during cement hydration. The alkalinity in cement is ruled by magnesium hydroxide, lime, sodium hydroxide, and sodium carbonate. The primary pH of the aqueous cement solution is around 11.20-12.10, which relay on the formations of the $Ca(OH)_2$ and C-S-H in dense composition were molded. When, the pH was decreased to 9.0-12 due to $Ca(OH)_2$ was consumed by SiO_2, CaO, and plentiful C-S-H and silica gel was molded, therefore less leachability was reported (Cerbo et al., 2017; Roy et al., 1992). The OPC configuration was administered by mainly the triplex combination of SiO_2, CaO and H_2O. S/S technique on five metals selected, namely Pb, Cr, Cd, As and Hg by

progressive group leaching on developed OPC based, determined that the metals' motion was on reliant of pH (Cerbo et al., 2017).

Figure 2.7 shows the dissolve-ability of the hydroxides form of metals as a purpose of pH. The minimum volume of contaminated metal in liquid phase could be produced by altering alkalinity pH condition (Du et al., 2014). The ideal pH is regularly in the range of 9 to 12.0 (Cheng, 2012). The minimum decomposition of metal hydroxides occured at pH of 8.5 to 12.0 (Cerbo et al., 2017).
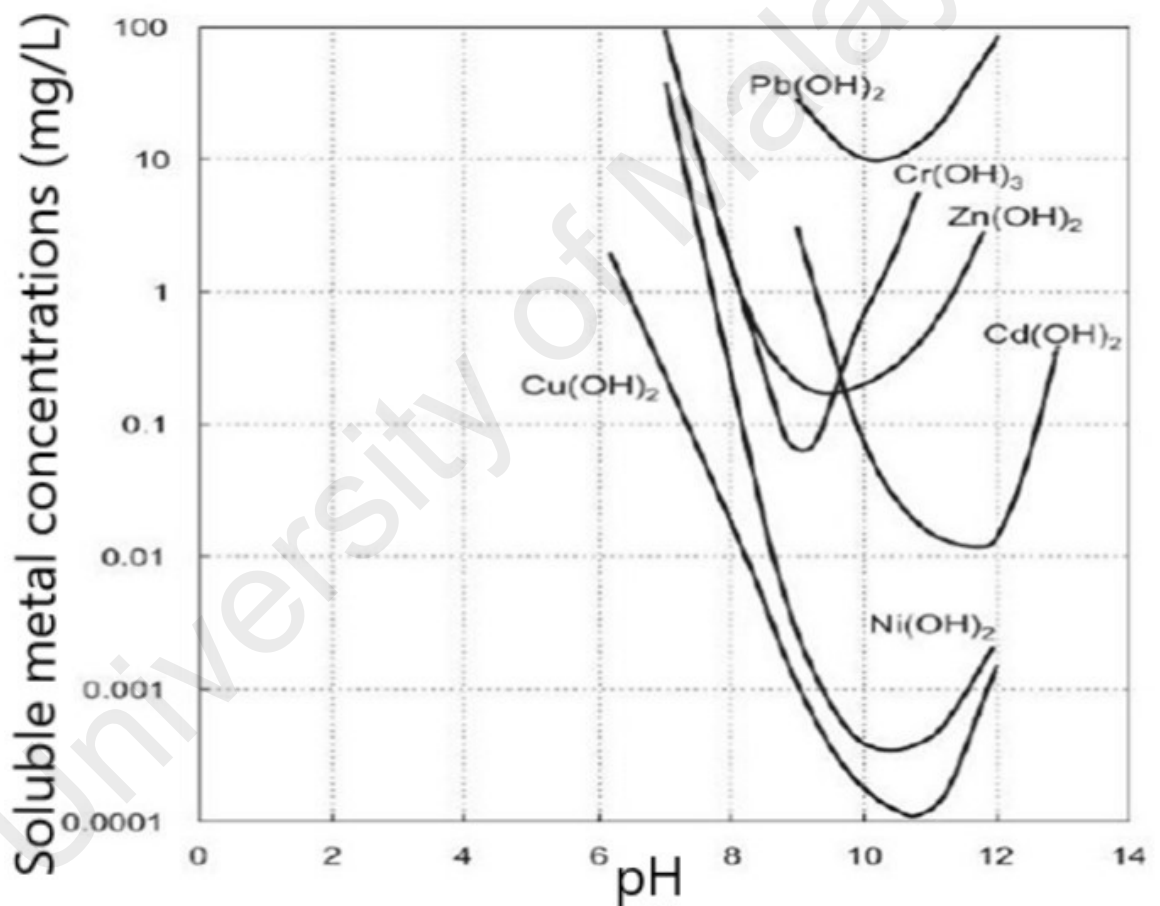
Figure 2.7: Dissolve-ability of hydroxides form of heavy metals as a role of pH (Cheng, 2012)

2.10.3.2 Sedimentation

Hydroxide sedimentation happens in OPC hydration feedback which is exposed to pH alkalinity. Some contaminated metal types are put out of actions with formation silicates, sulfates, carbonates, and non-metal components like sulfate, cyanide is accelerated as metals category. For example, Pb metal in the calcite phase of OPC based S/S technique produces lead sedimentaed recognized forms $PbSO_4(CO_3)_2(OH)_2$, and $3PbCO_3.2Pb(OH)_2.H_2O$ which fixed on external solidified/stabilized samples, that delay the continuing hydration of fundamental clinker substantial as distinguished through composition XRD analysis (Lee, 2004; Lee et al., 2017). Lead nitrate may alter the properties of solidified products and inhibit initial and final setting times (Stegemann & Zhou, 2009).

2.10.3.3 Adsorption

The high specific surface area of C-S-H in cement offers sorption with a formation comprising a bulk of calcium silicate coating with silicon at minimum level of polymerization. As a result, the irregular bulk of the dense sample, with individually 10-100 nm creates a teremendous capacity of microspores in size 0-10 nm (Conner et al., 1994; Hunce et al., 2012). The durable potentioal of sorption is provided by C-S-H surface area with a high mass of unbalanced hydrogen bonded, and rich calcium has a positive surface control and the anions metals absorbed especially when the pH is ranged as alkanility (Lee et al., 2017; Shi, 2004).

2.10.3.4 Ion exchange and Diadochy

The leaching solution is provided as the condition which some ion at the superficial coating is substituted with other ion's types. Cation Exchange Capacity (CEC) known as ion exchange, happens in most inorganic metals of hazardous waste composition. The

hydrated cation and its size in the acid extraction leaching is charged as significant ion exchange condition. The bonding control may arise from ionization of hydroxyl sets elaborated to silicon atom or isomorphous replacement. Isomorphous exchanges caused from metals Mg^{+2} for Al^{+3} or, Al^{+3}, Fe^{+3} for Si^{-4} (Chen et al., 2009; Conner, 1990; Paria & Yuet, 2006). Diadochy is detected once a component replaced by same element in size and bonded in a crystalline network. The diadochy feature can be instituted in substitution of Zn for Ca in calcite phase of cement (Cerbo et al., 2017; Chen et al., 2009; Conner, 1990).

2.10.3.5 Encapsulation

Most inorganic metals waste forms in S/S technique are maintained by microfixation, and these particle obstructions and accumulation can be easily defined by a SEM micro-structural analysis of solidified specimens (Bone et al., 2004; Conner, 1990; Lee et al., 2017).

2.10.3.6 Alteration

Prior, the solidified/stabilized of waste is determined by varying the properties of waste as a pre-remedy to the waste to improve the disable of waste reactivity, for instant, the decrease of waste magnitude and modification of waste solid into a less solvable level or deactivate acidic waste (Ahmaruzzaman, 2010; Conner, 1990).

2.10.4 Inorganic intrusion in Portland cement

The physicochemical effects of interposition on the OPC binder are listed in Table 2.6. They act against the paste hydration. The interference specifications may have opposing and advantageous consequence on the OPC hydration. The ultimate features of the solidified sample like mechanical and leachability may be substantial influenced by the response of interference categories. Inorganic metals have interposition result through

modifying the hardening process. They prolonged the cement hydration reaction, which caused variation in charactrizations of dried harden samples. Inorganic toxin such as heavy metals and inorganic metal salts may increase setting time and alter the charactristics of solidified waste. Some hydroxide formation of heavy metals like lead, zinc and copper may delay OPC reaction (Bone et al., 2004).

Table 2.6: Inorganic interference effects of cement (Bone et al., 2004)

Inorganic interference	Effects
Metals: Pb, Cr, Cd, As	May upsurge setting time of cement
Fe compounds	straggled and interrupt paste
Metal salts collections	Superior set time and inferior durability
Cu, Pb and Zn	Negative effect on physical properties of cement-treated waste
Cu $(No_3)_2$	Delay of set cement
Gypsum hydrate	Acceleration of set cement
Gypsum hemihydrates, lead nitrate	Obstruct setting
Silica	Setting/curing retardation

2.10.5   Organic intrusion in Portland cement

The significant interference effects of organic composite in the harden waste are known as blocking the bonding formation of OPC and waste, delaying in setting time of paste. Minocha et al. (2003) was indicated range of main organic compound's interference effects as shown in Table 2.7. These organic compounds may be reliant on together existence and the amount of other hazardous heavy metals and discovered variations in the C-S-H comparative ultimate phase, which weaken strength properties and it adversely effect on the holding of heavy metals in solidified waste.

Table 2.7: Organic interference effects of cement (Minocha et al., 2003)

Organic interference	Effects
Semi Volatile Organic (SVOC)	Fail in the binding of cement and waste
Volatile Organic (VOC)	Retarded setting of final product
Organic-polar: Phenols, organic acids	Reduction in durability and retarded setting time
Aromatic hydrocarbons, Polychlorinated biphenyls (PCBs)	Vaporization, diminish durability, impeded setting of binding
Hydrocarbon complex organic	Interfere cement hydration
Chlorinated organic	Increase set time, decrease durability

2.10.6   Common solidified/stabilized heavy metal elements

OPC-based solidifed/stabilized samples is reported wildly with inorganic heavy metal elements which consist of high concentration of copper, nickle, lead and cadmium (Ahmaruzzaman, 2010; Choi et al., 2009; Zhang et al., 2009).

2.10.6.1 Copper

Due to the discharges of copper in building materials and coal combustion industry, the rate of usage this heavy metal especially in coal ashe industrial is known as an alarm for disposing at landfill sites (Gildeh et al., 2013). S/S technique is used to safely alleviate copper from the hazardous materials (Zain et al., 2004). The sedimentation as copper hydroxide and alkalinity pH of extractions are two major immobilization that resulted in less concentration of copper (Cerbo et al., 2017; Polettini et al., 2004).

2.10.6.2 Nickel

The solidified/stabilized products of reduction Nickle's concentration has been considered through numerous investigators. Overall, Nickel is identified as the element to delay the OPC hydration. Moreover, the Nickle hydroxide formation was known as the key of immobilization stage (Fatta et al., 2004; Fuessle & Taylor, 2004).

2.10.6.3 Lead

The high rate of usage lead in most manufacturing like coal combustion power plants and gasoline combustion industry caused discharging of this heavy metal in the dumping areas (Hale et al., 2012). The amount of lead reduction in leachate extraction is strongly governed by the pH in the leaching solution (Halim et al., 2003; Fuessle & Taylor, 2004). Nearly, all the lead concentration transforms into unsolvable lead hydroxide formation between pH 9-12 . Moreover, the physical fixation of Pb is stated to be halted by the creation of a new point with Al and Si rich types in OPC- based composites (Paria & Yuet, 2006). Halim et al. (2004) observed that lead is consistently scattered top the C-S-H of the cementitious layer by SEM analysis. The prevention hydration of paste and prolongment of the setting time of OPC are concluded by lead ions like insoluble salts in the leaching solutions (Cerbo et al., 2017).

2.10.6.4 Cadmium

Fuessle and Taylor (2004) observed that the amount of cadmium in the stabilization process upsurges by late curing days. Figure 2.8 presents diamond shape which is cadmium concentration after 2 days, triangle shape that is cadmium concentration after (370 days), and the solid line is the cadmium solvability rate . The pH ranging defined the reduction concentrations of cadmium (Cerbo et al., 2017). Many studies have found the significant of pH range for immobilization of Cd exsited in leachate waste (Coz et al., 2004; Halim et al., 2004). The Cd $(OH)_2$ sediments were found to be condensed inside the cement base or stucked on the C-S-H layer, about maximum 30% amount at several areas (Paria & Yuet, 2006).
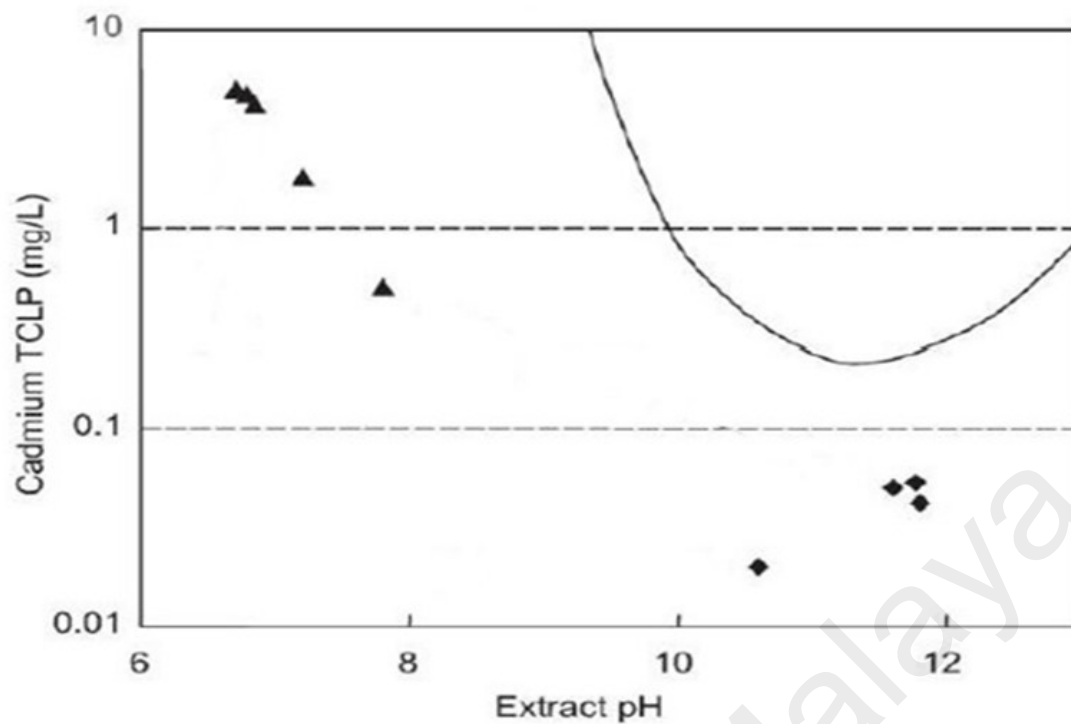
Figure 2.8: Cadmium solubility stabilized representative (Fuessle & Taylor, 2004)

2.11 Performance of OPC- based solidification /stabilization technique

Presentation of harden waste-based cement can be evaluated by numerous physical and chemical assessments. The main criteria test is leachability of solidified waste which defined by the United States Environmental Protection Agency S/S handbook standard (USEPA), (USEPA, 2000).

2.11.1 Leaching model of fixation waste

Leachability is described as the physio-chemical segregation of the waste into an extraction leachate. The rate of leaching progression is measured by relevance features that caused the demotion of harden waste. The pertinent model presented by Spence and Shi (2004) is created based on the environmental impact to the solidified waste. Recognized factors comprise pH, porosity, leachant flow level, and biological and

hydrological surroundings contribute to evaluate leaching rate. Mehta and Monteiro (2006) also, mentioned further aspects like specific surface area of waste, type of extraction vessel, sort of leachant, agitation method, interaction time and segregation of solid and liquid lead to effects in leaching process. The cement-based waste form leached model exposed to acid attack solution is shown in Figure 2.9. Environmental attack by H^+, CO_2, O_2, Cl^- and SO_4^{2-} will release Ca^{2+}, OH^-, trace elements and inorganic heavy metals. Those aspects are not enforceable because of the appropriate regulatory limits used for leaching test.

Discharge of heavy metal is largely reliant on pH value. Generally, in the pH range from 9.5 to 12.0 which considered as high pH, metal hydroxides have minimum solubility. High solubility in both acidic and alkaline solution is defined as an amphoteric behavior for some heavy metal compound for instant Cr, Pb and Zn (Bone et al., 2004).

Basically, the potential of a stabilized waste to release pollutants to the environment is measured by leaching test. The assessments of the leaching potential of the receiving medium is governed by two significant tests. The Toxicity Characteristic Leaching Procedure (TCLP) and Synthetic Precipitation Leaching Procedure (SPLP) by USEPA known as crushed sample into uniform size agitated extraction test, and for whole block test for sanitary disposal of waste in dumping sites. The Crushed Block Leaching TCLP method based on USEPA is tabulated in Table 2.8.

Whole block leaching (WBL) or semi dynamic leaching is used to designed simulation short-term leaching pattern of intact monolithic products when the harden waste was dumped in a catchment area. Although, crushed block leaching (CBL) quantity the severe lasting performance of the leaching by crushing the cube into small parts.
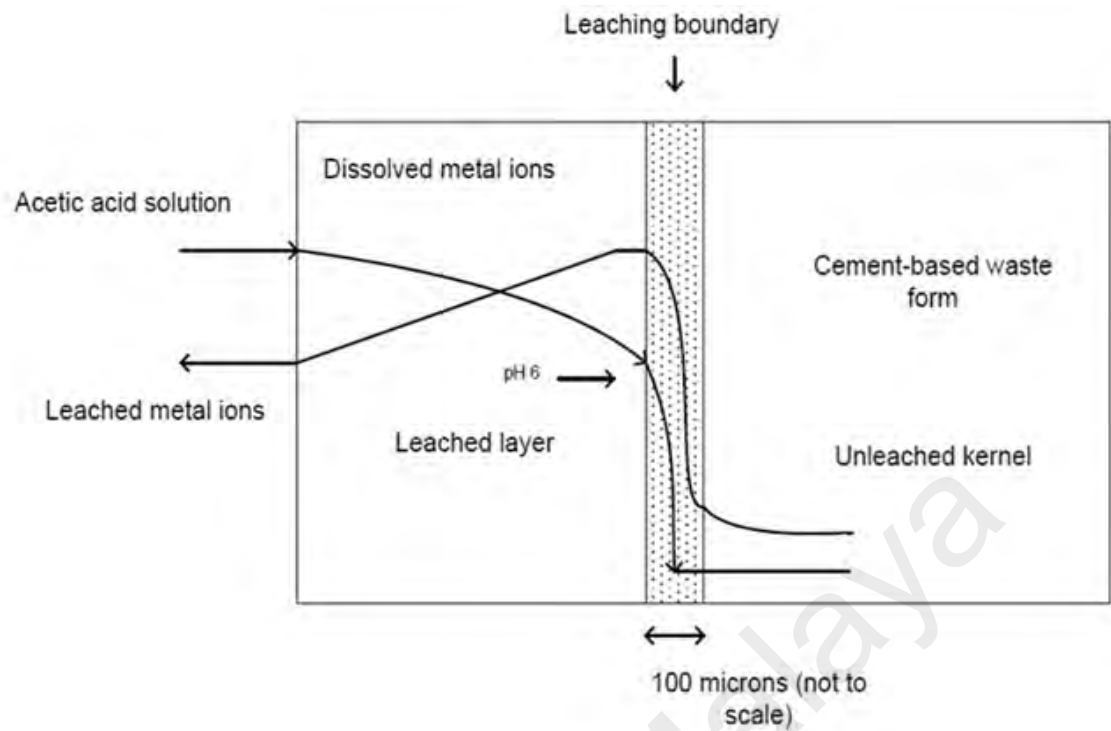
Figure 2.9: Cement- based leached model exposed to acid attacked solution (Cheng, 2012)

Table 2.8: TCLP procedure for Crushed Block Leaching (CBL) (USEPA, 1986)

Test standard	Size portion (mm)	Leachant	Extraction period	Mass of solid (g)	Solid/Liquid ratio
US EPA	< 9.5	Deionized water (Acetic acid/Nitric acid to pH 6.80, 2.88 and 4.20)	$18 \pm 2h$	50	50 g/2000 ml

2.12 Regulatory requirement of solidification/stabilization technique

The TCLP and SPLP procedures in accordance with US-SW-846 Method 1311 and 1312 are applied with the purpose toward the evaluation of leaching rate of contaminated metals with limitation Malaysian standard (USEPA, 1994b, 1994a). Acceptable leaching limit of Environmental Quality Act (EQA), industrial effluent regulations for metal concentration prior to hygienic landfill dumping was measured based on Standard A

(EQA). Table 2.9 displays the acceptance level of metals concentration and the pH limitation extracted from two sources; Malaysian standard and USEPA of S/S technique. The vulnerability of the treated wastes by S/S technique depends large extent on factors such as strength property, permeable porosity, chemical and mineralogical composition, and microstructure of the cement paste, as well as the cement and waste aggregates (Malviya & Chaudhary, 2006a).

Table 2.9: Limitation of heavy metals concentration in Malaysia (EQA, 1979) and USEPA standard (USEPA, 1993)

Type of metals	Standard A Malaysia (mg/l)	US EPA toxicity level (mg/l)
Aluminum	10	10
Calcium	-	10
Cadmium	0.01	1
Chlorine	1	5
Chromium	0.2	5
Copper	0.2	5
Iron	1	10
Magnesium	-	5
Manganese	0.2	5
Sodium	-	5
Nickel	0.2	5
Lead	0.1	5
Zinc	1	10
Arsenic	0.05	5
Cyanide	0.05	5
Free Chlorine	1.0	0.1
Phenol	0.001	0.1
pH	5.5-12	8-12

Table 2.10 lists two significant undertaking principles of final harden samples which were applied to estimate the efficiency of the strength behavior and permeable porosity. Due to unavailability of principal in Malaysia, these characterizations assembled and followed for assessment determinations in the chemical immobilization handling, according to the S/S treatment of United States Environmental Protection Agency (USEPA, 1993).

Table 2.10: Regulatory solidified waste acceptance parameters (USEPA, 1993)

Characteristics	Acceptance levels
Compressive strength (28 days)	Landfill disposal limit: 0.414 MPa
	Comparative mortar limit: 20 MPa
Permeable porosity (28 days)	Landfill disposal limit: 15-25%

2.13   Features of Portland cement pavement blocks

Portland Cement Pavement Blocks (PCPB) are applied in a diversity of trading, manufacturing and public usages. This form of interlocked paving blocks in term of pedestrian application is low maintenance, simplicity of settlement and immediate usage after fixing or repair as shown in Figure 2.10 (Ghafoori & Mathis, 1998). The key benefits of PCPB are resisted heavy loads and endured aggressive environments. It is tremendously durable. In addition, it provides the aesthetic appearance with its wide variety of colors, surfaces and forms. The uniquely elastic texture of PCPB, with its description of interlinked, avoids the block from moving in segregation and disperses made loads sideways and crossways downwards through the sub-ground for the basis.

These specifications with combination of higher strength property of the blocks, delivers a working surface with unusually high load volume (Pratt, 2003; Singh & Shah, 2017).

Main physical parameters of PCPB as determined by ASTM C936 is specified in Table 2.11. Preservation charge can be saved lower as it is possible to use the suitable waste material as a sustainable construction material in fabricating paving block and brick units (Poon & Chan, 2006; Zhang, 2013).

Figure 2.10 : PCPB application (Pratt, 2003)

Table 2.11: The physical requirements of PCPB (ASTM, 2016; MS, 2003b)

Parameters	ASTM C936	MS1380:1995
Compressive Strength	Individual strength unit. 45-50MPa	Average strength unit equivalent for production blocks and bricks <30MPa
Abrasion Resistance	Weight loss singular unit <3cm^3	Singular abrasion unit 20 mm
Water absorption	Value absorption singular unit <5%	-

One aspect of possible concern in use of CBA concrete/mortar, is stiffness (Elastic modulus). In pavement blocks this is not of significant concern. Typically, a significant reduction in E-modulus is associated with lightweight concrete, especially aerated or foam concrete, but also light weighted aggregate concrete. The E-modulus may be halved

for a density of 1600 or 1800 kg/m^3 compared with a standard density of 2400 kg/m^3 concrete. A remark on stiffness should be measured in future work to ascertain sound serviceability performance of CBA concrete, if it is to be considered for other structural applications. It is acknowledged that beam and slab type applications are significantly more dependent on stiffness than blocks and walls. but should structural application be considered, it may be dominant. the influence of CBA replacement of natural sand on the E-modulus of the composite

2.13.1 Aggregates properties

The bulk of PCPB is formed by fine aggregates. The production of cement blocks significantly influenced by the cost of using aggregates. The quality of the final product related to the properties of aggregates used. Aggregates used are commonly produced by natural solid rock, which has been crumpled or crushed down. Substitute aggregates or waste residues such as furnace fly ash, crushed clay, and slag are also applied broadly in the assembly of concrete pavement units (Poon & Chan, 2006). All characterizations of these aggregates should be checked to see if they have main acceptable properties. This might be completed by testing the aggregates in a small scale in laboratory then comparing values with reference to the successful presentation of the aggregates in concrete for long period (Ghafoori & Mathis, 1998; Pratt, 2003). The performance of aggregates at the hardened block depends on the combined effects of particle size distribution, grading, particle shape and hardness. Each of these properties is described as following sections.

2.13.1.1 Dimension

The suggested utmost size of aggregate for PCPB is 13.2 mm. Nevertheless, the determined size usually applied in preparation of PCPB is 9.5 mm. Minor dimension of 4.75 mm may be nominated to acquire an external surface. The size of aggregates should

be in a range of medium size of aggregates. Typically, the utilization of fine aggregate like natural sand as a substitution in production of paving blocks results in saving of total costs. All aggregate particle sizes are distributed in mean same range to attain good strength and satisfactory outward base. Th minimum and maximum dimension of block is in a range of 30-70 mm (Ghafoori & Mathis, 1998; Pratt, 2003; Singh & Shah, 2017).

2.13.1.2 Grading

One of the governing parameter affecting the characterizations of PCPB is grading of aggregate. The aggregate's grading ranging are specified in Table 2.12.

Table 2.12: Aggregate grading for the PCPB (MS, 2003b; Pratt, 2003)

Sieve size (mm)	Cumulative percentage passing
13.2	100
9.5	90-100
4.75	70-85
2.36	50-65
0.30	10-25
0.15	5-10
0.075	2-10

2.13.1.3 Particle configuration

The PCPB are constructed from bulky texture and dense surface that improved mechanical property. Natural sand as fine aggregate associated with this form of particles. As a result, adding natural sand as partial replacement aggregate is appropriate way because of its lengthened shape and irregular external texture (Ghafoori & Mathis, 1998; Pratt, 2003). Moreover, it may consequently be advantageous to use an amalgamation of natural sand as aggregate with residues for easy compaction and efficient strength (Singh & Shah, 2017).

2.13.1.4 Hardness

sands comprising large amounts of weak weathered particles which is sieved and oven dried before consuming as a substitution in production paving blocks. Natural sands with high silica content are appropriate for partial substitution in production interlocked pavement blocks. If aggregate texture is well paved at the base of the block, the package life of unit blocks can be prolonged by replacing the hard and strong aggregate with weaker aggregates to provide higher approaches of wearing surface. To boost the texture resistance, designated particles may be used in a stronger coating layer about 15mm dense molded in line with the foundation of blocks (Poon & Chan, 2006; Pratt, 2003; Singh & Shah, 2017).

2.13.2 Mechanical Properties

2.13.2.1 Compressive strength

PCPB contains of concrete blocks bedded and jointed in natural sand-based Portland cement. Consequently, the inclusive load carrying volume of a PCPB is contingent on the characteristics of these components, natural sand and other aggregates used as well as the interface between these aggregate particles. The overall performance of the paving block units is influenced by the size, thickness, laying patterns of aggregates (Panda & Ghosh, 2002). In general, the strength property of cement paving blocks is influenced by volume of the pores. The strength property does not offer any certain quantity of paver's toughness but does deliver a plain way for determining the global value of a paving concrete. Pavers must offer satisfactory mechanical property with stand to the struggle action and stresses caused by traffic (Raut et al., 2011). A universal investigation of PCPB characterizations proves that the compressive strength of an individual paver should record more than 50 MPa (Viana et al., 2009).

2.13.2.2 Abrasion resistance

The recent published literatures on abrasion measurement of CBA mixture are limited. Basically, a texture specification that is primarily reliant on the value of the surface layer features defines as abrasion resistance of block pavements. The upper layer about 1-3 mm of the paving products known as their most important part to evaluate the abrasion resistance (Humpola, 1996). Aggregate particle shape, texture, type of cement and quality of bond between aggregate and paste are the key aspects that effect on abrasion resistance. Basically, there is a relationship between PCPB compressive strength property and abrasion resistance (Ghafoori & Sukandar, 1995; Raut et al., 2011).

Ghafoori and Cai (1998) resulted that the penetration of wear of CBA roller compacted concrete reduced with intensification of cement proportion. Under air–dry conditions, the resistance to abrasion of roller compacted concrete containing high-calcium CBA was far superior to that under wet conditions. The depth of wear of CBA roller compacted concrete under damp situations was 7.25 times that under waterless conditions. This value released for 6.42 and 6.00 when paste proportion enlarged from 9 to 15%, respectively. Ghafoori and Bucholc (1997) investigated the impact of CBA with high calcium composition on resistance to abrasion of concrete. They observed that CBA concrete containing 50% CBA exhibited 13% higher resistance to abrasion as compared to normal concrete. CBA concrete mixtures incorporating 100% CBA as fine aggregate and containing 356 and 474 kg/m^3 cement contents displayed 47.5 and 35.2%, respectively, higher average penetration of wear than the conventional mixture.

Aramraks (2006) observed that the mass loss of CBA concrete mixtures containing 100% fine was 3.29 times that of normal concrete. The CBA concrete mixture containing 50% CBA as partial replacement of natural sand and with the use of 2% chemical admixture was the most appropriate concrete mixture concerning both abrasion resistance

and mechanical properties. Yuksel and Genç (2007) detected that chemical and physical properties of CBA affect the resistance to abrasion. The superior usage of CBA as a fine aggregate replacement in concrete, caused the inferior abrasion resistance.

2.13.3 Portland cement pavement blocks by using waste materials

The published literature on utilization of waste materials in producing PCPB is reported. It is assumed that the applicable structure of most coal wastes such as fly ash is useful for fabrication interlocked paving concrete units.

Nishigaki (2000) studied the producing water-permeable blocks (size: $200 \times 100 \times 60$ mm) by using melting slag ashes and shard (slag fly ash) obtained from plasma-melting furnace. They concluded that the heavy metals leaching test by selected elements data was within the environmental soil standard. On mean value, compression property of concrete mixture with shard two-layer block is improved by 37%. This is reported by the fact that the permeable porosity of the shard is so high. While, relative strength is lower with the using shard-based slag ash block that can be assumed as caused by the low affinity between the base and top layers of blocks.

Poon (2002) investigated possibility using recycle residues aggregates such as fly ash with OPC in the production of concrete paving blocks. They concluded that the substitution of such residues waste by natural aggregates at the levels of 25% and 50% had little effect on the strength property of the block specimens, but higher levels of replacement decreased the compressive strength. Using residues as the replacement of natural aggregates at the level of up to 100%, concrete paving blocks with a long curing age compressive strength of 49 MPa could be achieved.

Vinai et al. (2013) produced paving blocks using coal combustion products (CCPs) together with Portland cement and sand. The compaction property was higher about 49

MPa for blocks with proportion of 20% sand, 70% coal combustion and 10% cement after 45 days of curing for all specimens. The produced blocks showed good strength property, and light weight blocks.

Santos et al. (2013) studied the usage of coal waste to produce the concrete paving blocks. Their result shows that the concrete paving blocks with 50% of recycled coal waste in substitution of natural sand had satisfactory results in terms of mechanical strength property.

Ganjian et al. (2015) carried out a research on production environmentally-friendly paving block based-cement incorporated with ash wastes. The optimum concrete paving blocks produced with OPC 7.0% and ground granulated blast furnace (GGBS) 6.3%, meets the minimum requirements of compressive strength about 50 MPa at long curing days.

Singh and Shah (2017) investigated the utilization of cheap by-product such as fly ash as a pozzolanic binder geopolymer in production of interlocking paving block. They found that, fly ash based geopolymer concrete achieved relatively high strength interlocking paving blocks in 70 mm thickness at 7 days.

Overall, the production of PCPB applied for some waste materials such as fly ash and can be applicable for usage CBA as sustainable aggregate in manufacturing interlocked paving blocks.

2.14   Summary

Department of Environment Malaysia has announced scheduled wastes guideline to control the discharging of contaminated wastes. CBA is categorized as scheduled waste, that must be disposed at a licensed treatment plant. It formed in pulverized coal furnaces

that produced from the coal combustion power plants. Ash ponds exist as a huge surface impoundment and used to dispose of the coal ashes. CBA is considered as waste material owing to the blend of toxic elements such as Ni, Cu, Zn, Pb, Ba and Cd which are varying in concentrations depending on originate fed coal. The CBA as partial replacement aggregate in concrete investigated as fresh and harden properties. The workability of CBA concrete was decreased, permeable pore space increased in early age and there was a high-water demand in advanced CBA contents. It is challenging to define the exact water to cement ratio due to the extremely porous structure of CBA which capable to uptake more water then there is water caught inside the CBA through slender maintenance, which does not add to the development of cementitious gel. The water absorption by CBA alters the water required for the workability of the concrete. It acts as an aggregate with high pore size that functions as a reservoir for water in the future hydration of the cement mixtures. However, using CBA as fine aggregate in concrete may reduce the compressive strength at an early age due to the increase in the pore volume of the concrete. After 28 days curing, mixture with CBA up to 30% replacement did not have an adverse effect on compressive strength. The early age mechanical property reduced for CBA concrete compare to control mix without CBA, but strength resulted good improvement at 56 days of curing. Not much work has been reported on the microstructure chemical bonding of CBA in cement mixtures. The CBA disposal landfills are often exposed to open air which cause risk to human well-being and surroundings. Therefore, concern should be taken in the pre-treatment of this waste before they can be considered as a safe material for either landfilling or construction. Solidification /Stabilization (S/S) method is known as a progressively efficient technique to rectify the inappropriate hazardous or toxic material disposal. The principal of this technique is to limit the mobility and solubility of toxic elements through binding them into safe compounds. This procedure is frequently found application in remediation of waste materials because of its practical reduction in

leachability of dangerous elements of huge dumped waste in landfills. Solidification of the residue waste through combination with cementitious materials would be an easy and low-cost method to utilize these materials in application of construction as a sustainable replacement of aggregates. Despite the high potential of CBA in infrastructures, its application is not a common practice in Malaysia. The heavy metals of CBA may have the neutralization effect based on the chemical bonding and interaction cement hydration in the S/S technique. The performance of solidified waste is subjected to the local requirement and USEPA standard which must be achieved prior in utilizing the CBA as sustainable construction application such as paving blocks or safe disposal in landfill areas.

CHAPTER 3: MATERIALS AND METHODOLOGY

3.1 Introduction

Basically, this section presents the selected implementation tests of OPC-based solidified/stabilized specimens and experimental steps that are presented in Figure 3.1and Figure 3.2.

Figure 3.1 shows four main tests to evaluate the efficient performance of solidified/stabilized samples compared with appropriate standard of solidification and stabilization techniques.
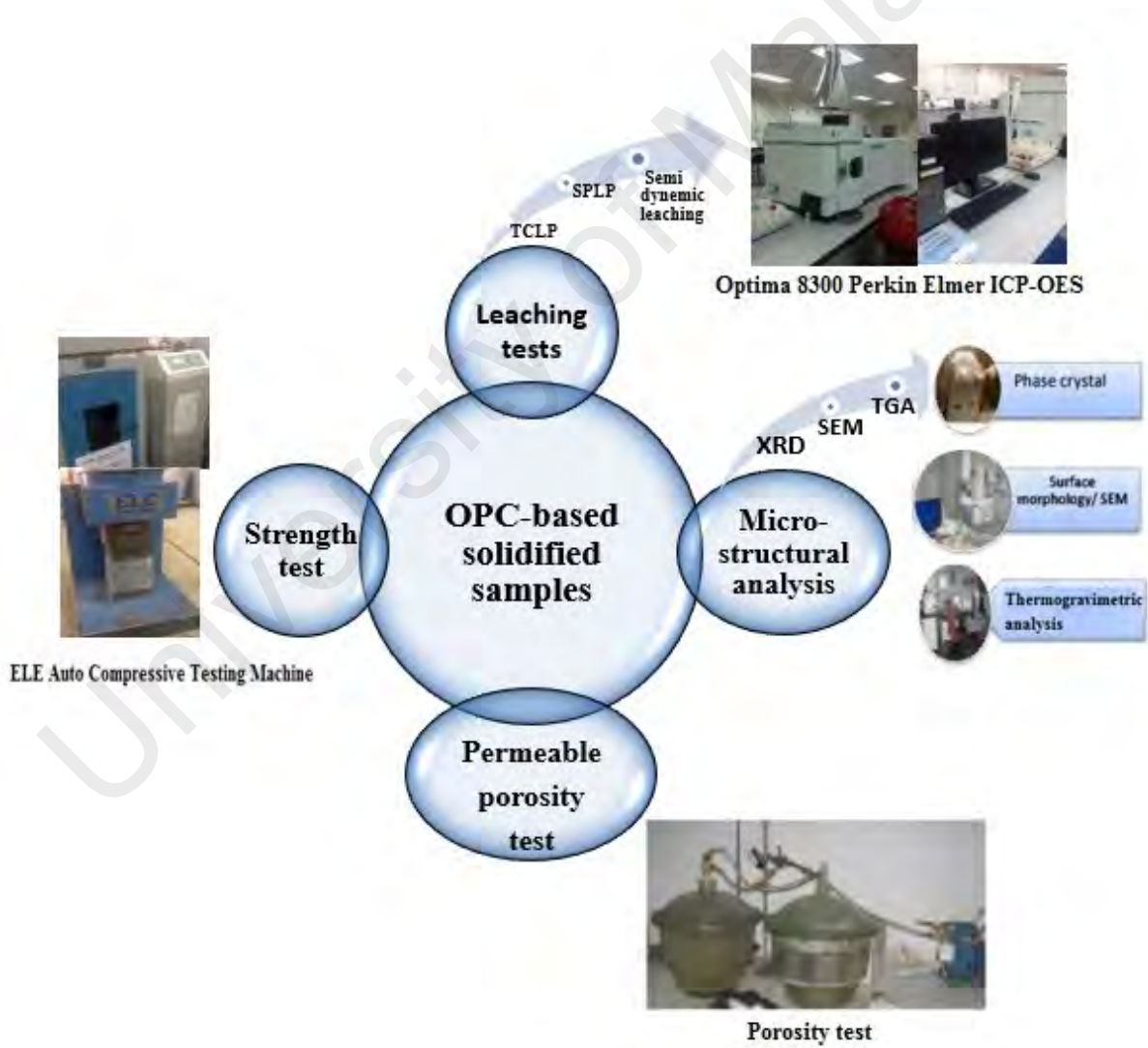
Figure 3.1: Performance tests for OPC based solidified/stabilized samples by S/S technique

Figure 3.2 illustrates five-main series of research experimental. In the first step materials were characterized for its physical, chemical and microstructural properties. Second and third steps were conducted to determine the optimal design mixture of mortar and solidified/stabilized mixtures, respectively. The microstructural properties of normal mixture and composites containing CBA were evaluated in the step four. The application of paving block containing CBA were performed in fifth step.
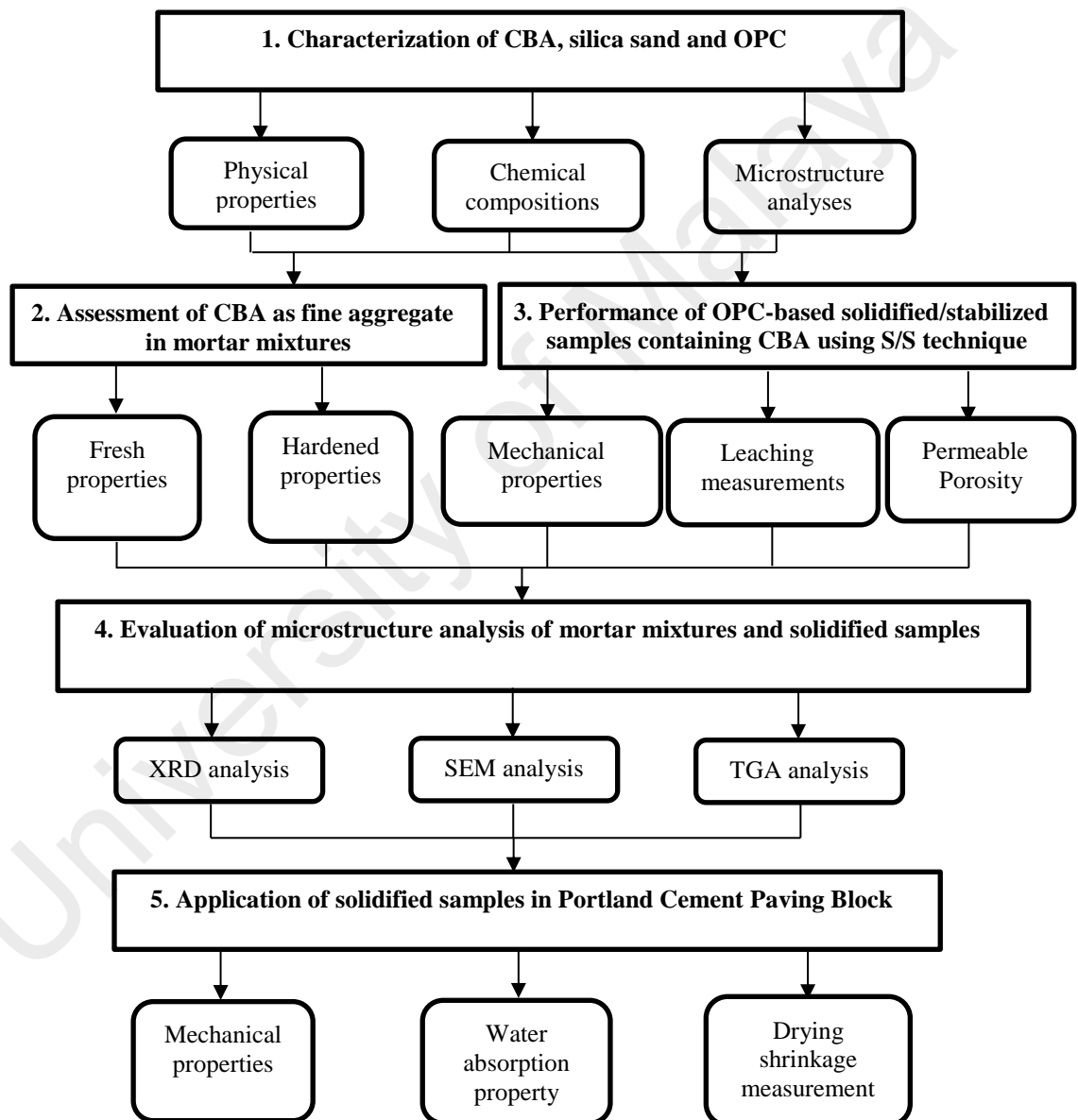
Figure 3.2: Flowchart of experimental methods

3.2   Raw materials

Materials, chemicals and moulds were used in this study are explained as following sections:

3.2.1   Coal Bottom Ash

The CBA used in this research was obtained from a coal-fired power plant (Jimah station) sited in the state of Selangor, Malaysia. It was tagged and kept in a plastic container at room temperature of 28 ˚C.

3.2.2   Silica sand

Silica sand was collected from the local Malaysian facility. The sample kept in a plastic bucket at room temperature of 28 ˚C.

3.2.3   Ordinary Portland Cement

A local Ordinary Portland Cement (OPC) CEM1 was utilized as the main binder in this research. It is complied with the Malaysian Standard specification (MS, 2003a). The OPC was stored in steel drum to preserve from humidity.

3.2.4   Chemicals

A Polycarboxylate Ether, superplasticizer (Sika Viscocrete-2199) was used, to evaluate flowability of CBA mortar mixtures to improve strength property. Merck glacial with 100% purity acetic acid and nitric acid with 65% purity were used as additive chemical in preparation of solution for leaching test in the S/S experimental work. The metal absorption and cleaning of flasks and moulds were done by nitric acid with 65% purity. Decont90 was used to wash contaminated bottles and flasks.

3.2.5   Deionized water

Deionize water was utilized for providing leaching solution and samples of leachability tests.

3.2.6   Moulds

The Perspex cubic moulds with size $50 \times 50 \times 50$ mm used for casting mortar mixture and stabilized leaching samples. The 100×50 mm small steel cylinder moulds used for permeable porosity test of solidified samples. Shrinkage measurement and paving blocks specimens are cast in rectangle Perspex mould with the size of $215 \times 105 \times 65$ mm. All moulds are ringed by Decon90 to remove any contaminated residues.

3.3   Experimental Procedures

The five series of experimental methods: 1. Characterization of CBA, Silica sand and OPC, 2. Assessment of CBA as fine aggregate in mortar mixtures, 3. Performance of OPC-based solidified/stabilized samples using S/S technique, 4. Evaluation of microstructure analysis of mortar mixtures and solidified samples, 5. Application of harden samples in paving block, are explained as following sections:

3.3.1   Characterization of CBA, silica sand and OPC

The raw materials are analyzed for physical properties, chemical compositions, and micro-structural analyses prior main experimental stages as following sections. Characterizations are specific to this type of CBA and cannot necessarily be extrapolated to other type of CBAs. However, water absorption is not chosen as a parameter, and that a specific CBA is used throughout the experimental.

3.3.1.1 Physical properties

Physical properties test presented in the raw materials is as following sections:

(a) **pH value**

The pH of the raw materials was gauged by HI 8417pH meter. 1g dried grounded raw materials was mixed with 9ml of deionized water (pH:7) and stirring at the speed of 150 rpm for 20 minutes. It is then measured pH while the samples are stirred. The triplicate average pH value was recorded.

(b) **Specific gravity and water absorption**

Specific gravity of the raw materials was determined using pycnometer according to ASTM C128-15 standard (ASTM, 2014a). Specific gravity and water absorption were calculated using Equations 3.1 and 3.2:

$$Specific\ gravity= = \frac{A}{[S-(C-B)]} \tag{3.1}$$

$$Water\ absorption_{\%} = \frac{S-A}{A} \times 100 \tag{3.2}$$

Where:

$A=$ Weight of oven-dry specimen in air, *(g)*.

$S=$ Weight of saturated specimen, *(g)*.

$B=$ Weight of the pycnometer filled with water, *(g)*.

$C=$ Weight of pycnometer with specimen and water to calibration mark, *(g)*.

(c) **Moisture content**

In accordance to ASTM C566 - 13 standard (ASTM, 2014b) the CBA, sand and OPC which placed in container were weighed *(M₂)*, and oven dried at 110 ˚C for 24 hours. After oven dried, the samples were cooled down for 1hours, then weighted as *(M₃)*.

As shown in Equation 3.3 the moisture content of samples calculated:

$$Moisture\ content = \frac{M_2 - M_1}{M_3 - M_1} \times 100 \qquad (3.3)$$

Where:

M_1 = Mass of dry container, *(g)*.

M_2 = Mass of container and sample in room temperature, *(g)*.

M_3 = Mass of the container oven dried sample, *(g)*.

(d) Specific surface area

The Brunauer– Emmett– Teller (BET) specific surface areas apparatus based on nitrogen adsorption isotherms using a BELSORP-max. 2g of raw materials samples were oven dried for 24 hours for the test(Ranjbar et al., 2014).

(e) Particle size distribution

The sieve analysis of aggregates was performed using Master-sizers (Malvern Instruments) in accordance to BS 812: part 103 standard (BSI, 1983). The CBA and silica sand were oven dried at 110°C for 24 hours and thereafter cooled down to room temperature. 1000 g of each dried sample was mechanically sieved through a set of sieves starting with 9.5 mm sieve on top, 4.75 mm, 2.36 mm, 1.18 mm, 600 μm, 300 μm, 150 μm, 75 μm and pan at bottom. The material retained on each sieve for each sample was recorded.

3.3.1.2 Chemical compositions

The raw materials were assessed for the leachability of contaminated metal. According to Method 3050B standard (USEPA, 1993). 1g dried grounded raw materials was mixed with 9ml of deionized water (pH:7) and stirring at the speed of 150 rpm for 1 week. It is then placed in a centrifuge at the speed of 6000 rpm to balance the leachant: specimens

mass ratio into 9:1 (g/ml). After all, the leachate was filtered and digested by nitric acid prior to analyzed toxic concentration of metals. It was operated using Nitric acid (HNO_3) 65% method for heavy metals concentrations by Optima 3000 Perkin Elmer Inductively Coupled Plasma mass spectrometry (ICP) test. The triplicate average testing value was recorded. The organic contaminated of CBA was determined by Shimadzu using Gas chromatography Mass Spectrometry, USEPA 3540C, 3570 (USEPA, 1993).

The chemical composition of the raw materials was defined by X-ray fluorescence (XRF) using the PANalytical Axios mAX instrument.

The reactive fraction of silica sand and CBA was studied using a hydrofluoric acid (HF) solution. A similar method was used to quantify the reactionary content of materials in the same nature of CBA such as fly ash (FA) (Ranjbar & Kuenzel, 2017b). About 100 g CBA and silica sand were oven dried at 105˚C for 24 hours. As shown in Equation 3.4, the dried aggregate was then sieved to 200µm. After that, 5 g *(w_0)* of sieved aggregate was dissolved in 500 ml of 1% hydrofluoric acid, and then stirred for 6 hours. After stirring, it was rinsed twice with deionized water and then centrifuged. The weight of aggregate after being centrifuged was denoted as *(w_1)*.

$$W_{Reactivity} = \left(\frac{w_0 - w_1}{w_0}\right) \times 100 \tag{3.4}$$

Where:

w_0 = The initial weight of aggregates, *(g)*.

w_1 = The final weight of aggregates after centrifuging, *(g)*.

3.3.1.3 Micro-structural properties

The 2 *g* of raw materials were oven dried at 105˚C for 24 hours. They were then tested for microstructure analysis as follows:

(a) Pore volume distributions

The pore volume distributions of sample were measured by BET of Quantachrome Autosorb using nitrogen gas based on Langmuir multiple layer adsorptions samples(Ranjbar et al., 2014).

(b) Scanning Electron Microscopy (SEM)

The samples were used for SEM imaging using a Quanta FEG 450 to detect the microstructure of the surface interaction between the CBA, silica sand, and cement particles.

(c) X-ray diffraction analysis (XRD)

The X-ray Diffraction (XRD) patterns were performed using an Empyrean Panalytical diffractometer with monochromated Cu α radiation (λ = 1.54056 Å), operated at 45 KV and 40 MA with a step size of 0.026 deg and a scanning rate of 0.1 deg s^{-1} for 2 hours, at a range of 5–75 deg (Ranjbar et al., 2016b).

(d) Thermogravimetric analysis (TGA)

The thermal stability of the materials was obtained by thermogravimetric analysis using a Mettler Toledo SDTA at a heating rate of 10 °C/min and the specimens were heated from the ambient temperature to 1000 ˚C. The sample was used to measure based on the weight variation as a function of temperature.

3.3.2   Assessment of CBA as fine aggregate in mortar mixtures

The usage of CBA as partial/full replacement of sand in mortar mixtures may influence the final product performance. The main aim of this section is to investigate the effect of the use of CBA as fine aggregate at various percentages (0–100%) on the features of fresh and hardened in mortar mixtures such as flowability, compressive strength, density and total porosity. Furthermore, the utilization of superplasticizer to overcome the high-water demand of CBA based mortar is also studied. Hardened samples were then tested for morphology, compound formation using XRD, SEM, and TGA analysis. To fabricate each specimen, CBA and silica sand were dried at 105°C for 24 hours and sieved in order to achieve particles size 4.75mm and below. Then, the dried CBA, and sand were mixed homogeneously for 7 min in 1- liter SPAR type mixer. Then, 10% water was added. Afterward, cement was added to the paste with the 50% additional water and mixed for another 5 min. The remaining water was then added to those mixtures with the superplasticizer so that a uniform mix could be achieved. The mixtures were then poured into cubic, small cylinder and rectangle block molds. All specimens were prepared in triplicates to average the results. The specimens were covered with damp cloth and kept under ambient conditions for 24 hours; then, the specimens were demolded and cured for 56 curing days in both deionized water tank at an average temperature of 35 °C and humidity of 90%.

3.3.2.1   Fresh properties of mortar mixture

(a) Flowability measurement

Flowability test was conducted to determine the workability of cement paste mixtures. The flow measurement was carried out according ASTM C1437-13 standard (ASTM., 2013). Freshly mixed mortar was poured into a flow mold with a bottom diameter of 10 cm (D_0) on a flow table. The flow mold was then lifted off and the flow table was vibrated.

The mean diameter (*D*) of the resulting flow was calculated using results obtained after conducting the test four times, as follows: the flow *(S)* is the result of an increase in base diameter of the paste *(D)*, expressed as a percentage of the original based bottom diameter *(D₀)* by the following Equation 3.5.

$$S = \left(\frac{D - D_0}{D_0} \right) \times 100 \tag{3.5}$$

(b) ***Bleeding test***

The quantity of mixing water that bleed from a mortar mixture was measured as per procedure in ASTM C232–09 standard (ASTM, 1997). After mixing the ingredients of mortar mixtures, the rectangle Perspex mould having an internal diameter of 235±5 mm and inside height of 65 mm was filled in with the freshly made mixture. The fresh mixture in the rectangle mould was vibrated in three layers. The top surface of the concrete was levelled with the help of a trowel. Immediately after the troweling the top surface of specimen, mass of mould and the mixture was recorded. Stop watch was set on and the mould was covered to prevent the evaporation of the bleed water. The mould was sloped by insertion a chock under its one side and the gathered water at the top surface of the mixture was accumulated with the help of pipette at an interval of 10 min during first 40 min and at 30 min thereafter until ending of bleeding. After the collection of bleeding water, the mould was brought to level position without jarring. The mass of bleeding water, excluding the mass of solids was recorded. Percentage of accumulated bleeding water of net, mixing water contained within the test specimen was calculated as shown in Equations 3.6 and 3.7.

$$C = \left(\frac{w}{W} \right) \times S \tag{3.6}$$

$$Bleeding_\% = \left(\frac{D}{C} \right) \times 100 \tag{3.7}$$

Where:

C = Mass of water in the test specimen, *(g)*.

w= Mass of the total mass of the batch, *(g)*.

W= Mass of the total amount of water, *(g)*.

S= Mass of the sample, *(g)*.

D= Mass of the bleeding water, *(g)*.

3.3.2.2   Harden properties of mortar mixture

(a) Compressive strength test

A compressive strength test was done using ELE Auto Compressive Testing Machine at the rate of 0.9kN/s in accordance with ASTM C109 standard (ASTM, 2005a). The strength test of the specimens was performed after 1, 7, 14, 28 and 56 water curing days.

(b) Density test

The density test was performed by Archimedes' principle at 28 days water curing in accordance with ASTM C-20 standard (ASTM, 2015). The test procedure was first done for suspended and soaking conditions and then for dried condition of specimens. The saturated and suspended weight measured after 2 hours boiling was followed by immersing specimens under deionized water in vacuumed condition for 24 more hours; to obtain the dry weight, the specimens were kept in an oven at 105 °C for 24 hours more hours to remove the moisture and obtain the dry weight (Ranjbar et al., 2016b).

3.3.2.3 Microstructure analysis of CBA mortar mixture

The hardened matrix pieces were manually crushed for 2g after 28 days of water curing. They were then tested for pore volume distribution, SEM, XRD and TGA analyses as mentioned details of apparatus type were used in section 3.3.1.3 (a), (b), (c) and (d).

3.3.3 Performance of OPC-based solidified/stabilized samples

Performance of cement-based solidified samples applied by main physical and chemical tests. The tests are in accordance with the USEPA, S/S handbook standard (USEPA, 1993). Significant implementation tests contain permeable porosity, strength and leachability mechanisms of solidified samples.

The solidified/stabilized samples were directed by a series of important performance tests to access for full-scale handling to judge for effectiveness of selected OPC as a main binder.

The OPC was added to the control hydrated OPC mixture or (OPC/CBA) mixture ratios of 0.5, 1, 1.5 and 2. The dried CBA and OPC were homogenized in a 1- liter SPAR type mixer for 5 min prior to the adding of deionized water in the W/C ratio of 0.55. The OPC/CBA mixture was then mixed at high speed for 6 minutes to become homogenous. The mixtures were cast in three layers into 50 mm Perspex moulds cubic for compressive strength and leaching measurements. The mixture was compacted by using a vibrating table. Then, the specimens were covered by damp fabric in the laboratory for 24 hours. After which, they were demolded. The samples were kept in a cabinet for 56 air curing days in a relative humidity of 90% and temperature of 30˚C.

3.3.3.1 Setting time of solidified mixtures

The initial and final setting times of OPC/CBA mixture were evaluated according to the ASTM C 191 - 04b using Vicat Needle. The initial setting time was determined as the required time for 25 mm penetration and the final setting time as the total time elapsed until the needle stop completely at the paste surface (ASTM, 2005c) .

3.3.3.2 Mechanical properties of solidified samples

Bulk density was measured by Archimedes' principle after 28 days air curing in accordance with ASTM C20. The strength test of the samples was performed after 1, 7, 14, 28, and 56 air curing days which complied with ASTM C109. Details of apparatus type were used as mentioned in section 3.3.2.2 (a) and (b).

3.3.3.3 Leachability of solidified samples

The solidified samples were analyzed for assessment of possible leachability of selected contaminated heavy metals. According to crash block leaching, and whole block leaching methods.

Crash block leaching (CBL) is performed under two methods: Toxicity Characteristic Leaching Procedure (TCLP) and Synthetic Precipitation Leaching Procedure (SPLP) methods (USEPA, 1994b, 1994a). They are based on simulating the worst leaching case conditions through landfill and catchment areas and leaching solution that simulated acid rain respectively. The TCLP test regulates the impact of CBA as toxic waste in groundwater even when the CBA is disposed in non-landfill conditions or using as sustainable material in construction fields (Yin et al., 2007).

In terms of TCLP test, 50 g of manually crushed specimens were placed in low-density polyethylene (LDPE) containers. Then, leaching solution of acetic acid (pH=2.88) and deionized water (PH=6.80) were added in two separate containers to provide a ratio of 20:1 mass ratio of leachant to specimens (Table 2.8). Then leachate samples were agitated using a shaking extractor at 30 rpm for 18 hours. Subsequently, leachate specimens were filtered through vacuum filtration using a 0.45 mm membrane filter (USEPA, 1986; Yin et al., 2007). The filtrate was then acidified with nitric acid 65% to pH<2 and stored under refrigeration (<4 ˚C) prior to heavy metal analysis The SPLP test was slightly different

from the TCLP as it required a leaching solution of nitric acid (pH = 4.20) while other attributes remained the same. All TCLP and SPLP investigation were completed on sample triplicates and average values were used. The whole block leaching (WBL) was evaluated to ascertain the leachability of heavy metals from the uniform solidified blocks subsequent to 56 days. The term semi-dynamic refers to the leachant being substituted sporadically after intermissions of static leaching (Sri Bala Kameswari et al., 2001). Moreover, semi-dynamic leaching test was based on the solution renewal period for solutions which was added into the leaching system to enable the rate of acid penetration to stay at a moderately constant speed (Figure 3.3). Apart from modified renewal solutions (acetic acid and deionized water), all other aspects of the testing remained the same. The schedule of leaching test of this study is shown in Figure 3.4.

The leaching concentration after stabilization, (L_r), is calculated by the total leaching concentration of 56 days, (L_{sum}), over the initial leaching, ($L_{initial}$) and reported in percentage format as in Equation 3.8.

$$L_r = \frac{L_{sum}}{L_{initial}} \times 100 \tag{3.8}$$
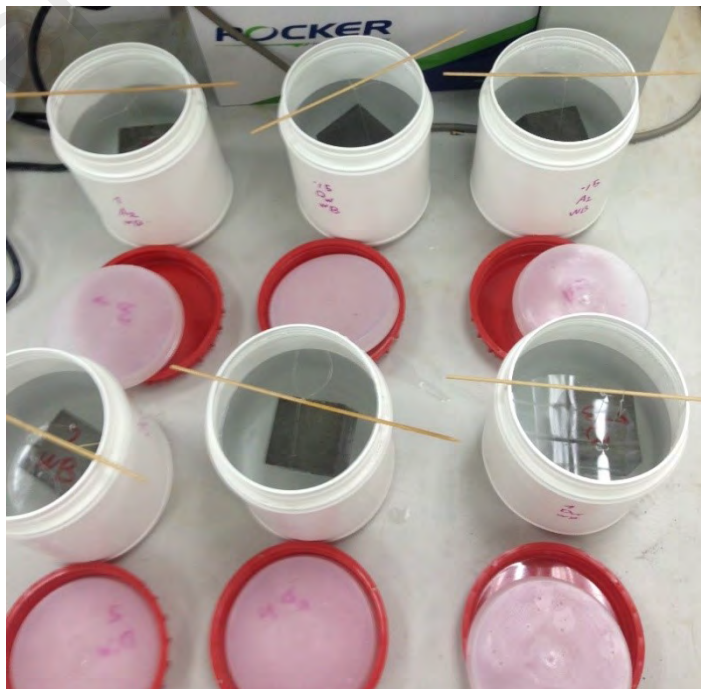
Figure 3.3: Semi-dynamic leaching test
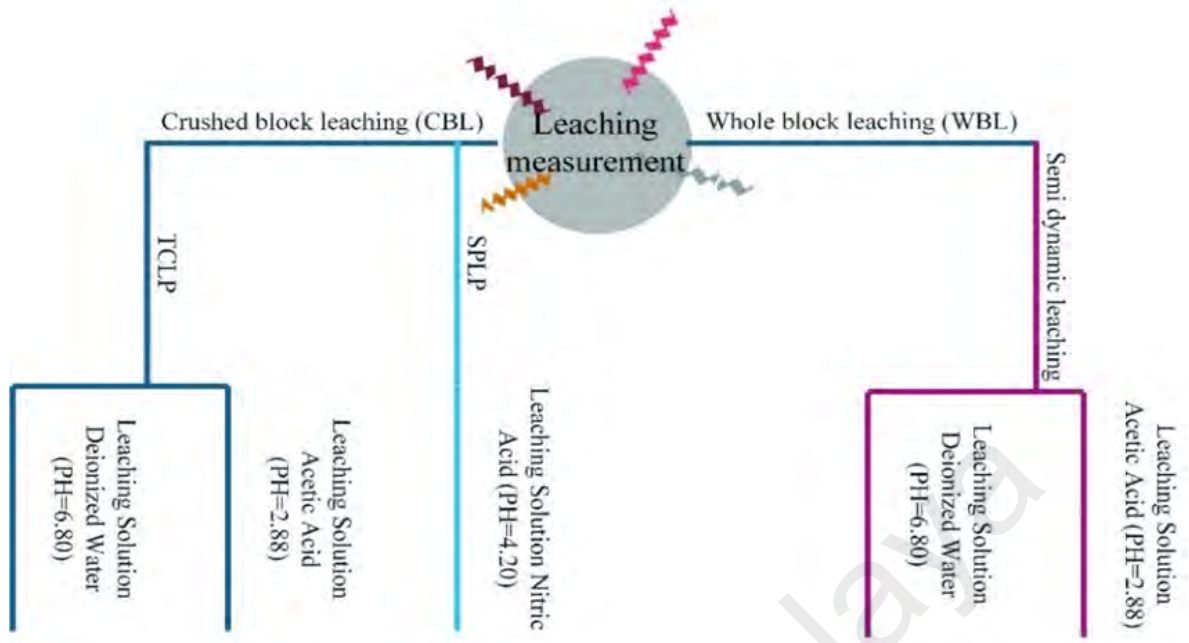
Figure 3.4: Schedule of leaching measurements

3.3.3.4 Permeable porosity of solidified samples

Three saturation wet, boil and vacuum method were used to define the permeable porosity of harden samples (ASTM, 2005b; Safiuddin & Hearn, 2005). Triplicate 100×50 mm small cylinder specimens with volume of 785 cm^3 were tested at 28 curing days. As shown in Equation 3.9 the permeable porosity was calculated based on concept of weight gain due to water absorption and weight loss because of floating.

$$Permeable\ Porosity = \left(\frac{W_C - W_A}{W_C - W_F}\right) \times 100 \tag{3.9}$$

Where:

W_F = The floating weight of the specimen in water, *(g)*.

W_A = The oven-dried weight of the specimen in air, *(g)*.

W_c = The weight of the saturated surface-dry of the specimen in air, *(g)*.

71

3.3.3.5 Microstructure analysis of Solidified samples

The hardened matrix pieces were manually crushed for 2g powder sample after 28 air-curing days. They were then tested for SEM, XRD and TGA analysis as mentioned details of apparatus type were used in section 3.3.1.3 (b), (c) and (d).

3.3.4 Application of harden samples in Paving Block

The paving blocks were designed as substitution of silica sand mixtures, in ranges of 0% -100% with increments of 20%. Their main technological requirements included optimization of particle size distribution of materials, mechanical properties, drying shrinkage measurement, and water absorption. The productivity of paving block samples was evaluated in accordance with selected parameters stated in ASTM C936 as following sections (ASTM, 2016).

3.3.4.1 Abrasion resistance test

The Dorry abrasion machine was applied to assess the abrasion. The test was carried out essentially in accordance with BS 812 Part 113 standard (BSI, 1993). The abrasion value measured based on the volume loss during the abrasion test. Tests were performed on average of triplicate specimens at the curing age of 28 and 56 days. Cube specimens with a 50-mm diameter and 50 mm thick were prepared and cut into two. Cut surface was used for abrasion measurements. During this investigation, Leighton Buzzard silica sand which complies with BS 812 standard was used as the abrasive criteria assessment.

3.3.4.2 Drying shrinkage measurement

The block mould size $210 \times 105 \times 65$ mm were prepared to measure the drying shrinkage after one day demoulded. After 24 hours of oven-dried at a temperature of 105 °C, the specimens were taken out from the oven and Demec points fixed to the surfaces

of the specimens by using Araldite 5-minute AB Epoxy adhesive. To measure the variation of shrinkage over time a Mitutoyo Absolute Digimatic Indicator ID-C112B apparatus was used with the range and resolution of 12.7 mm and 0.001 mm, respectively. Figure 3.5 shows the shrinkage measurement tools used in this study. Drying shrinkage of paving blocks was measured as per ASTM C 157-03 standard (ASTM, 2004; Ranjbar et al., 2016b).The length of rectangle block was recorded as initial comparator reading for period of 56 days and specimens were stored in the drying room. The length change at any age after initial reading was calculated as Equation 3.10.

$$\Delta L_\% = \frac{L_2 - L_1}{G} \times 100 \tag{3.10}$$

Where:

$\Delta L_\%$ = The length change of specimen at any age, *(%)*.

L_2 = The difference between the comparator reading of the specimen at any age, *(μm)*.

L_1 = The initial comparator reading of the specimen at any age, *(μm)*.

G = The gauge length, *(200 μm)*.

Figure 3.5: Drying shrinkage measurement

3.3.4.3 Water absorption test

The specimens were tested for water absorption at 28 and 56 curing days in accordance with ASTM C642 standard (ASTM, 2005b). The specimen was oven dried at 110 ˚C for 24 hours. After removing specimens from the oven, they are allowed to cool down in dry air for 5 minutes to determine the dried mass *(A) (g)*. Then, immerse the specimen in water at 21 °C for 2 hours. After immersion, the samples were surfacing-dried by towel to remove surface moisture and the surface-dry mass *(B)(g)* is weighted. The Equation 3.11 was used to calculate the absorption percentage.

$$Water\ absorption\ _{\%} = \left[\frac{B - A}{A}\right] \times 100 \qquad (3.11)$$

3.4 Summary

This chapter describes the general experimental techniques employed in this research project. The physical, chemical properties and micro- structural analysis (XRD, SEM, TGA) of the raw materials are studied. The effect of CBA as replacement of fine aggregate on properties of mortar mixtures are evaluated in terms of fresh and harden properties and microstructural analysis. The assessment is based on the effect of CBA as replacement of sand on properties of crystalline phases with cement paste mixtures. Moreover, comprehensively investigates the S/S technique of CBA using ordinary Portland cement (OPC) as the main binder of mixture according to USEPA S/S handbook standard. Besides, the strength and microstructure properties of their solidified/stabilized samples were analyzed based on changes in crystalline phases (XRD), morphology (SEM), and thermal characteristics (TGA), porosity and density. In addition, main parameters for manufacturing the paving block to explore the capabilities usage of such waste material which can be successfully applicable as sustainable construction material.

CHAPTER 4: RESULTS AND DISCUSSIONS

4.1 Raw materials Characterization

Characterization of the CBA, silica sand and OPC in the mortar mixtures and final solidified/stabilized products were analyzed for physical, chemical and micro-structural features. These properties may impact on final product paving application. The physical properties of raw materials such as pH, water absorption, specific gravity and specific surface area were analyzed. The chemical composition affects the chemical bonding in the cement hydration and final products in such a way that it will influence the contaminated heavy metals released in leaching and mechanical property. Micro-structural analysis will present the surface of raw materials morphology, crystalline phases and loss weight of raw materials.

4.1.1 Physical properties of raw materials

OPC (CEM1) was used as the main binder. The cement was supplied by local Malaysian manufacture. The average size of cement is 4992.33 nm with specific surface area 3.89 m^2/g. The binder property is important for designing the mixture proportion. This can have significant effect on the strength. The practical validation for its selection was due to the fact that configuration of OPC was much more reliable, thus removing some of the many metal elements in studying chemical stabilization and capsulation processes (USEPA, 1993; Yin et al., 2007). Summary of binder's physical properties are given in Table 4.1.

Table 4.1: Physical properties of OPC

Physical Properties	OPC (binder)
Specific gravity	3.15
Density (kg/m^3)	2870
Setting time- initial (min)	125
Setting time- Final (min)	175

The average pH value for CBA, silica sand and OPC measured by pH meter was almost alkaline range of 12,11.5, and 12 at room temperature of 26.0 ˚C, respectively. Specific gravity of the CBA and silica sand was 1.80 and 2.60, respectively. Water absorption value for the CBA and sand was 2.77 and 1.98 g/cm^3, respectively. Moisture content for the CBA was 13% and 3% for silica sand. The specific surface area of fine aggregates was 1.05 and 0.80 m^2/g for CBA and silica sand, respectively. Because the larger surface area of the fine aggregate higher water requirement was needed and CBA perform as reservoir water contents. The BET surface charge may give a direct effect on the hardened samples properties. These specifications are in agreement with other research work as mentioned in section 2.3.

The particle size distribution of fine aggregates and binder is illustrated in Figure 4.1and Figure 4.2. As shown in Figure 4.1 Both particles are almost similar in size distribution for fabrication of mortar samples. CBA contains 70% particles finer than 1.18 mm as compared to silica sand. Particle sizes coarser than 1.18 mm in silica sand is 8% more than that in CBA.

The particle size distribution of the ground CBA and OPC is shown in Figure 4.2. The production of OPC-based CBA solidified samples need to achieve ground particles size of 2 mm and below to homogenized particles distribution. This is achieved by grinding in a Los Angeles abrasion machine for 30,000 cycles. The mean grading particle size for CBA and OPC were 32.53 and 127.45 µm, respectively. Details of data for the particles distribution of raw materials are given in Appendix A (Table A-1).
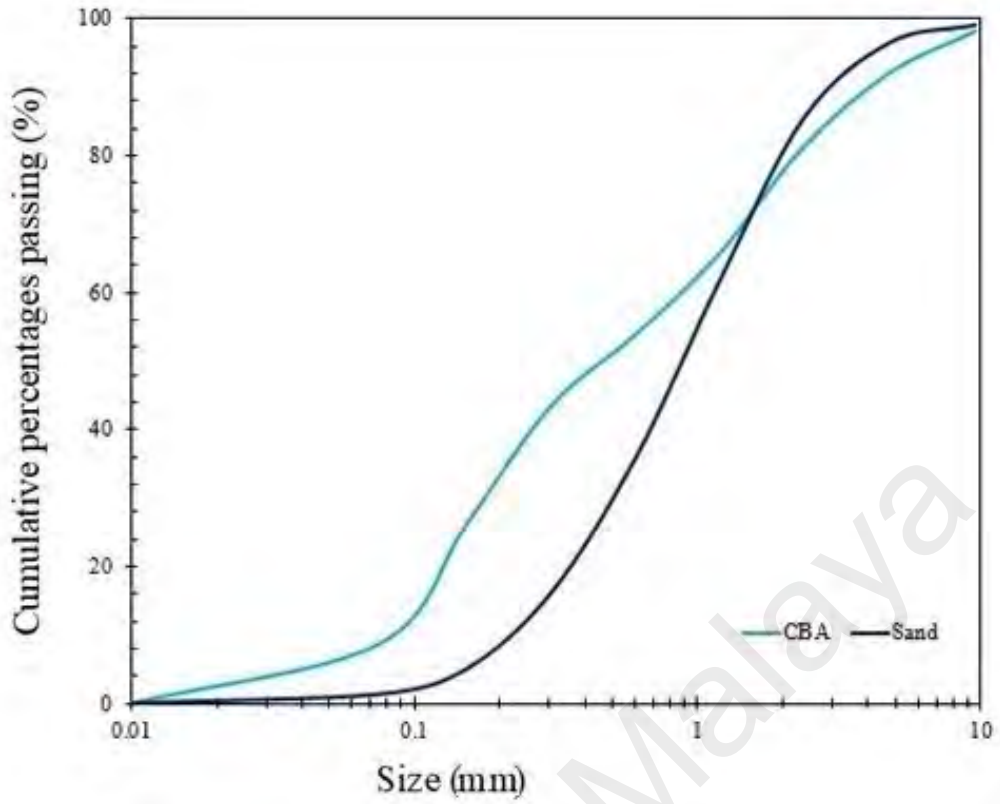
Figure 4.1: Sieve analysis of fine aggregates
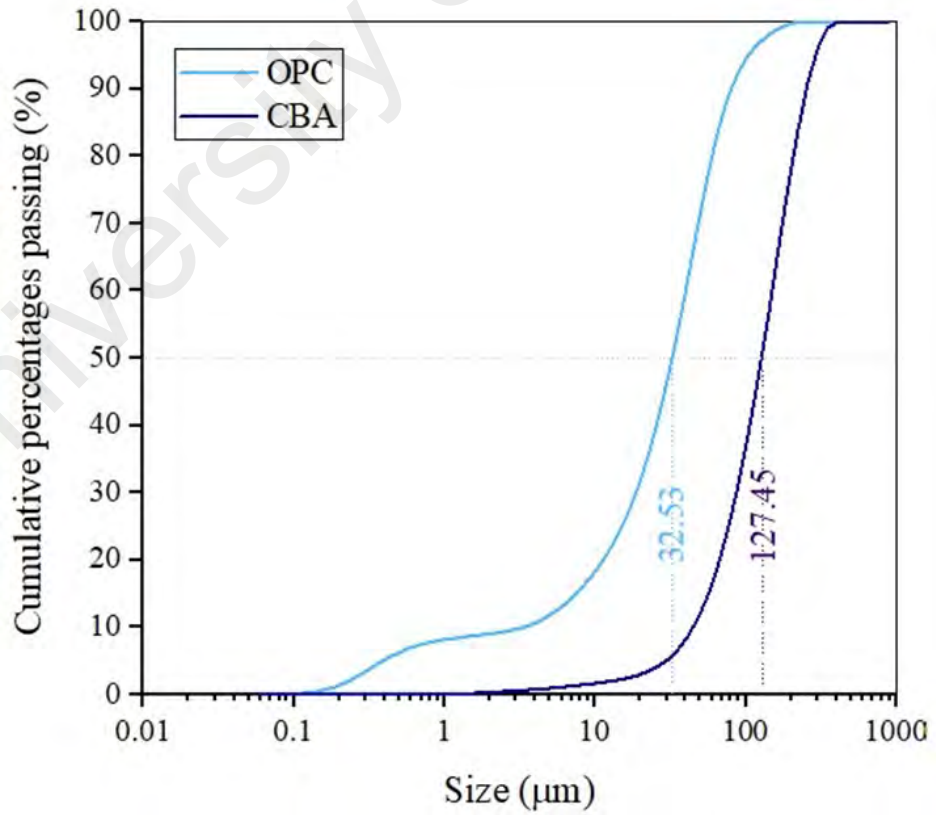
Figure 4.2: Particle size distribution of the ground OPC and CBA

The raw materials in powder form are depicted in Figure 4.3. The CBA collected is dark black in colour due to the coal combustion at the bottom of the furnace, while silica sand is lighter in colour.
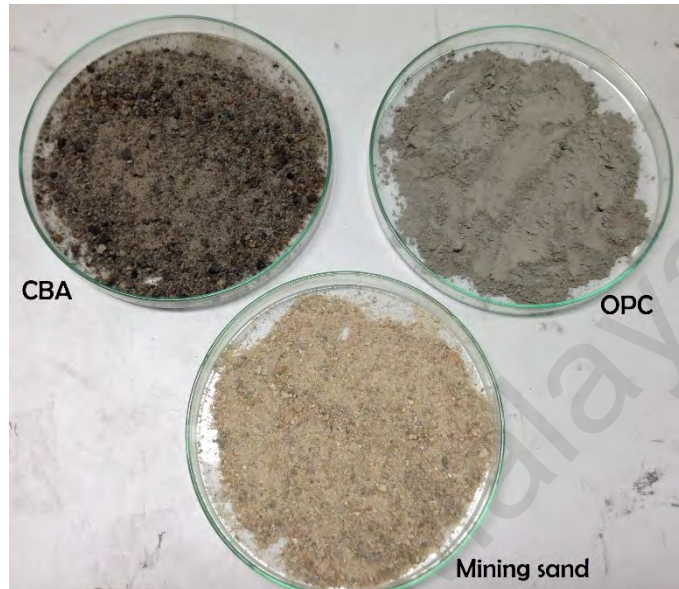
Figure 4.3: Raw materials in powder forms

4.1.2 Chemical composition of raw materials

The chemical oxide compositions of raw materials are presented in Table 4.2. The characterization of OPC as a main binder was important in the research. It controlled interaction with the chemical bonding CBA and creating satisfactory monolith final products. OPC consists mainly of 82% composition of SiO_2 + CaO. The MgO formed 2.60% of the total oxide and the remaining alkalise are derived in form of K_2O (0.32%) and N_2O (0.07). As shown in Table 4.2 CBA and silica sand are rich in silicon dioxide. CBA has significantly high composition of iron oxide of about 10.93% while it is less than 1% in silica sand. The composite oxide of SiO_2 + Al_2O_3 was at 78.05% for CBA, while it was 96.33% in silica sand. The LOI value was marginally higher for CBA than silica sand (Mehta & Monteiro, 2006).

Table 4.2: Chemical compositions of raw materials

Chemical composition (wt.%)	CBA (%)	silica sand (%)	Ordinary Portland Cement (%)
SiO_2	50.49	91.99	16.96
K_2O	0.82	0.99	0.32
Fe_2O_3	10.93	0.54	3.68
CaO	4.19	0.14	65.12
P_2O_5	0.24	0.03	0.05
MgO	1.24	0.13	2.60
Al_2O_3	27.56	4.34	3.36
SO_3	0.10	0.02	4.04
TiO_2	2.23	0.44	0.15
Na_2O	0.57	0.17	0.07
MnO	0.08	0.03	0.18
SrO	0.12	0.00	0.02
ZrO_2	0.11	0.04	0.01
LOI	1.11	1.04	3.38

The heavy metals concentration leachates of raw materials were analyzed to discover its interaction to stabilized OPC-based final hardened products. These heavy metals may affect the stabilized samples.

As a result, it is very important to recognize the heavy metals to forecast potential chemical bonding reactions occurred during setting of cement paste, which subsequently will influence the mechanical and leachability properties of the stabilized samples. CBA has significant inorganic heavy metals of copper, cadmium, nickel, and lead of 2.66, 0.07, 0.34 and 0.20 (mg/l) respectively (Table 4.3). The concentration values for the dominant contaminated elements of Cd, Cu, Ni and Pb in CBA particles exceeded by 6%, 12%, 5% and 5% the Malaysian Environmental Quality Act standard, respectively (Figure 4.4) (EQA, 1979). While the other elements were below the toxic limit concentrations and acceptable for discharging in landfills or catchment areas. Nevertheless, the cement and silica sand itself does meet criteria for the metal contents (Table 4.3). CBA is considered as dangerous material owing to the blend of toxic elements such as Ni, Cu, Zn, Pb, Ba

and Cd which are varying in concentrations depending on originate fed coal (Anastasiadou et al., 2012; Rafieizonooz et al., 2016; Ranjbar & Kuenzel, 2017a). OPC has considerable amount of aluminum 9.66 (mg/l) which is less than the limit in Malaysian standard (EQA, 1979; MS, 2003a). The highest metal concentration of Fe belonged to OPC and CBA of 0.9856 and 0.9112 (mg/l) respectively.

Organic content measurements in CBA are the focus as the waste contains semi volatile organic carbon (SVOC), Pentachlorophenol Herbicides, volatile organic carbon VOC, Trichloroethylene, Pesticides and Polychlorinated biphenyls (PCBs). These compounds have been acknowledged to interfere with Portland cement hydration (Conner, 1990). Their concentrations did not exceed the limit regulated by Malaysian standard (Table 4.4) (EQA, 1979).

Table 4.3: Inorganic heavy metals analysis of raw materials

Inorganic elements	CBA (mg/l)	OPC (mg/l)	Silica sand (mg/l)	Malaysian standard (A) (mg/l)
Al	2.1856	9.668	0.4804	10
Cd*	0.07156*	0.00187	0.00	0.01
Cr	0.1984	0.00301	0.00	0.2
Cu*	2.6644*	0.00164	0.00	0.2
Fe	0.9112	0.9856	0.7568	1
Mn	0.12504	0.03709	0.00	0.2
Ni*	0.3436*	0.0014	0.00	0.2
Pb*	0.20324*	0.0050	0.00	0.1
Zn	0.98102	0.0412	0.00	1

* selected elements
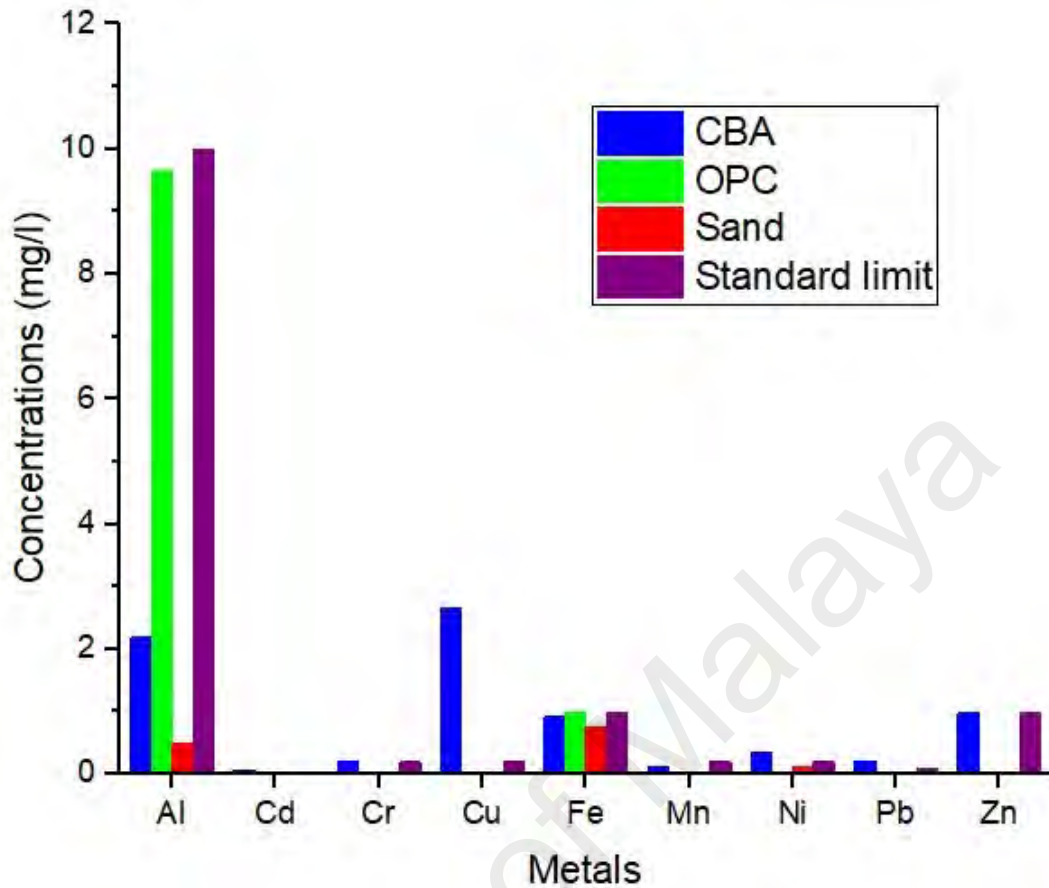
Figure 4.4: Metal concentrations in raw materials and Malaysian Quality Act standard

Table 4.4: Organic contents analysis of CBA

Organic elements	CBA (mg/l)	Malaysian standard (A) (mg/l)
SVOC, Pentachlorophenol	0.002	1
Herbicides	0.001	1
VOC, Trichloroethylene	0.009	0.5
Pesticides and PCBs	0.004	0.5
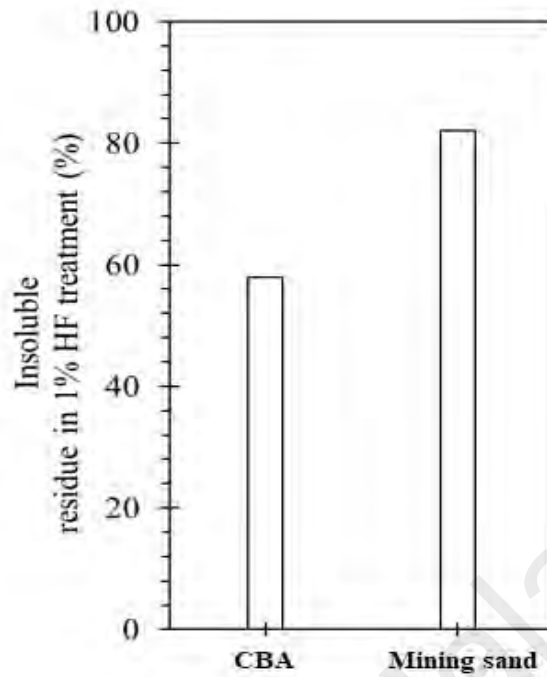
**Figure 4.5: The reactive fraction measurement of CBA
and silica sand**

Figure 4.5 shows the reactive fraction of CBA and silica sand. When the material was exposed to hydrofluoric (HF) acid for 6 hours, almost 40% of the CBA dissolved, while a large volume of silica sand remained undissolved. This is attributed to the vitreous fractions of the CBA. Similar quantifications were reported to evaluate the reactive fraction of fly ash (Aughenbaugh, 2013; Ranjbar & Kuenzel, 2017b). Although the dissolvable fraction of CBA is much lower than FA, this could be beneficial for OPC based composites and provides stronger interaction compare with that of silica sand.

4.1.3   Micro-structural analysis of raw materials

The SEM, XRD and TGA analysis of binder and fine aggregates report as following sections:

4.1.3.1 SEM analysis

The SEM morphology of the OPC powder resembles that the sample consists of angular particles as shown in Figure 4.6. The OPC particles have specific surface area of 3.89 m^2/g

which is slightly higher than its micro-pores of 3.54 m^2/g. OPC has a total pore volume of 0.0102 (cm^2/g) with average pore size of 105.0 (Å).

In Figure 4.7, the particles of CBA are porous and irregular in shape and have rough texture. Some disordered shape particles are also presented in CBA micrograph (Figure 4.7b). CBA particles with porous characteristics are lighter and stiffer. The CBA particles are easily degraded under compression and this reduces the mechanical properties of specimens containing them (Singh & Siddique, 2014). The CBA has considerable porosity which increases the risk of higher water absorption and corresponding leaching.
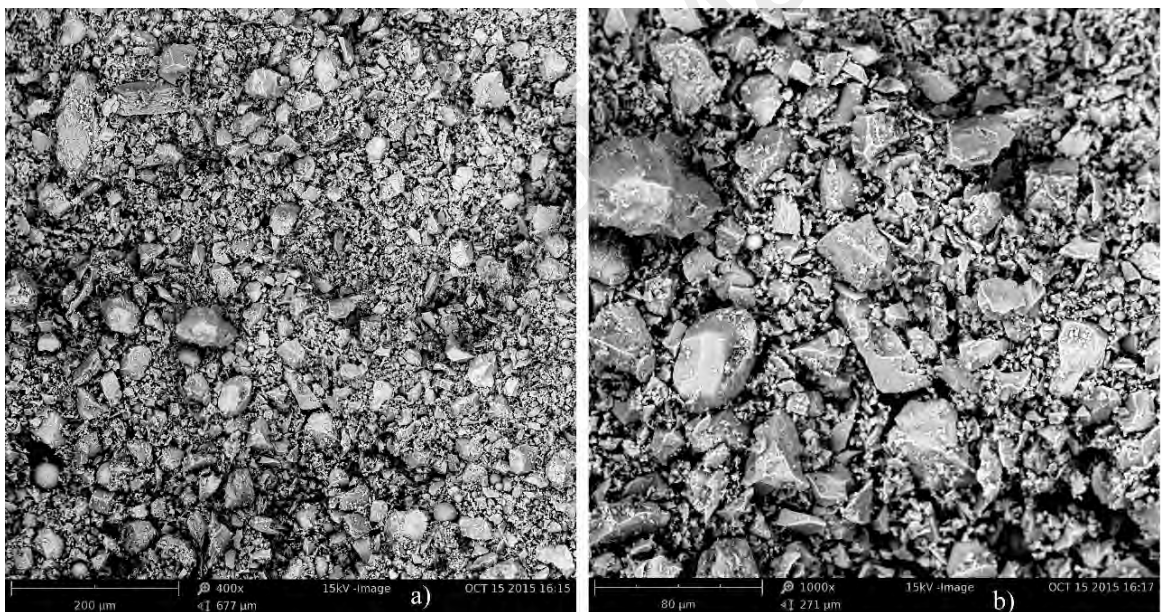
Figure 4.6: Micrographs of OPC at (a) 400x and (b) 1000x
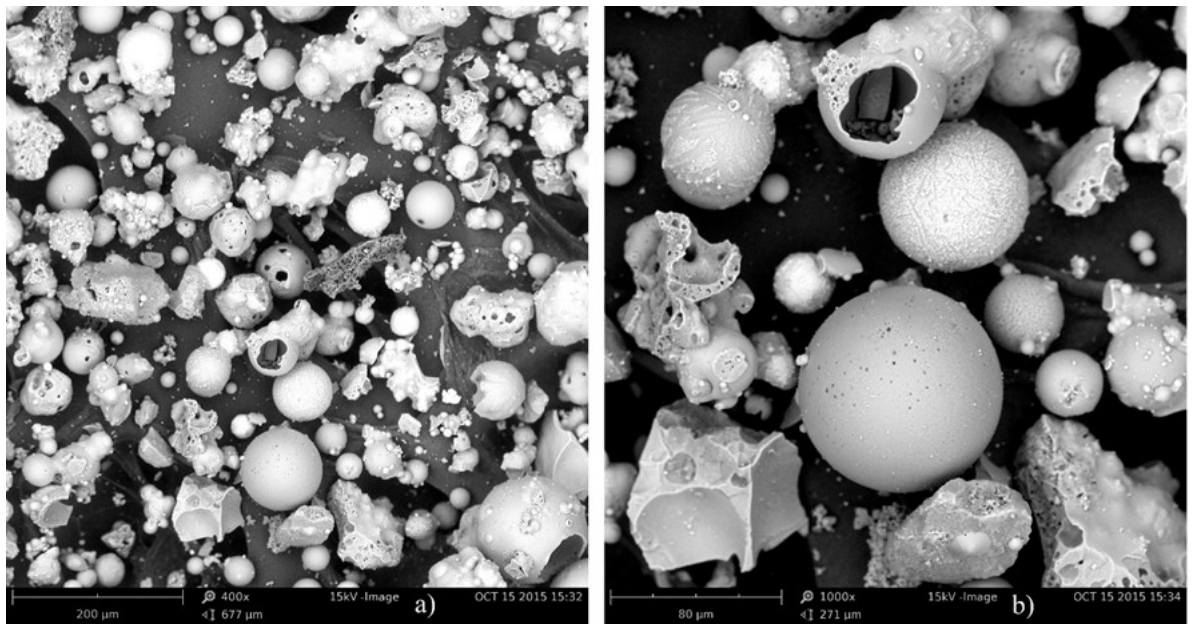
Figure 4.7: Micrographs of CBA at (a) 400x and (b) 1000x
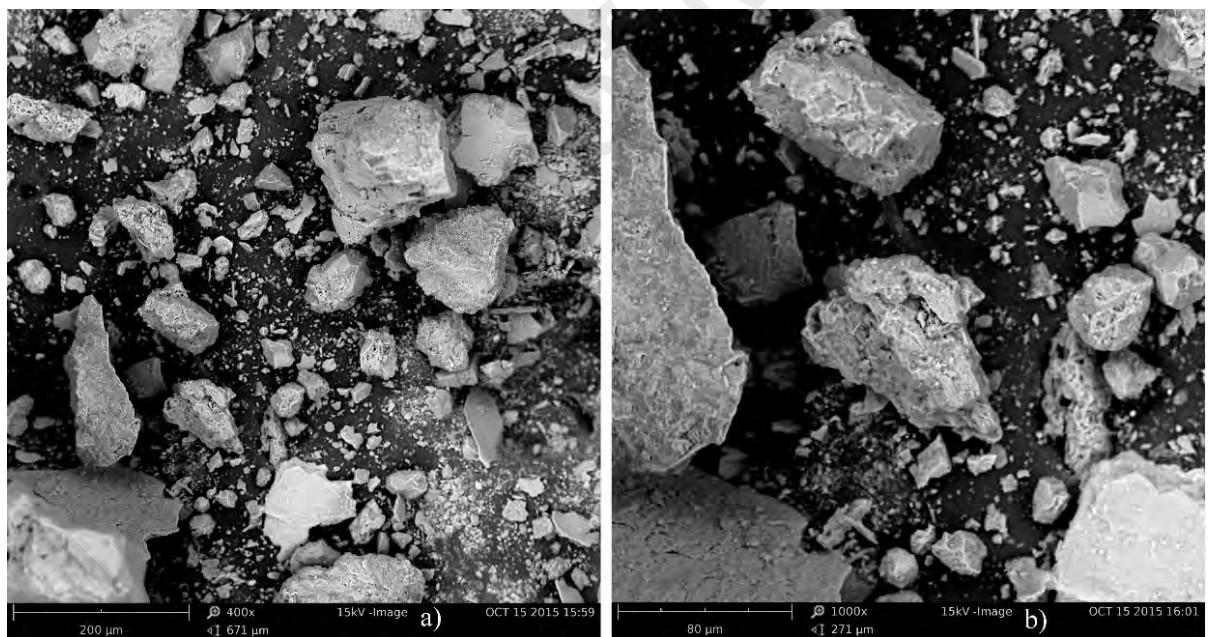
Figure 4.8: Micrographs of silica sand at (a) 400x and (b) 1000x

As shown in Figure 4.8, silica sand particles are angular in shape compared to those of CBA which have porous structures with disordered spherical shapes.

Figure 4.9 presents cumulative distribution of pore volume and pore area of CBA and sand. The highest pore volume belongs to CBA particles (3.8×10^{-4} m^2/g) compared to silica sand particles (1.2×10^{-4} m^2/g). The maximum pore area for CBA and silica sand are 0.030, and 0.015 (m^2/g), respectively. The CBA contains higher porosity, which provides a high potential for water retention and thus flowability of mixtures. In contrast, the smaller particle size of CBA, compounds the situation leading to the use of extra water to lubricate the particles (Singh & Siddique, 2016).
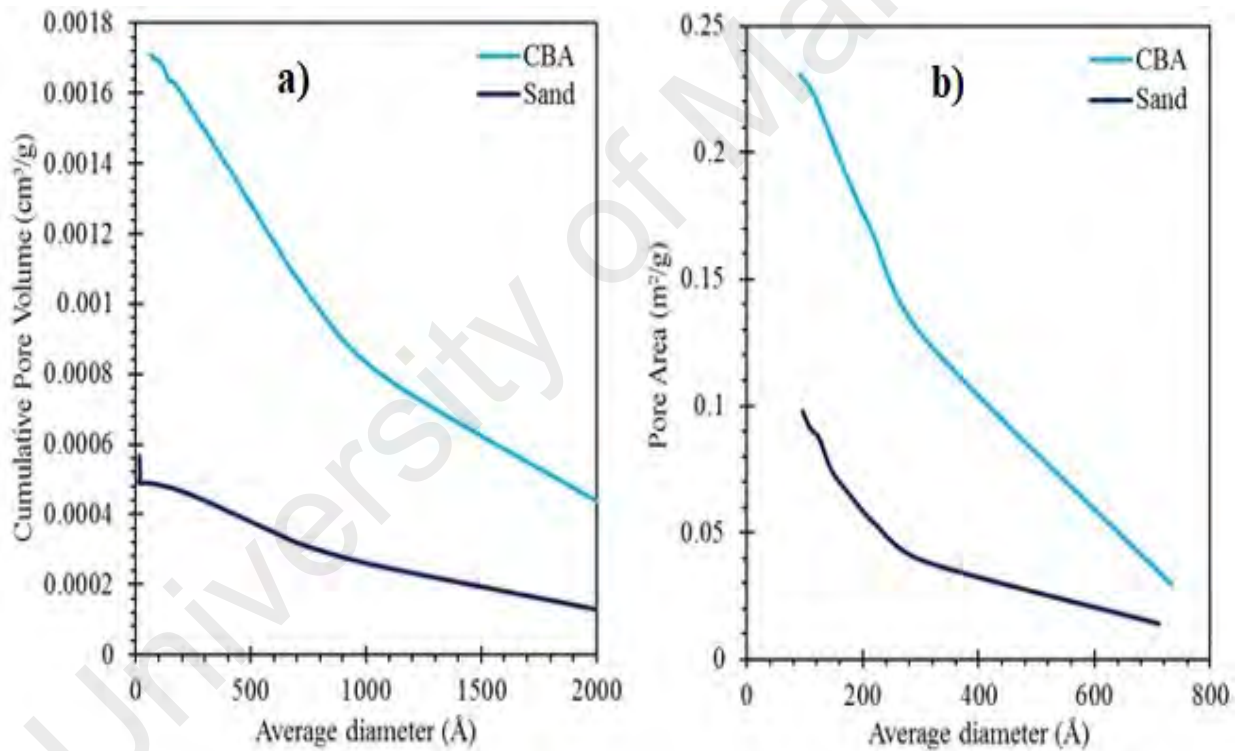
Figure 4.9: Cumulative distribution of a) Pore volume and b) Pore area of CBA and silica sand

4.1.3.2 XRD analysis

The X-ray diffraction (XRD) analysis of OPC as the main binder is presented in Figure 4.10. The strong mineral peaks in Portland cement are Alite and belite. They are in triclinic and monoclinic shapes, respectively. While, minor mineral peaks in the OPC are tricalcium aluminate, calcium aluminum iron oxide and calcium sulfate hydrate. The pozzolanic activity of OPC is normally associated with presence of $Ca(OH)_2$ or portlandite which, was presented. However, the OPC shows the major crystalline structure of tricalcium silicate, dicalcium silicate, calcium sulfate hydrate and calcium aluminum iron oxide.
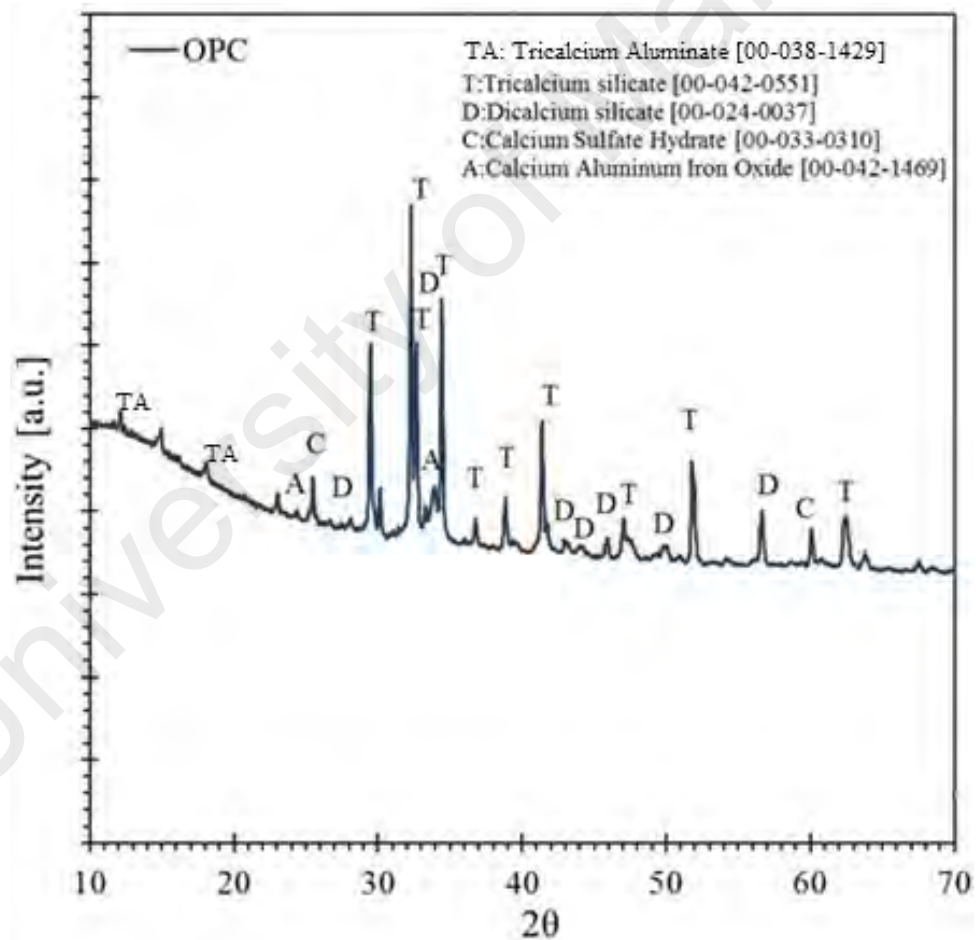
Figure 4.10: XRD pattern of OPC binder

The X-ray diffraction (XRD) analysis of CBA and silica sand is illustrated in Figure 4.11 (a) and (b). As shown in Figure 4.11a, the XRD pattern of the silica sand is quartz type, while the CBA is mostly mullite with only a trace of quartz (Figure 4.11b). However, the hump at about 18 to 32 2θ in the XRD pattern of CBA associated with glassy phases.
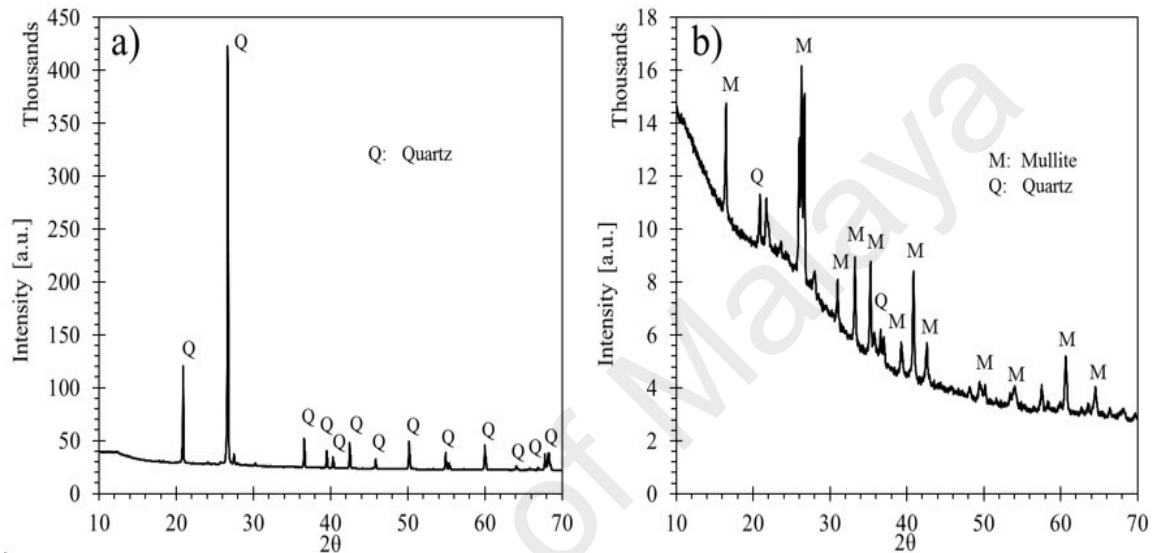
Figure 4.11: XRD patterns of a) silica sand and b) CBA

4.1.3.3 TGA analysis

Thermogravimetry analysis (TGA) was used to investigate the chemical and physical properties of materials during heating by measuring the mass loss of the samples. Weight loss was measured as specimens were exposed to gradually increasing temperatures. The thermal gravimetric analysis of the OPC is shown in Figure 4.12. The total weight loss of OPC is around 32.5 to17.5 wt.%. Moreover, the OPC binder with LOI >3% has significantly larger mass decomposition at temperature of 600 to 1000 ℃. The thermal gravimetric analysis of the CBA and silica sand, is shown in Figure 4.13. The CBA and sand have insignificant weight loss of around 0.6 and 0.9 wt.%, respectively. It also corresponds to the water loss physically adsorbed or contained inside the pore structure in the case of CBA.
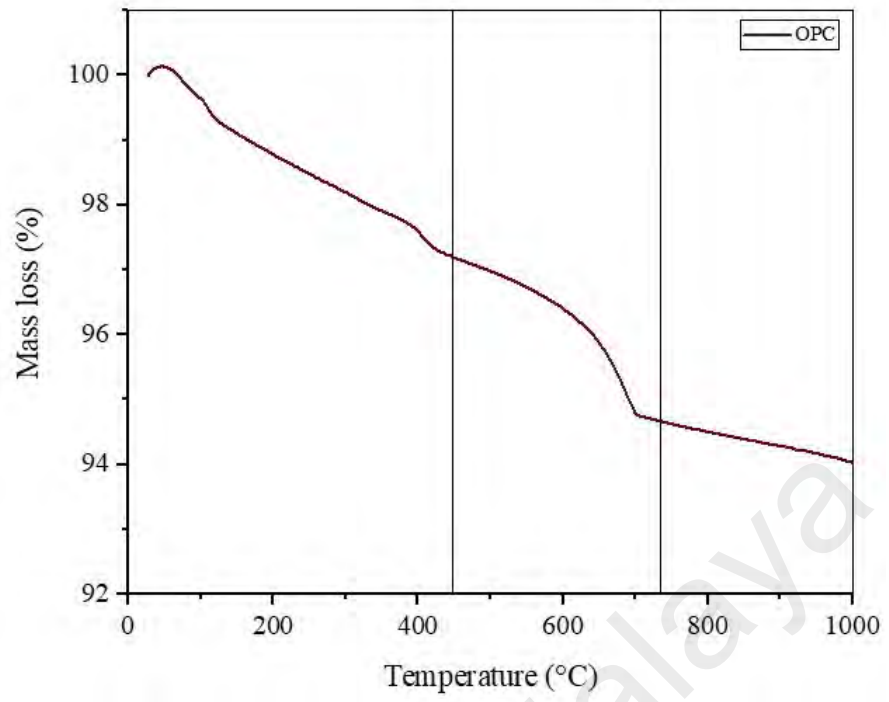
Figure 4.12: TGA pattern of OPC binder
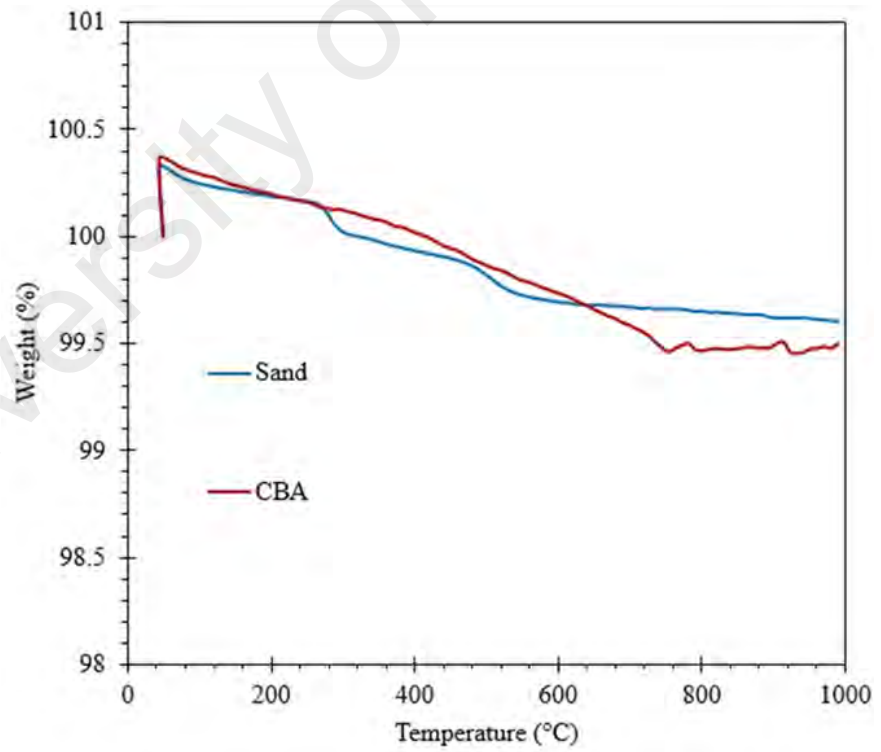
Figure 4.13: TGA patterns of CBA and silica sand

4.1.4 Summary of raw materials characterization

The salient points derived from raw materials characterization are summarized as given in Table 4.5 :

Table 4.5: Summary of raw materials characterization

Raw materials	Physical, chemical and micro-structural characterization
OPC binder	Its specific surface area was 3.89 m^2/g which provides adsorption sites to the contaminants in waste, especially for contaminated heavy metals adsorption. Its pH value was in an alkaline range. OPC (CEM1) mainly consists of 82% composition of $SiO_2 + CaO$. The MgO formed 2.60% of the total oxide and the remaining alkaline are derived in the form of K_2O (0.32%) and N_2O (0.07%). The surface morphology of OPC showed that, its specific surface area is slightly higher than its micro-pores 3.54 m^2/g. The main OPC mineral consists of alite, and belite. Although, minor mineral peaks in the OPC are tricalcium aluminate, calcium aluminum iron oxide and calcium sulfate hydrate. The total weight loss of OPC is around 32.5 to17.5 wt.% due to decomposition of organic structure.

Physical properties

	pH value	Specific gravity	Specific surface area (m^2/g)	Water absorption (g/cm^3)	Moisture content (%)
Fine aggregates (CBA and silica sand)	Alkaline-12	1.80	1.05	2.77	13
	Alkaline 11.5	2.60	0.8	1.98	3
Remarks	The CBA performs as reservoir for water with higher surface area which leads to higher the water requirement. CBA and silica sand have similar particle size distribution. While CBA contains 70% particles finer than 1.18 mm as compared to silica sand. Particle sizes coarser than 1.18 mm in silica sand is 8% more than that in CBA.				

Chemical compositions	
Fine aggregates (CBA and silica sand)	The composite oxide of $SiO_2 + Al_2O_3$ was 78.05% for CBA, while it was 96.33% for silica sand. CBA can be considered as hazardous waste since it comprises a substantial total of contaminated heavy metals and acceptable less concentration of volatiles organics. CBA has significant amount of copper, cadmium, nickel, and lead of 2.66, 0.07, 0.34, and 0.20 (mg/l), respectively. These values exceeded the Malaysian EQA standard limit.
Micro-structural analyses	
Fine aggregates (CBA and silica sand)	The CBA surface morphology resembles high porous structured and disordered shape particles formed by interlocking characteristics. While, the silica sand particles are angular in shape and lesser porous texture. The CBA contains higher porosity, which provides a high potential for water retention. In contrast, the smaller particle size of CBA, compounds the situation leading to the use of extra water to lubricate the particles. The XRD pattern of the CBA and silica sand is mostly Mullite and quartz types, respectively. The CBA with vitreous fractions compounds and silica sand with inert compounds have insignificant weight loss around 0.6, and 0.9 wt.%, accordingly.

4.2   Mixture proportioning of mortar mixes

Three series of mixes were designed (A, B, C). The first series of mixes (A) focused on the effect of silica sand replacement by CBA in OPC-based mortar mixture with constant water to cement ratio 0.55 in the range of 0-100% at increments of 20%. Then, optimum mix in terms of higher strength and lower flowability obtained from the substitution CBA/sand mixes (A) was used in the considering effects of water to cement ratios, it was varied from 0.2-0.55 (Mix B). Lastly, the water reduction by using superplasticizer, with a dosage of 1% cement content with a water to cement ratio of 0.4 was studied (Mix C). Details of these mixes are shown in Table 4.6.

Details of data for fresh and hardened properties of CBA mortar mixtures are given in Appendix B (Table B-1).

Table 4.6: Mix proportions of specimens

| Mix series	Mix Numbers	CBA: Silica sand (%)	OPC (kg/m³)	W/C ratios	CBA (kg/m³)	silica sand (kg/m³)	Water (kg/m³)	Super plasticizer (kg/m³)	OPC/ filler ratio
A	A1	0: 100	670	0.55	0	1340	368	none	2
	A2	20: 80	614	0.55	245	983	337	none	2
	A3	40: 60	580	0.55	464	696	319	none	2
	A4	60: 40	552	0.55	662	441	303	none	2
	A5	80: 20	515	0.55	824	206	283	none	2
	A6	100:0	507	0.55	1014	0	278	none	2
B	B1	40: 60	580	0.55	464	696	319	none	2
	B2	40: 60	588	0.5	470	705	294	none	2
	B3	40: 60	594	0.45	475	712	267	none	2
	B4	40: 60	601	0.4	480	721	240	none	2
	B5	40: 60	609	0.35	487	730	213	none	2
	B6	40: 60	618	0.3	494	741	185	none	2
	B7	40: 60	621	0.25	496	745	155	none	2
	B8	40: 60	628	0.2	502	753	125	none	2
C	C1	40: 60	556	0.4	444	667	222	5	2
	C2	40: 60	577	0.35	461	692	201	5	2
	C3	40: 60	609	0.3	487	730	182	5	2
	C4	40: 60	670	0.25	536	804	167	5	2
	C5	40: 60	696	0.2	556	835	139	5	2

4.2.1 Fresh properties of mortar mixtures

4.2.1.1 Flowability of mortar mixtures containing CBA

Flowability is the property of freshly mortar mixture, which determines the ease and homogeneity which it can be mixed, placed, compacted and finished. It is the amount of energy to overcome friction and cause full consolidation. Ease is related to rheology of fresh mixture, which includes performance parameters of stability, mobility and compact-ability. These parameters are predominantly dependent on consistency of the fresh mortar mixture. Thus, usual measurement of consistency of mortar mixture is flowability test. In accordance with the formula in ASTM C1437-13 (Equation 3.5), using a flow table of 25.4 cm diameter, the maximum flow value would be 154% (i.e., $(25.4 − 10)/10 \times 100\%$). In addition, all the mortar mixtures presented good flow values not less than and up to not exceeding of 10%-154% limit, respectively.

Figure 4.14 shows the flowability results of the OPC-based mortar mixtures incorporating CBA/silica sand replacements. Figure 4.14a show that at constant W/C ratio of 0.55, flowability values of CBA mixtures decreased with increases in CBA content in the mortar mixture. However, this reduction varies based on using different mix proportions such as CBA/silica sand, water/cement ratio, and effects of superplasticizer (Aggarwal & Siddique, 2014). The flowability values was 120% in control sample, but decreased to 10% on substitution of 100% CBA samples at constant W/C ratio of 0.55 (Figure 4.14a). Aramraks (2006) and Chun et al. (2008) also observed reduction in flowability on the use of CBA as substitute of sand in concrete mixture. The flowability values decreased with reduction in W/C ratios from 37% to 0% at W/C ratio of 0.2 (Figure 4.14b). However, by adding 1% superplasticizer as shown in Figure 4.14c, the flowability value of mortar mixes at W/C ratios of 0.4, 0.35, 0.3 and 0.25 increased

to 25, 20, 15 and 5%, respectively. Therefore, using SP improved lubrication of particles and increase the flowability of mixes.
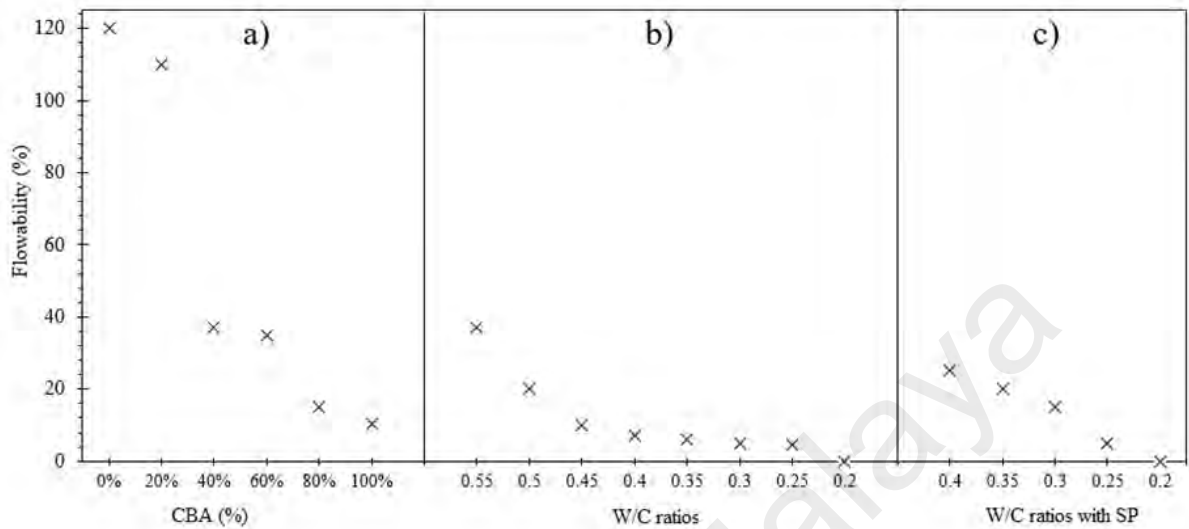
Figure 4.14: Flowability measurement of mortar mixtures based on the variations of the a) CBA (%), b) Water/cement ratios and c) Effect of superplasticizer

Flowability test results are in line with the porous structure of CBA compared to the silica sand. The substitution of silica sand with CBA also caused growth in specific surface area of fine aggregate in the mortar mixtures. The irregular texture and disordered shape of CBA particles also played significant role in increasing the interparticle friction. The water absorption of CBA is higher than that of silica sand (Table 4.5). Moreover, the CBA contains higher porosity, which leads to higher water absorption; consequently, more water is required to cover the surface of CBA particles and subsequently to increase the flowability. In contrast, the smaller particle size of CBA compounds the situation leading to the need of additional water to lubricate the particles. To compensate for the loss of flowability, higher water content is needed for similar flowability design, as shown in Figure 4.14b. In contrast, the addition of water increases the porosity of the matrix, and thus, a reduction in the compressive strength (Ranjbar et al., 2016a; Singh & Siddique, 2014). Therefore, to avoid such an adverse effect, an increase in flowability can be provided by adding a superplasticizer, as shown in Figure 4.14c.

Therefore, reduction in flowability of concrete by incorporations CBA in mortar mixes, is the result of increased specific surface area, increase in internal friction and rate of absorption of water internally by the high porous particles of CBA.

4.2.1.2 Bleeding of mortar mixtures containing CBA

After vibrated newly mixture placed in molds, the cement and fine aggregate particles settled to the bottom of the mold. Besides, segregation takes place and water rises to the top surface of the freshly mixture due to the difference in the mass of component raw materials. These waters collected at top surface of mixtures known as bleeding. Bleeding results in the formation of porous, weak and non- durable concrete layer at the top of placed mortar mixture.

Figure 4.15 presents the water loss of CBA replacement mixtures through bleeding. It is observed that bleeding decreased with the increase in the CBA content in the mortar mixture. The bleeding decreased from 7.66 to 1.80% when 100% CBA was used as substitute of silica sand in the mortar mixture. The volume of water accumulated per unit top surface area of mortar mixture decreased from 27.74 g/cm^2 to 10.55 g/cm^2 by incorporation of 100% CBA as substitute of silica sand. The regression line with higher value of determination coefficient R^2 of 0.986 indicates good relationship between the results and regression curve (Figure 4.15). The low effect of CBA in the mortar mixtures through bleeding of less water, attributed to porous particles in the CBA that internally water was absorbed during the mixing process. Because of the increased demand for mixing water, the CBA mixtures displayed a much higher degree of bleeding than the control mixture (Ghafoori & Bucholc, 1996). Andrade et al. (2009) reported that higher water loss through bleeding was observed by incorporation of CBA in concrete mixtures. They reported, the amount of bleeding water in concrete depends largely on the water to cement ratio. Higher amount of water was applied in the CBA concrete mixtures

compared to the control mixture which reached the desired workability. Consequently, it resulted in higher loss of water through bleeding in the CBA mixtures. Their investigation was based on 378 kg/m^3 of water content being added to concrete mixture containing 100% CBA against 219 kg/m^3 of water content needed for control concrete mix. In the present study, a fixed water-cement ratio of 0.55 was maintained in the six main CBA mortar mixtures as well as the control mixture. Therefore, with constant W/C ratio, water loss through bleeding in the higher CBA proportions reduced, compared to control mixture.
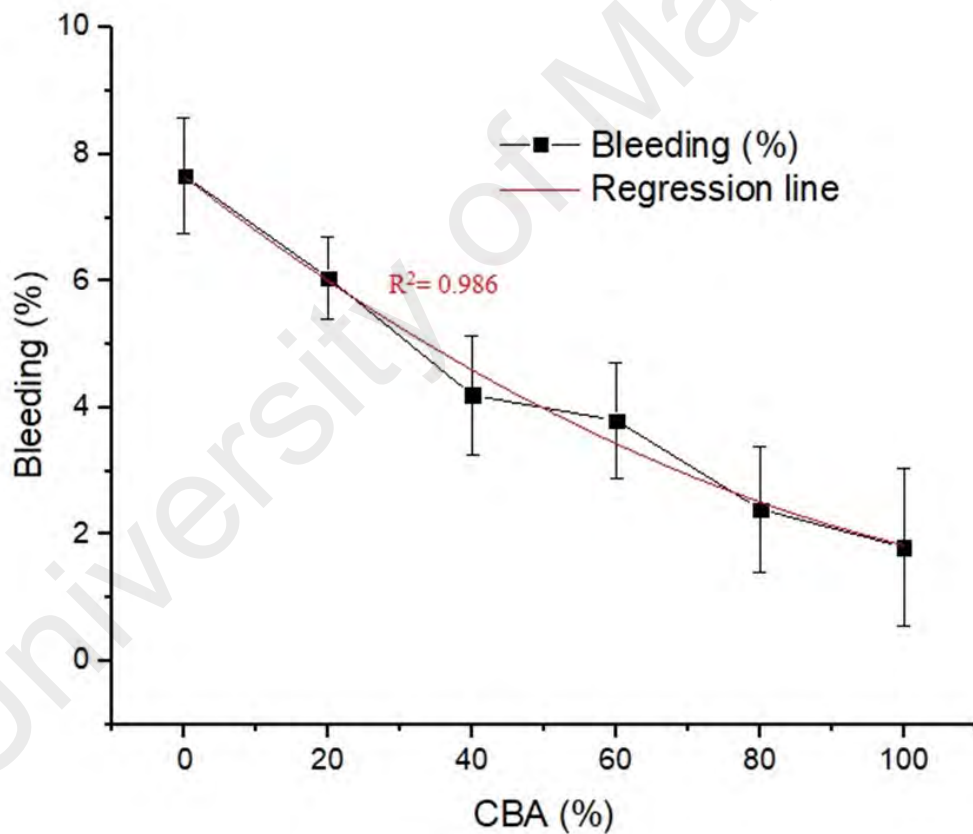
Figure 4.15: Effect of CBA replacement mortar mixtures on loss of water through bleeding

4.2.2   Harden properties of mortar mixtures

4.2.2.1 Compressive strength of mortar mixtures containing CBA

Strength property of specimens was measured immediately after removing the cubes from the water at the specified curing ages. Surface water and grit were wiped off and the cube was placed in the compression testing machine. The harden properties results of CBA mixtures and control mixture are given in Appendix C. The effect of levels of silica sand replacement with CBA, water/cement ratios and effect of adding SP on compressive strength of mortar mixtures are discussed in the following sections.

4.2.2.2   Effect of CBA and silica sand replacement

Figure 4.16 shows the compressive strength of CBA mortar mixture at all levels of sand replacement. At the early curing age of 7 days, CBA mortar mixtures exhibited higher compressive strength than that of the control mortar mixture. At 7 days, mortar mixtures containing 20, 40, 60 and 80% CBA as fine aggregate substitution achieved 6.4%, 6.8%, 16.4%, and 1.6% over compressive strength of the control mortar mixture, respectively. However, the mixture replacement of 100% CBA achieved lower compressive strength than the control mortar mixture at all curing ages. At 14 days, CBA mortar mixtures exhibited lower compressive strength than that of the control mortar mixture. At 28 days, although compressive strength of CBA mortar mixtures containing 20, 40 and 80% CBA as fine aggregate substitution was slightly lower than that of the control, the 60% CBA mixture achieved 1.4% higher compressive strength than the control mortar mixture. The target strength of mixtures designed for 45 MPa at 28 days was achieved by mixture containing 60% CBA (A4). Mortar mixture containing 40% CBA (A3) as fine aggregate substitution at 56 days achieved 54.96 MPa which was 2.1% higher compressive strength than the control mortar mixture (53.80 MPa). Therefore, the optimum mixture incorporating CBA was up to 40% and water/cement ratio of 0.55.

Bai and Basheer (2003) reported that, at a fixed cement content and fixed W=C, the compressive strength decreased with the increase in the replacement level of natural sand with the CBA. As shown in Figure 4.16, the enhancement in compressive strength of CBA mortar mixtures is continuous with increasing curing age days. It is apparent from the test results of the present study that incorporating CBA by up to 40% in silica sand-based matrices does not have a tangible adverse effect on the compression strength of the matrices, while further replacement reduces the compressive strength. The factors causing the decrease in the compressive strength of the CBA mixtures can be credited to the replacement of the stronger material (silica sand) with a weaker one (CBA), and the increase in the pore fraction of the concrete (Singh & Siddique, 2015). Consequently, additional porosity to the matrix leads to a decrease in effective cross section. When the material is under compression, a lateral tension maximizes around the pores and cause local failure in these areas and reduce the strength of the matrices (Ranjbar & Kuenzel, 2017b).
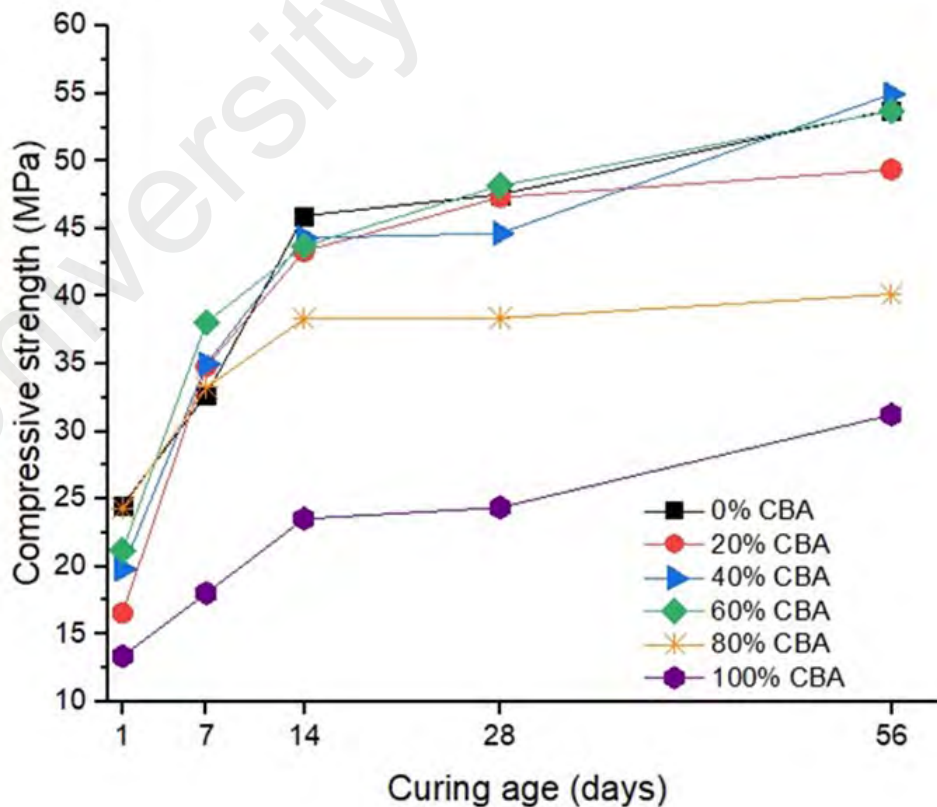

Figure 4.16: Compressive strength of CBA replacement mortar samples (Mix A)

As mentioned in section 4.2.1.2, with increasing CBA proportions in the mixture, reduction of bleeding of water was noticeable. Consequently, there are more chances of bleeding water getting trapped into porous structure of CBA mixtures and this resulted in the formation of numerous small pores close to the aggregate surfaces. These micropores prevent the excellent bonding of cement paste with the aggregate. Therefore, the transition zone between the aggregate and cement paste becomes weak and porous, which ultimately results in reduction in strength of CBA mixtures. The weak microstructure obtained with the use of CBA mixture is responsible for the decrease in compressive strength. As a result, the decrease in the free water/cement ratio of the CBA mixtures due to absorption of part of water by the porous particles of the CBA internally during the mixing process, also contributed to some extent in negating the effect of the factors responsible for lower compressive strength. In other words, at early curing age, the compressive strength of CBA mixtures improved to some extent due to the reduced free water/cement ratio but the net effect of all the factors mentioned above was reduction in compressive strength by using CBA as fine aggregate.

Previous studies showed that the pozzolanic activity of CBA is slow up to 14 days of curing and after this period, the CBA particles start reacting with calcium hydroxide to form CSH gel and needles (Cheriaf et al., 1999; Singh & Siddique, 2013). With increasing age, reactive silica in the CBA reacts with alkali calcium hydroxide produced during hydration of cement and forms calcium silicate and aluminate hydrates. The formation of stable calcium silicate and aluminate hydrates by chemical reactions between cement paste constituents and aggregates result in filling the voids in the interfacial transition zone and improving its compressive strength. At 28 days, the increase pozzolanic activity of the CBA negated the effect of factors responsible for reduction in strength and played its role in improving the compressive strength. As such, the decrease in compressive strength of CBA mixtures was not significant except CBA mixture containing 100%

CBA. After 28 days of curing, pozzolanic effect of CBA overcame all the negative effects and enhanced the strength properties of CBA mixtures (Lee et al., 2017; Singh & Siddique, 2014). Our results show that in mix A, compressive strength of CBA mortar mixtures of A2, A3, A4, A5 and A6 at 56 days achieved 13.2%, 4.3%, 23%, 11.5%, 4.7% and 28% over compressive strength at 28 days. Therefore, the pozzolanic reaction of CBA mixtures overcame all the negative effects and improved the strength property.

4.2.2.3 The effect of water/cement ratios

Figure 4.17 shows the effect of reduction in water /cement ratios from 0.55 to 0.2 on strength development of optimum mixture A3 which is obtained from mix A. At 7 days of curing, compressive strength of B1, B2, B3, B4, B5 at W/C ratios of 0.55, 0.5, 0.45, 0.4, 0.35 achieved 34.98 MPa, 28.18 MPa, 28.13 MPa, 25.65 MPa, 19.06 MPa, respectively. It is evident that, a decrease in the water content of the pattern does not necessarily increase the compressive strength. This is due to the dominant role of the porosity of CBA compared to that induced by the higher water content. However, reducing the water content weakens the hydration and the cementitious gel formation and therefore, influence the compressive strength of the matrix.

The compressive strength result of B1, B2, B3, B4, B5 at water/cement ratios of 0.55, 0.5, 0.45, 0.4, 0.35 achieved 44.66 MPa, 40.02 MPa, 45.58 MPa, 35.45 MPa, 24.14 MPa at 28 curing days which is gained over their 7 days compressive strength results. Increase in curing period, brought about a minimal increase in compressive strength of B1-B5 mixture with W/C ratios of 0.55 to 0.35. While, the compressive strength result of B6, B7, and B8 at W/C ratio of 0.3, 0.25, 0.2 achieved lower compressive strength at all curing ages which is not acceptable and required chemical admixture to improve flowability and strength property. The reduction in compressive strength reported in can also be attributed to non-proper consolidation of CBA structure, which was partly compensated for use of

SP. The B3 samples with W/C ratio of 0.45 archived the target strength of 45 MPa at 28 days and gained 2% over that compressive strength of W/C ratio 0.55 at 28 days. While, the B1 samples with W/C ratio of 0.5 achieved higher compressive strength of 54.96 MPa at 56 days (Figure 4.17). Due to the high absorption rate, angular shape, and very porous surface of the CBA, higher water content is required to achieve the degree of lubrication needed for a workable mix. The increased water demand has a moderate effect on early-age characteristics of CBA concretes (Ghafoori & Bucholc, 1996). Aggarwal et al. (2007) reported that the CBA texture caused the W/C ratio of the concrete to not be taken as exact. This is because of the amount of internally absorbed water by CBA is released to the concrete over time, being part of the production process with the concrete still in the fresh state. As a result, the particles of CBA increased the quantity of water loss by bleeding and the higher the CBA content of the concrete leads to the greater this effect (Kanadasan & Razak, 2014).
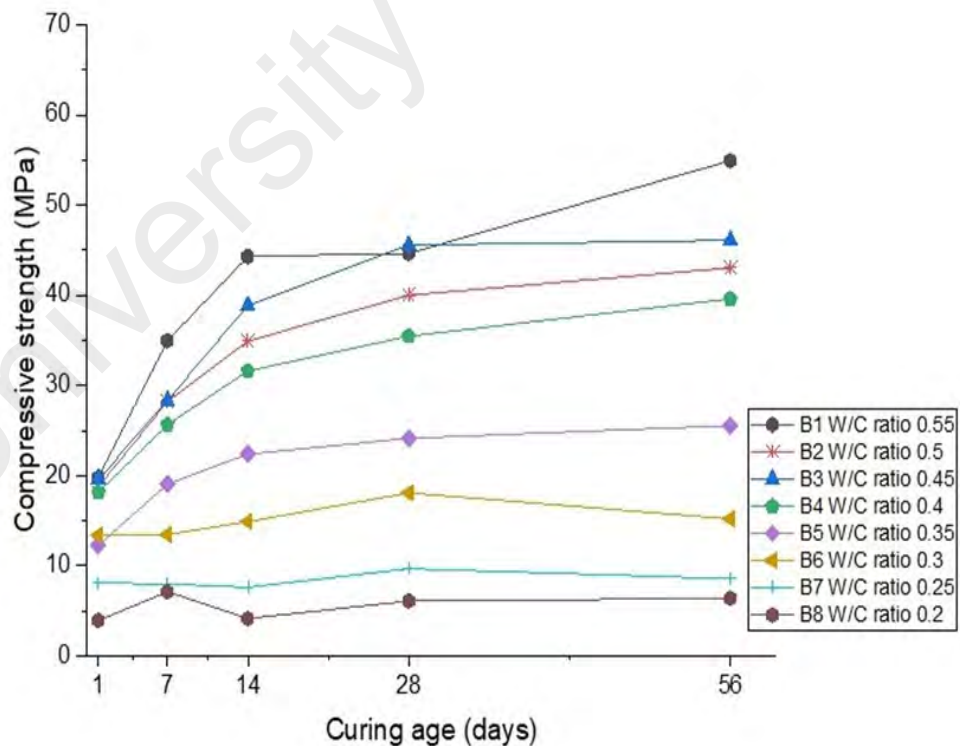
Figure 4.17: Effect of W/C ratios on compressive strength development of mortar samples (Mix B)

4.2.2.4 Effect of addition superplasticizer (SP)

Figure 4.18-Figure 4.20 present the compressive strength of incorporating superplasticizer into the optimum mixtures (A3) at W/C ratio of 0.4-0.2 at 1, 7, 28 and 56 days. The amount of SP added was kept constant for all mixes to increase cohesiveness and not significantly affect their flowability. Although flowability is heavily impacted by W/C ratios and SP; since the amount of binder was kept almost the same, the changes in flowability can directly be connected to changes in different material used such as fine aggregate and their characteristics such as water absorption. Incorporating a superplasticizer into the mix could compensate for some of the adverse effects such as a high-water requirement of CBA.

At 7 days, the compressive strength of C1, C2, C3, C4, C5 at W/C ratios of 0.4, 0.35, 0.3, 0.25 and 0.2 achieved 58.2%, 27.7%, 53%, 32.5% and 16.6% respectively, over compressive strength of mixtures B4-B8 without SP (Figure 4.18). Therefore, the compressive strength of C1, C2, C3, C4, C5 at W/C ratios of 0.4, 0.35, 0.3, 0.25 and 0.2 achieved 38.8%, 41.7%, 49.2%, 12.9% and 16.7% respectively, over compressive strength of mixtures B4-B8 without SP at curing period of 28 days (Figure 4.19).

Furthermore, as the CBA has some reactive phases, it has potential to cause a slow pozzolanic reaction over time and react with portlandite to form extra C–S–H gel. In such reaction, the interaction of paste and aggregate is improved, the mechanical properties of the matrices are enhanced subsequently and reached at 50 MPa at 56 curing days. Therefore, the compressive strength of C1, C2, C3, C4, C5 at W/C ratios of 0.4, 0.35, 0.3, 0.25 and 0.2 achieved 26.5%, 52%, 59.2%, 34.5% and 25.5% respectively, over compressive strength of mixtures B4-B8 without SP at curing period of 56 days (Figure 4.20).
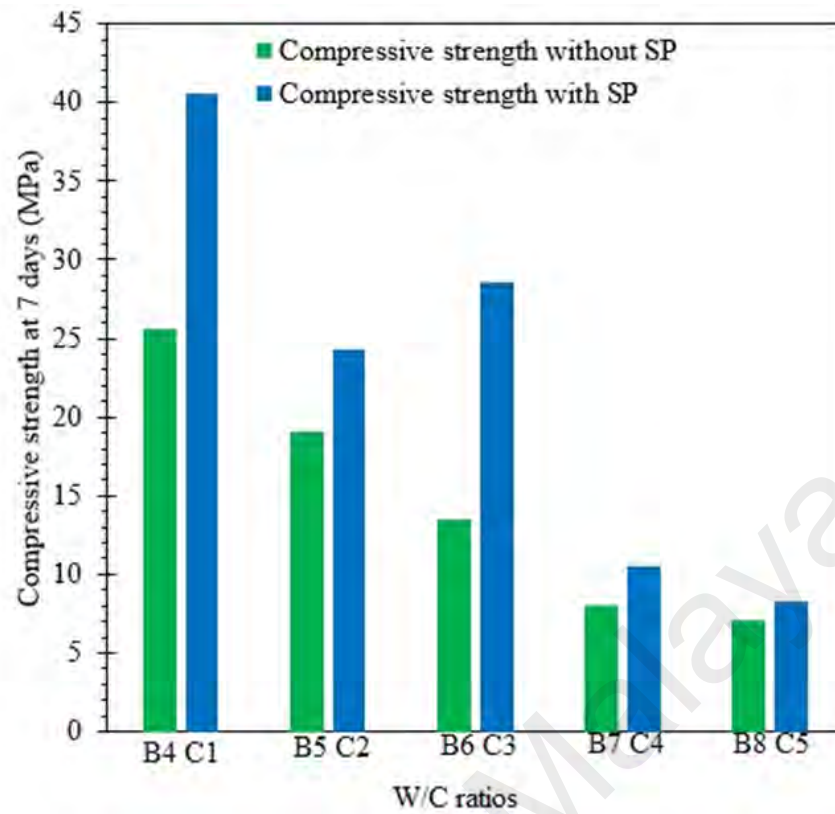
Figure 4.18: Compressive strength of superplasticizer mortar samples with 40% CBA at 7 days
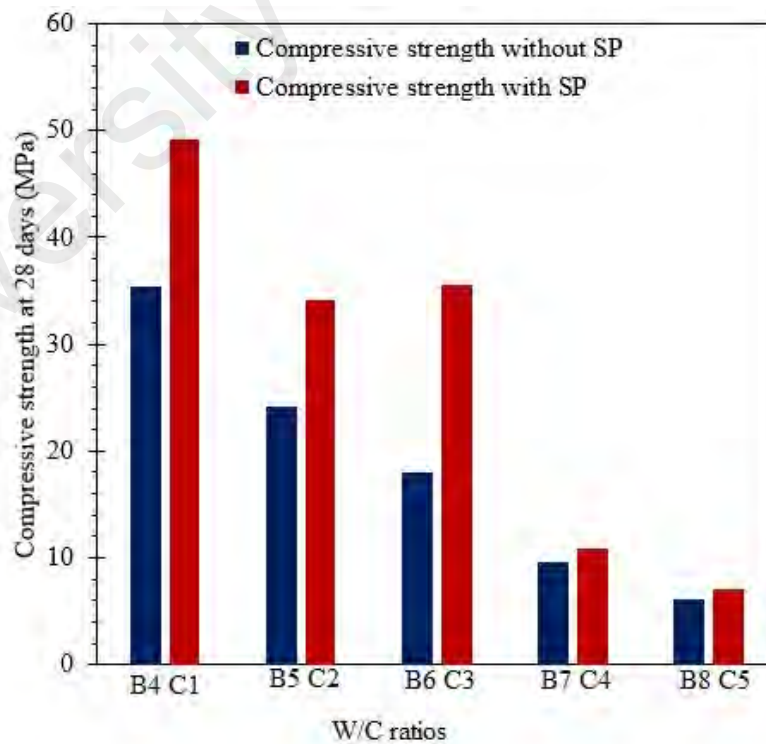

Figure 4.19: Compressive strength of superplasticizer mortar samples with 40% CBA at 28 days
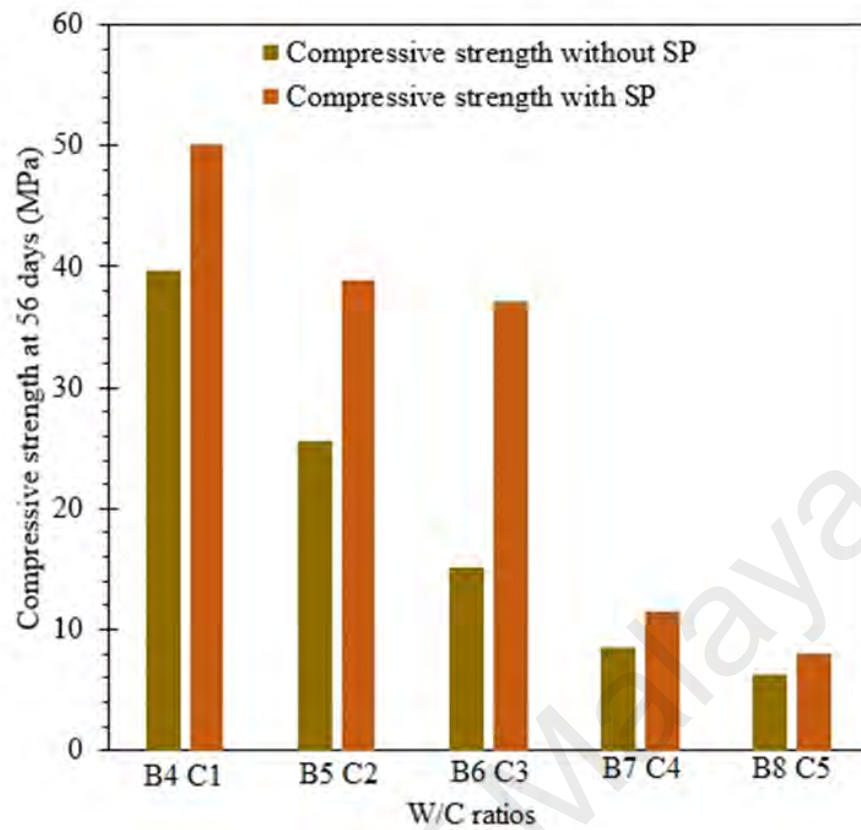
Figure 4.20: Compressive strength of superplasticizer mortar samples with 40% CBA at 56 days

The research carried out by Aggarwal et al. (2007) reported that, using the highest and lowest amounts of SP in the concrete mixture of 50% and 30% CBA, respectively. It resulted in expressively reduction the flowability values. Although, the strength property of 50% CBA mixture with highest amount of SP not significantly improved. In this study the SP portion was constant at 1% of cement weight for all optimum mixtures (A3) and addition SP at mixture C1-C5 to achieve improvements of flowability less than 10% and target compressive strength of 45 MPa at 28 days. Therefore, the optimal mixture of 40% CBA at W/C ratio 0.4 with and without 1%SP achieved compressive strength of 39.62 and 50.13 MPa at 56 days respectively (Figure 4.20).

4.2.2.5 Density of mortar mixtures containing CBA

The air-dried density results of CBA mixtures and control mixture are given in Figure 4.21a, b, c. The result of levels of silica sand replacement with CBA, water/cement ratios and effect of adding SP on density are presented. Figure 4.21a, presents the 28 days air-dried density of the mortar mixtures varies between 1830 kg/m^3 for 100% CBA (A6) content and 2380 kg/m^3 as a control mortar mixture (A1). This is because of the low specific gravity of CBA compared to the silica sand as mentioned in Table 4.5.

On replacement of CBA with the silica sand in mortar mixture, lighter particles are substituted with heavier particles. The density of mortar mixtures containing 40% (A3) and 100% (A6) CBA as substitute of sand decreased by 320 kg/m^3 (13.4%) and 580 kg/m^3 (24.4%), respectively. The increased in pores of the mixture by using CBA as substitute of sand also resulted in lower density. In addition, the CBA based mixture can be classified as lightweight concrete. The results of present study are in good agreement with the results reported by Andrade et al. (2007), Aggarwal et al. (2007) and Kim and Lee (2011). In addition, a decrease in the water/cement ratio (Figure 4.21b) can cause a reduction in the weight of the specimen from 2060 kg/m^3 at W/C ratio 0.55 to 2011 kg/m^3 at W/C ratio 0.2.

The unit weight decreased by an average of 7.1%, 5% and 1% with a low dosage of 1% SP at samples with W/C ratio of 0.4 (C1), 0.35 (C2) and 0.3 (C3) respectively in comparison with samples B4-B6 without SP (Figure 4.21c). While, the unit weight increased by an average of 8.2% and 11.2% with a low dosage of 1% SP at samples with W/C ratios 0.25 (C4) and 0.2 (C4), respectively, over samples B7 and B8 without SP (Figure 4.21c). This is associated to the compaction of the sample at lower W/C ratios by using SP which caused expansion of cement particles inside pore structure and enhanced fluidity therefore, higher density.
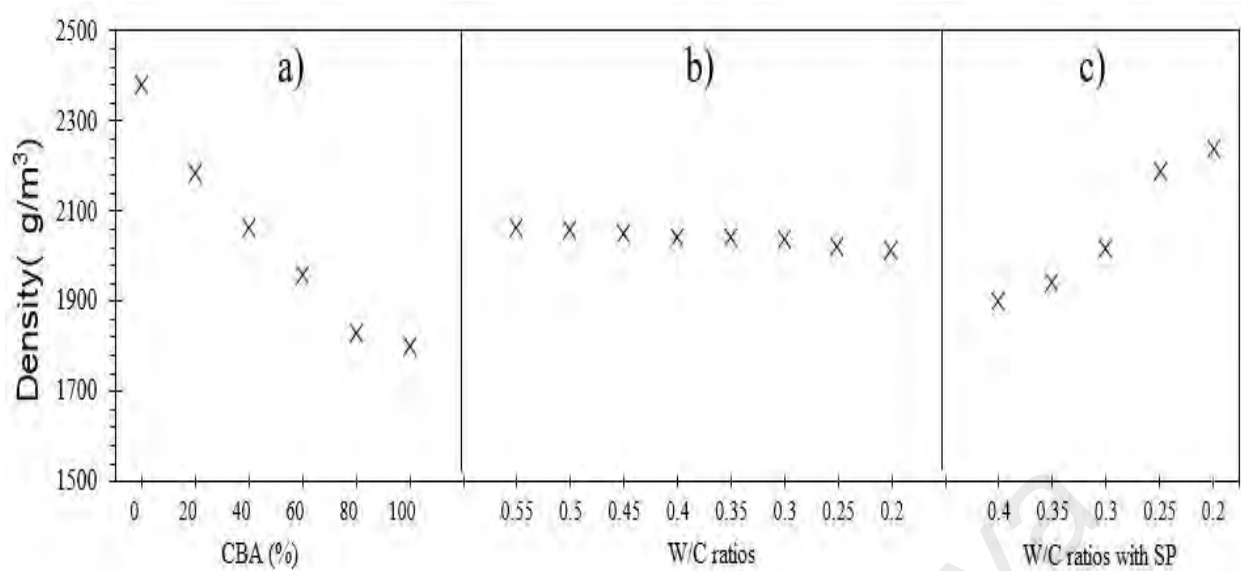
Figure 4.21: Density measurement of mortar samples based on variations of the a) CBA/sand replacement, b) Water/cement ratios and c) Addition of superplasticizer

4.2.3 Micro-structural analysis of mortar mixtures

The hardened properties of samples depend on its inherent microstructure. Principally, microstructure properties are influenced by the type of cement and the fine aggregates used in the production of mortar mixtures. The microstructure of samples consists of hydrated cement paste, aggregate and interfacial transitional zone. The pore volume distribution play substantial role in determining the microstructure of samples. SEM provides compositional micrograph analysis. In this study, pieces of samples after the compressive strength tests at 28 curing days were used for the SEM analysis. Moreover, the crystalline zones and weight loss of the composites were also analyzed, in terms of XRD and TGA properties.

4.2.3.1 Pore volume distribution

Pore size distribution was measured based on the cycle of adsorption-desorption isotherms balance. The pressure increases as the nitrogen adsorption raised to the maximum level, then by the decreasing of pressure, desorption happened and formed as cycle. The pore size can be considered as micro-pore, meso-pore and macro-pore with

diameter of < 20 Å, 20 to 500 Å and > 500 Å respectively. The cumulative adsorption pore volumes of the CBA mortar samples were plotted according to the Barrett-Joyner-Halenda (BJH) method as shown in Figure 4.22. It is observed that samples composed of significantly meso-pore and macro-pore volumes. The pore volume distribution for CBA samples at 28 days showed that their pore spaces increased with increase in the CBA contents. The macro-pore volumes of the composite matrix increase in diameter of 500-2200 (Å). The sample with more CBA proportions exhibit increases in average pore volume more than 0.035 (cm^3/g), except for the control sample that reached the lowest value of cumulative pore volumes which is less than 0.02 (cm^3/g). The sample with 20% and 60% CBA replacements reached lower pore volumes distribution at 28 days (Figure 4.22). This agrees with strength property results. At 28 days, with increase in CBA proportions, the pore volumes increased. Therefore, the sample with higher pore volume under compression leads to decrease in effective cross section., a lateral tension maximizes around the pores and cause local failure in these areas and reduce the strength of the matrices. The sample with 100% and 60% CBA achieved lowest and highest strength with the highest and lowest pore volume distributions, respectively.
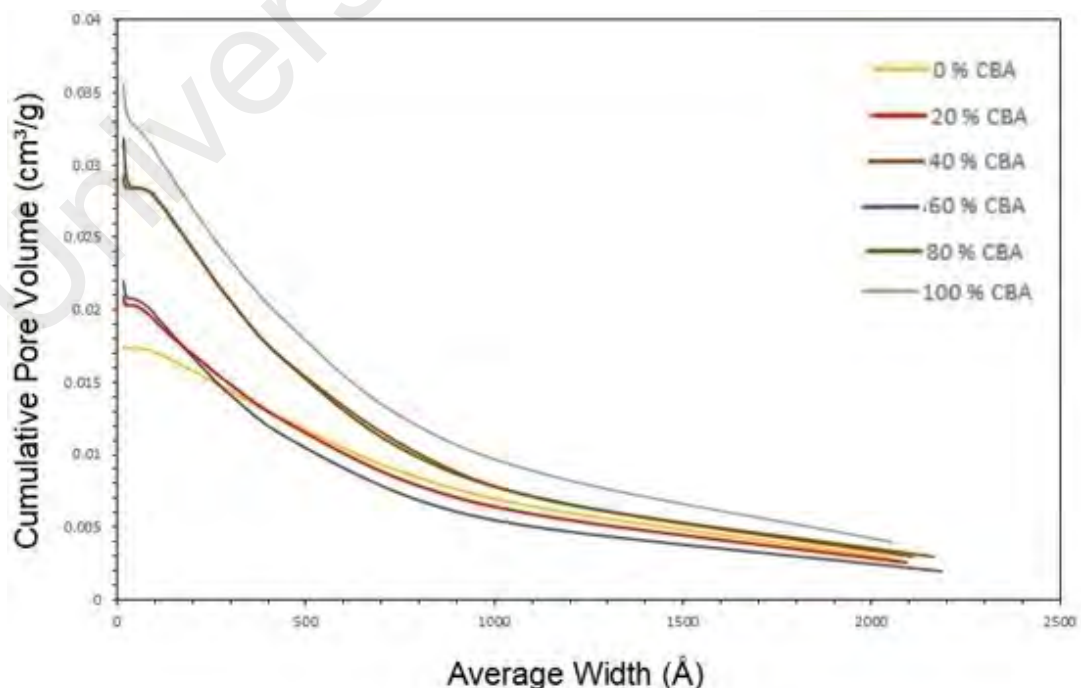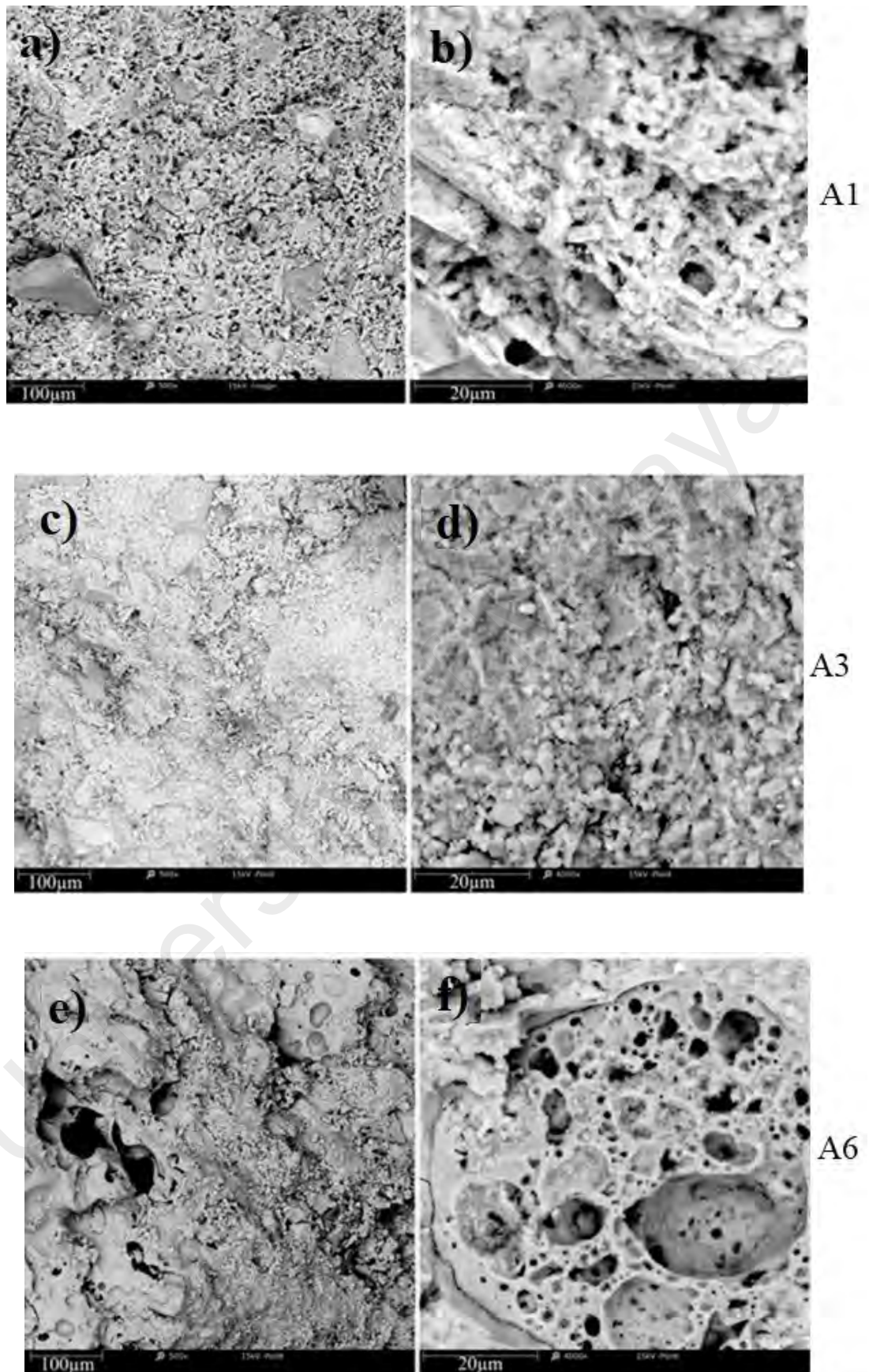

**Figure 4.22: Pore volume distribution of mortar samples**

4.2.3.2 SEM analysis

The SEM micrographs of specimens at A1, A3 and A6 CBA replacement with silica sand samples in high and low magnifications at 28 days are shown in Figure 4.23a-f. Figure 4.23a and b show the control mortar mixture that is surrounded by a binder with microporous cement dense, compact and continuous structure. The pore size is about 5 μm because of the high-water cement ratio of 0.55 (Figure 4.23b). When the sand was replaced with 40% CBA (Figure 4.23c and d), the composite shows dense structure (Figure 4.23c). In these specimens, the pore size was reduced by 2 μm (Figure 4.23d). This is attributed to the pozzolanic reaction of CBA which causes an expansion with CSH gel through the material and filling of some pores over time. Also, the higher water demand of CBA results in a reduction in water/cement ratio that leads to smaller pore structure of the produced cementitious gel. The porous structure of CBA is dominant in samples with high volume of this fine aggregate (Figure 4.23f). As observed in Figure 4.23f, the pore size increase to about 100µm which is attributed to the porosity of CBA particles and the air which was trapped among the agglomerated particles and the cement paste (Figure 4.23e). The induced pore fractions affect the mechanical performance of the composite although the result is a lighter weight material (Kurama & Kaya, 2008; Singh & Siddique, 2014). Also, the high utilization of CBA can cause decrease in strength of concrete due to delay in hydration and slow pozzolanic action of CBA in early curing period (Singh & Siddique, 2014). Yuksel and Genç (2007) reported that when natural sand was replaced with CBA in concrete, the microstructure changed its network structure. Instead of irregular grains in the case of natural sand, the grains become circular and pores become smaller and more distributed with the incorporation of CBA. As the replacement of sand with CBA increased, the detachment of grains in the network structure increased (Figure 4.23e and f).

**Figure 4.23: SEM analysis of CBA/silica sand matrices based on A1 (a and b),
A3 (c and d), A6 (e and f)**

The SEM micrographs of specimens at A2, A4 and A5 CBA replacement with silica sand samples in high and low magnifications at 28 days are shown in Figure 4.24g-l. Figure 4.24g shows the composite is dense, compact almost like control sample Figure 4.23a and b. While Figure 4.24h, observed the agglomerated particles of CBA, were expanded through the condensed composite. Figure 4.24 i and j, show samples containing 60% CBA (A4). The sample A4 is similar the sample A3 micro structural (Figure 4.23 c and d). Figure 4.24j observed of dense composite with crumped sheet surrounded by pore space. Figure 4.24K and l, show samples with 80% CBA (A5). The sample A5 show small sized pores less than 50 μm in cement compacted cement structure (Figure 4.24k). As observed the cement structure was slightly less monolithic as surrounded by more pore spaces than that of control mixture (A1) in Figure 4.23a and b.

Therefore, the samples A3 and A4 show the micrograph almost like that of control sample structure (A1) with lower pore space and dense structure. This resulted in the higher strength at late ages.
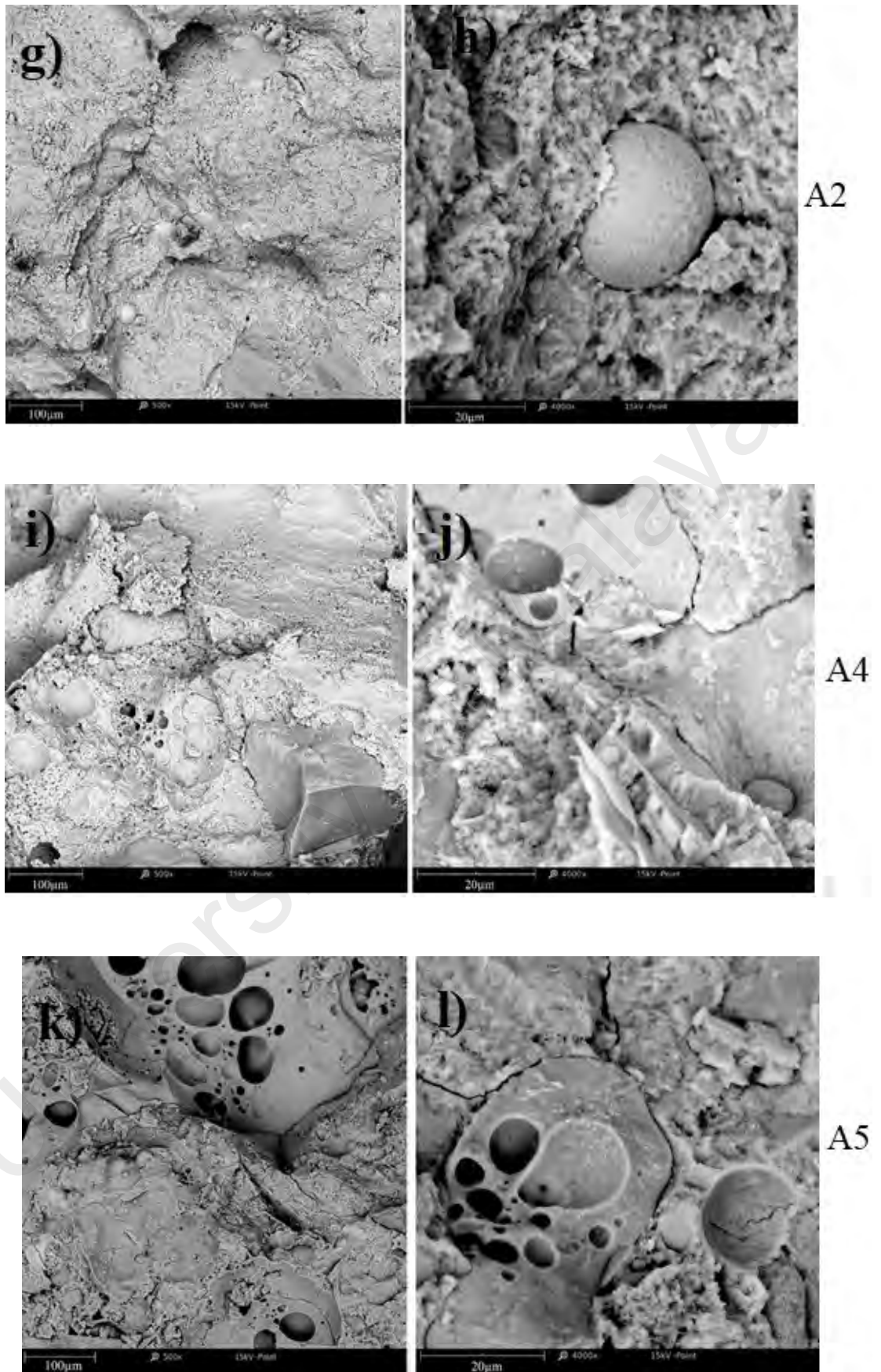
Figure 4.24: SEM analysis of CBA/silica sand matrices based on A2 (g and h), A4 (i and j), A5 (k and l)
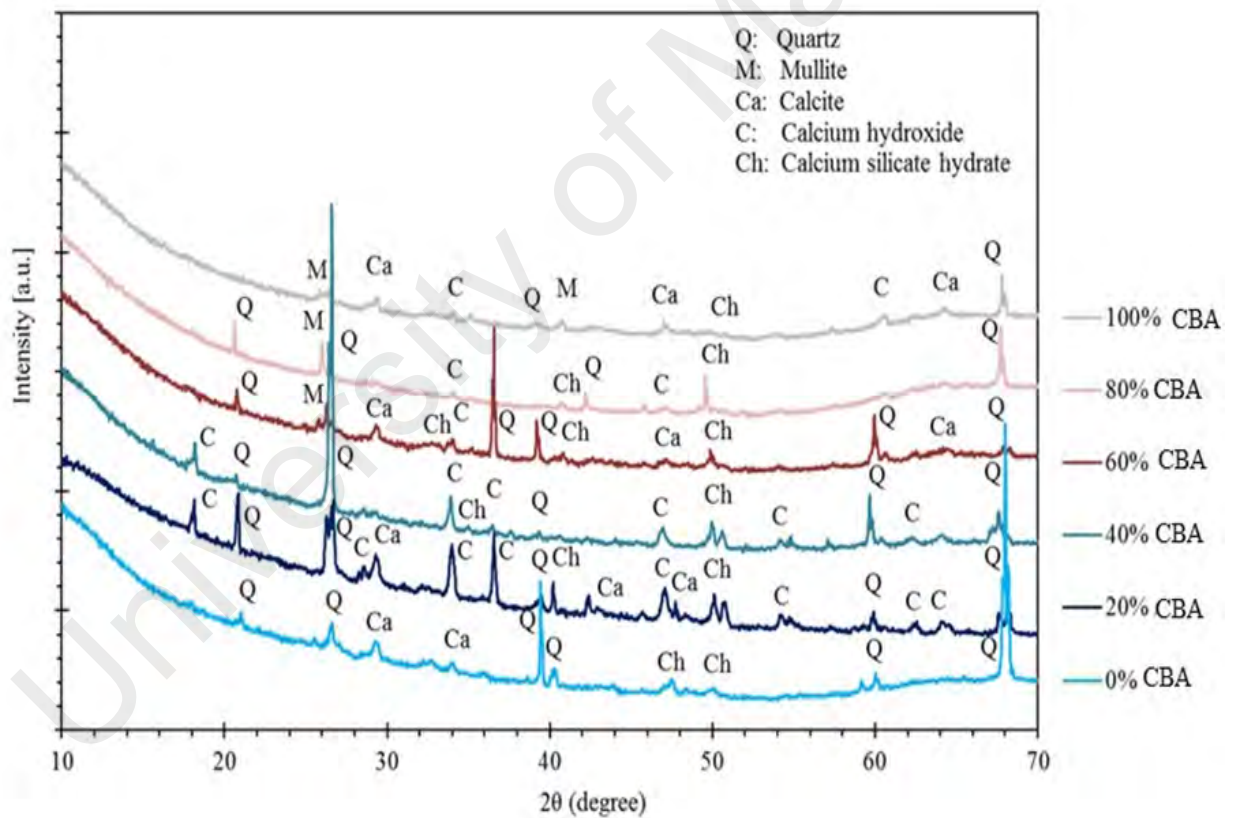
4.2.3.3 XRD analysis

The micro-structural of the crystalline phases of CBA/ silica sand composites varies from that of control OPC hydrated. Diffraction peaks of minerals present in aggregate may interfere to identify the hydration phases of composites. The X-ray diffraction of crystalline phase was used for identification of various peaks present in the hardened samples as well as control sample at the age of 28 curing days. The XRD investigations were performed for diffraction angle 2θ ranged between 10° to 70°.

XRD diffractograms of powder control and hardened samples containing 20, 40, 60, 80 and 100% CBA are presented in Figure 4.25. The graphs show the presence of quartz and mullite originating from the silica sand and CBA, respectively. These crystalline are structurally stable and remains almost intact in the reaction (Vassilev et al., 2004). The hydration reaction products, such as calcium hydroxide and calcium silicate hydrate (CSH), were observed. Another mineral, calcite ($CaCO_3$) that is produced from the reaction of the hydrated phases with atmospheric CO_2 was also present. The diffraction peak characteristics of CSH are not well resolved or visible. This is because of the poorly crystalline nature of CSH phase, and to the interference with diffraction peaks of minerals from aggregate which are predominant in the samples. In addition, there is an overlap of the peak characteristics of C-S-H with that of calcite (Figure 4.25). This has been reported to be due to the late hydration process that occurs in aging specimens (Abo-El-Enein et al., 2015). This phenomenon is fostered in the current system by the pozzolanic activity of CBA at later age, which enhances the hydration process (Cheriaf et al., 1999). The predominant diffraction peak phase in control sample (A1) is calcium silicate (Ch) compared to that in A2, A3, A4, A5, A6 CBA samples. The evaluation of XRD spectrums intensities revealed that the total intensity of Ch in CBA samples of 40% and 60% was higher almost like control samples (Figure 4.25). At 28 days, total intensity of calcite

increased on substitution of CBA in the mixtures. At this age, the evaluation of XRD spectrums intensities revealed that the total intensity of portlandite in CBA samples (20%, 40%, 60% CBA) was higher than that in control sample. The relative evaluation of peak intensity revealed that the influence of the vitreous fraction of CBA is significant in case of portlandite phase (Figure 4.25).

Therefore, the intensity peak crystalline phase of $Ca(OH)_2$ with pozzolanic reaction to produces CSH gel known as Tobermorite gel leads to higher strength resulted in the samples of A3 and A4.

Figure 4.25: XRD analysis of mortar samples at different CBA contents

4.2.3.4 TGA analysis

The thermal gravimetric analysis of the CBA mortar mixtures samples at 28 days, is shown in Figure 4.26 and Figure 4.27. Thermal change accompanying mass change includes decomposition, reduction, absorption and vaporization. As shown in Figure 4.27, the curve of the CBA mortar samples presents three major weight losses with maximum at 80-116, 374-498 and 772-787°C, which correspond to the decomposition of the CSH gel, calcium hydroxide, and calcite, respectively.

As shown in Figure 4.26 quantification of weight loss corresponding to the CSH gel decomposed in the control mortar mixture specimen (A1) which is measured 5 wt.%.
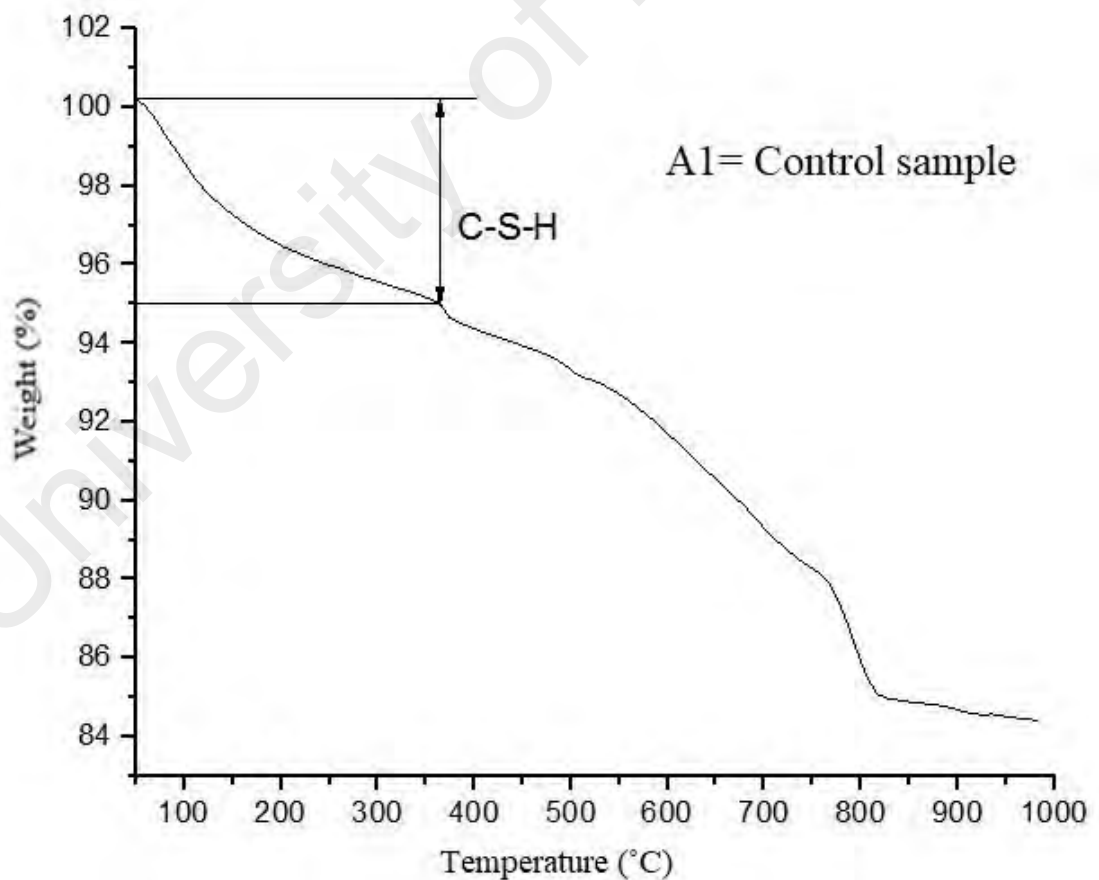
Figure 4.26: TGA analysis of control mortar sample

The quantification of weight loss corresponding to the CSH gel in all the CBA mortar mixture specimens gives, respectively, 5, 5.1, 5.2, 5.4, 5.8 and 6.9 wt.%. The amount of CSH gel formed increases with the silica sand replacement by CBA. This is due to the pozzolanic activity of CBA, which reacts with the calcium hydroxide from the hydration reaction to give the more CSH gel in the system. The present result corroborates the strength increase with sand replacement, as reported earlier. Therefore, the decomposition of CSH gel results in higher weight loss and consequently reduction in the strength of samples A5 and A6, with higher CBA proportions.
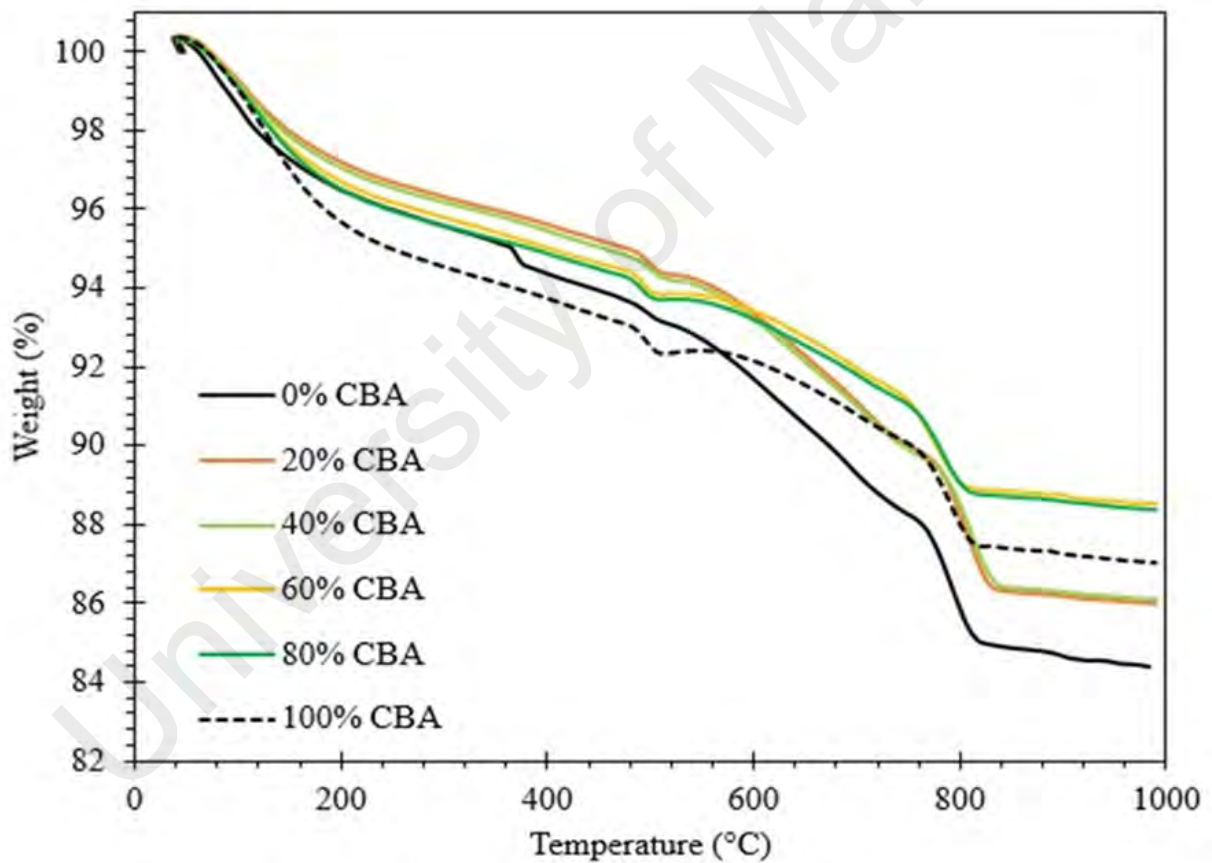
Figure 4.27: TGA analysis of mortar samples at different CBA contents

4.2.4 Summary of using CBA as fine aggregate substitution with silica sand in the mortar mixture

(1) Fresh properties of the mortar mixtures containing CBA: All the CBA mortar mixtures achieved the flowability requirement at minimum and maximum standard limit (10%-154%). The flowability values of CBA mortar mixtures decreased with the increase in the CBA contents. However, for the mixture with 40% CBA by adding 1% of cement weight superplasticizer at lower W/C ratios, the flowability up to 25% increased. Higher CBA proportions in the mortar mixtures resulted in lower water bleeding as compared to control mortar mixture. This is because of irregular porous texture and agglomerated shape of CBA particles increase the interparticle friction and water absorbed in inter particle voids and pores in the CBA mixtures.

(2) Mechanical properties of the mortar mixtures containing CBA: the compressive strength result of the CBA mortar samples at 28 days was over their 7 days compressive strength. However, the mixture incorporating 100% CBA achieved lower compressive strength than the control mortar mixture at all cuing ages. The target strength of samples designed for 45 MPa at 28 days was achieved by mixture containing 60% CBA (A4). Mortar samples containing 40% CBA (A3) as fine aggregate substitution at 56 days achieved 54.96 MPa which was 2.1% higher compressive strength than the control mortar sample (53.80 MPa). Therefore, the optimum mixture incorporating CBA was up to 40% and water/cement ratio of 0.55. While further replacement reduces the

compressive strength. It is evident that, a decrease in the water content of the mixture does not necessarily increase the compressive strength. This is due to the dominant role of the porosity of CBA compared to that induced by the higher water content. Moreover, by adding 1% SP, the compressive strength of mortar mixtures with lower W/C ratios improved up to 49% at 28 days. Since the CBA has potential slow pozzolanic reaction over time and react with portlandite to form extra C–S–H gels, this caused the interaction of the paste and aggregate, subsequently the mechanical properties of the matrices are enhanced. The increased pores in the mixture by incorporation of CBA as substitute of sand also resulted in lower density. In addition, a decrease in the water/cement ratio can cause a reduction in the density of the specimen. The unit weight increased by an average of 11% with 1% inclusion of SP.

(3) Micro-structural analysis of the mortar mixtures containing CBA: with increase in CBA contents, the pore volumes increased. Therefore, the sample with higher pore volume under compression leads to decrease in effective cross section, a lateral tension maximizes around the pores and cause local failure in these areas and reduce the strength of the matrices.

- SEM analysis shows that, the higher water demand of CBA results in a reduction in water/cement ratio that leads to smaller pore structure of the produced cementitious gel. The induced pore fractions affect the mechanical performance of the composite although the result is a lighter weight material. When the sand was replaced with 40% CBA, the composite shows dense structure with the pore size being reduced. This is

attributed to the pozzolanic reaction of CBA which causes an expansion with CSH gel by filling of the pore over time.

- XRD analysis shows that, the peak hydration reaction crystalline products, such as calcium hydroxide and calcium silicate hydrate (CSH) and calcite (CaCO3). The influence of the vitreous fraction of CBA is significant in the case of portlandite phase and the total intensity of CSH gel in mixtures containing of 40% and 60% CBA was higher like that of control sample. There is an overlap of the peak characteristics of C-S-H with that of calcite. This phenomenon is fostered in the current system by the pozzolanic activity of CBA at later age, which enhances the hydration process.

- TGA analysis shows that, the amount of CSH gel formed increases with the silica sand replacement by CBA. This is due to the pozzolanic activity of CBA, which reacts with the calcium hydroxide from the hydration reaction to give the more CSH gel in the system. The present result corroborates the strength increase with sand replacement. Therefore, the decomposition of CSH gel results in reduction strength in the samples with higher CBA proportions.

4.3 OPC- based solidified/stabilized specimen

The current section comprehensively investigates the S/S technique of CBA using ordinary Portland cement (OPC) as the main binder of samples. The OPC was added to the control hydrated OPC paste mixture and (OPC/CBA) mixtures ratios of 0.5, 1, 1.5 and 2 with constant W/C ratio of 0.55. The leachability of specific contaminated inorganic heavy metal concentrations of solidified samples subjected at deionized water, acetic acid, and nitric acid solutions was investigated. Moreover, the solidified/stabilized samples were analyzed based on standard specifications (Malaysian and USEPA) in terms of strength properties, porosity and leachability characteristics. Besides, the solidified samples evaluated for morphology performance, changes in crystalline phases and thermal characteristics. These characteristics investigation by means of OPC-based S/S technique are reported in the following sections.
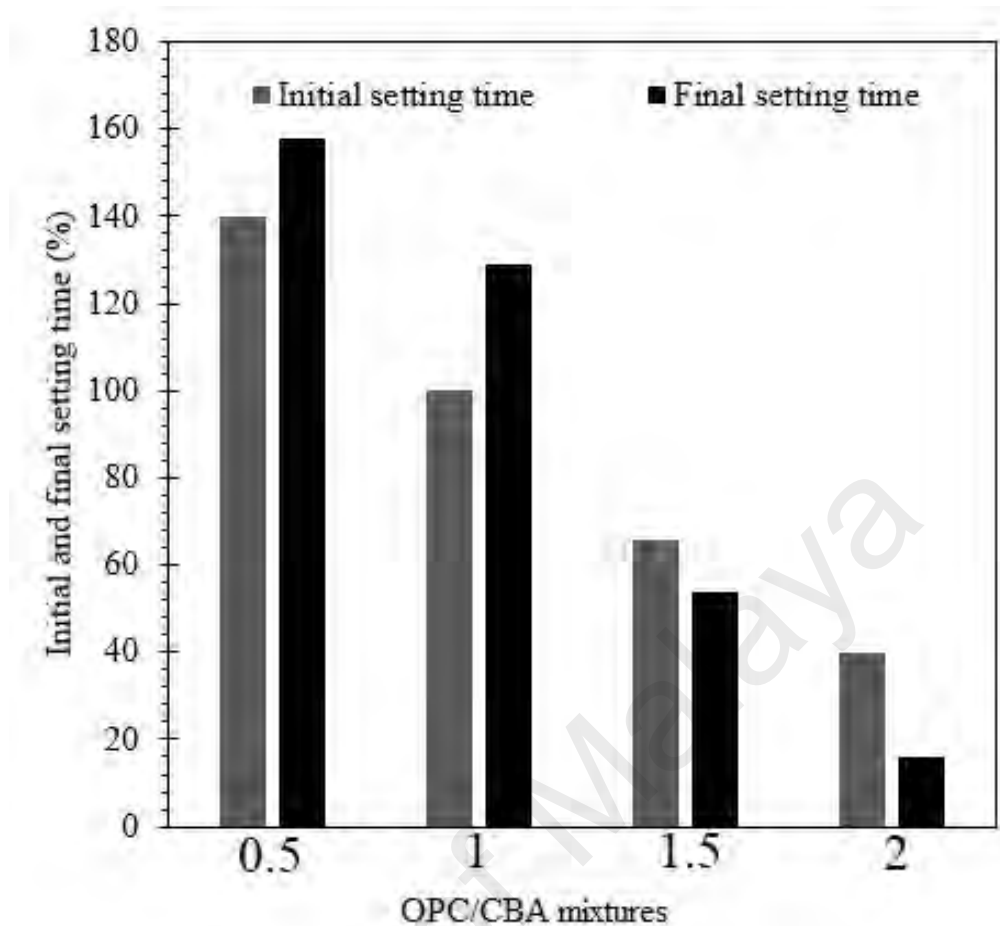
4.3.1 Initial and final setting time of solidified mixtures

The dynamic hydration process occurs, once cement reacted with water. Then, the cement phase is transformed from wet paste to solid during active hydration period. The significant of cement products such as C-S-H gel and portlandite formed at hydration process. To ascertain the appropriate mixture of cement to be used, initial and final setting time was measured. The setting time results for the OPC to CBA ratios of 0.5, 1, 1.5, and 2 mixtures is presented in Figure 4.28. The higher CBA contents will result in significantly increase initial and final setting time rates. The OPC/CBA ratio of 0.5 recorded significantly lengthened final sets of cement (>9 h) compared with hydrated control OPC (<4 h). The existence of some heavy metal contaminants such as Cu, Cd and Pb in the CBA could cause hindrance in the setting of cement and modification features of solidified samples (Stegemann & Zhou, 2009).
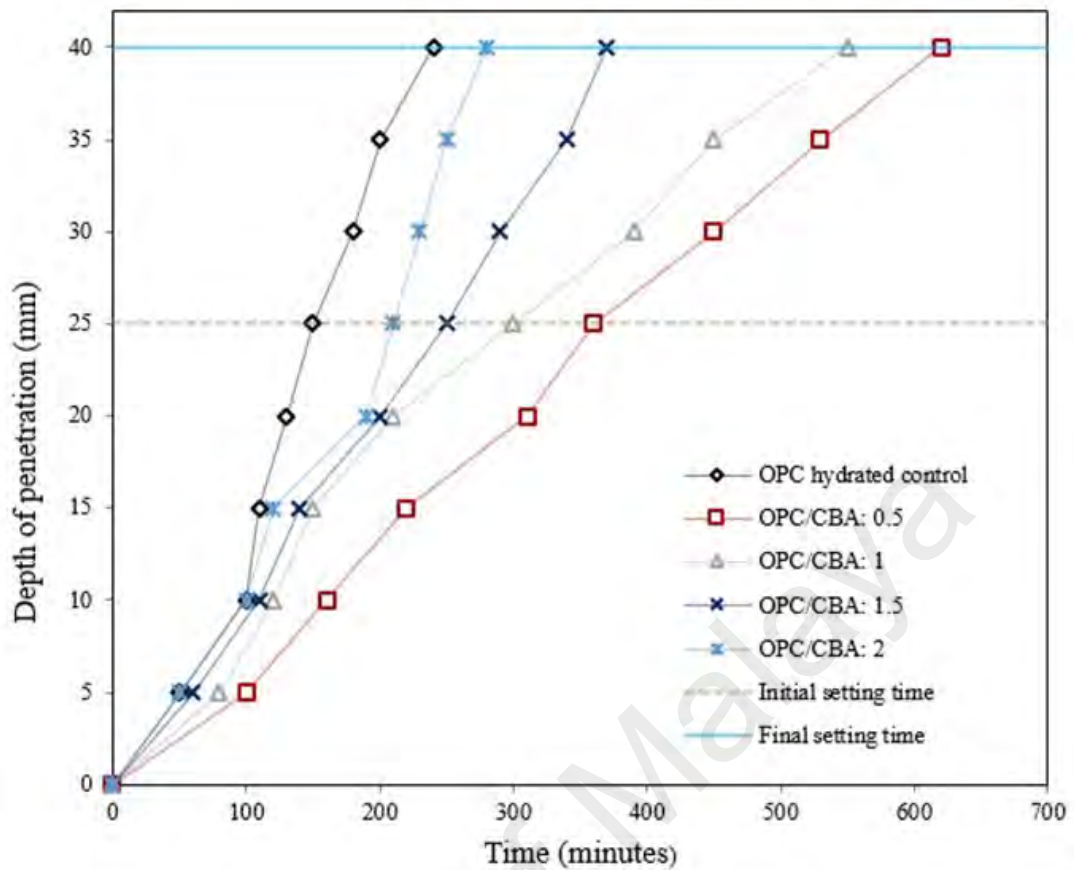
Figure 4.28: Initial and final setting times of OPC/CBA mixtures

Incorporation of CBA into OPC (OPC/CBA ratio=0.5 and 1) lengthen the setting time of cements by increase the initial and final setting times of 140 to 158% and 100 to 129%, compared to hydrated OPC control mixture, respectively (Figure 4.29). While, increase in OPC proportions in the mixtures OPC/CBA ratio=1.5 and 2 decreases the initial and final setting times 66 to 54% and 40 to 16%, respectively (Figure 4.29). Moreover, CBA up-takes more mixing water in paste mixtures, which leads to decrease in water content for OPC hydration mixtures. This would manifest by postponement or reduction in hydration actions of the OPC contents (Jaturapitakkul, 2003). Therefore, the OPC/CBA ratios mixtures =1.5 and 2 achieved well treated by OPC as initial and final setting times reduced up to 23% compared to hydrated OPC control mixture.

Figure 4.29: Performance of initial and final setting times of OPC/CBA mixtures

4.3.1.1 The effect of heavy metals on OPC hydration setting times

Generally, the constitute of C_3S in cement makes forming crystalline products C-S-H gel and $Ca(OH)_2$ that lead the setting of cement hydration. The cement alkaline with pH of about 12 is resulted by calcium hydroxide (Mehta & Monteiro, 2006). Hydration of typical Portland cement involving the setting time of major products are illustrated in Figure 4.30a. The cement setting of crystalline models, the hydration growth of hexagonal calcium hydroxide crystal starts and fills up the space between the cement granules with rich silicate layer on its surface, which stop to release of calcium and silicate ions from cement by reducing the movement of water to cement surface. The calcium silicate hydrate raises external of cement granule and design needles such as ettringite. The needle progress linked with other needles and shaped Tobermorite crystal.

Figure 4.30 shows the mechanism of interference by some contaminated metals such as Zn, Cr, and Cu that caused delaying in hydration process. The pure OPC hydration known as the aluminate structures are accomplished by producing ettringite forming around gel coating less than 10 min of mixing cement with water. Normal hydration reaction is proceeding and further products of hydration "burst" through (Figure 4.30b1). The formation of the gel around cement grains is an important reaction rate determining step, when waste is introduced this step is modified (Figure 4.30b2). Modification may be complexation or precipitation effects rendering the gel layer essentially impermeable, e.g. complexation and removal of calcium at the surface of hydrating cement grains by anionic or cationic agents will limit the production of both $Ca(OH)_2$ and C-S-H (Malviya & Chaudhary, 2006b).

a)

b)
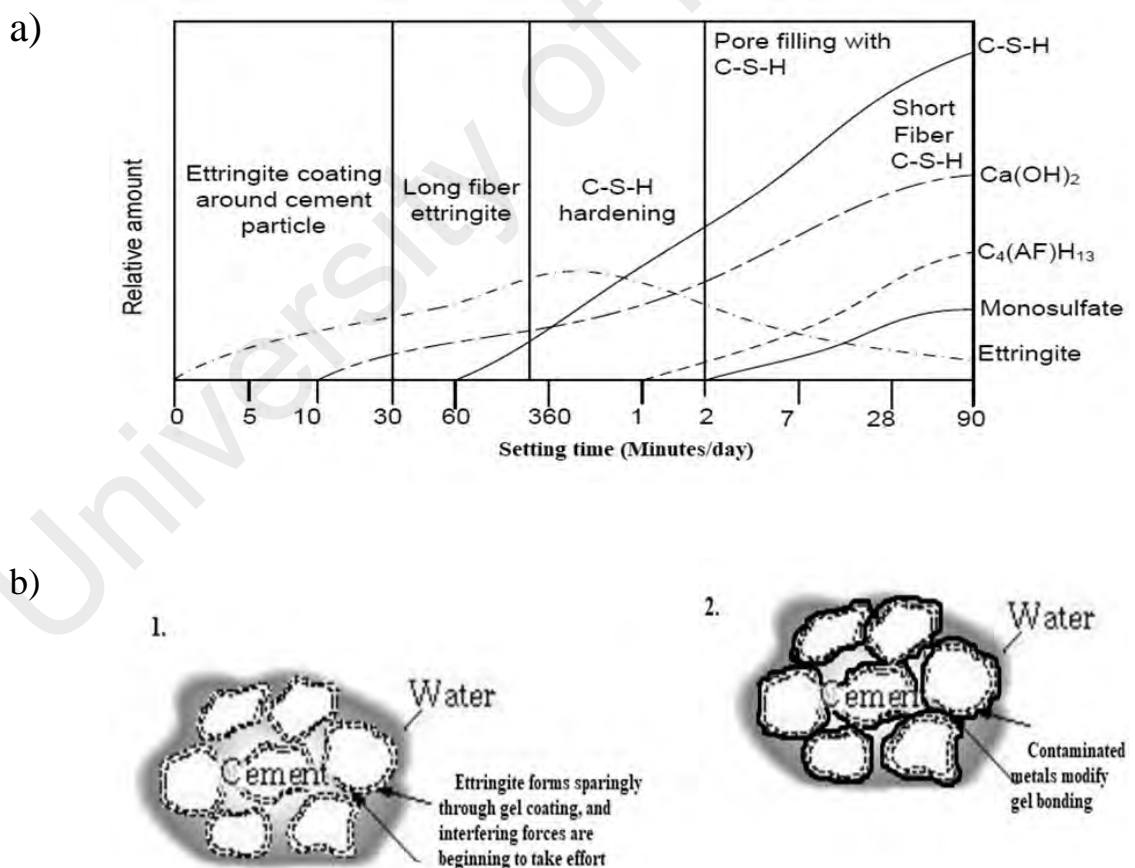
Figure 4.30: Mechanism of a) Hydration on the cement products b) Effect of heavy metals on hydration process

4.3.2 Compressive strength of solidified samples

The strength development of solidified samples at OPC/CBA ratios of 0.5-2 is presented in Figure 4.31. The strength increased as the ratio of the OPC content was increased in which the hydrated sample of pure OPC recorded compressive strength of 48.1 MPa, that is higher than the strength of the CBA mixtures at all ages. At 7 days, the compressive strength value of solidified samples at OPC/CBA ratios of 0.5, 1, 1.5, and 2 compared to control OPC hydrated sample decreased by 45%, 32.5%, 19%, 8.8%, respectively. At 28 days, the compressive strength value of solidified samples at OPC/CBA ratios of 0.5, 1, 1.5, and 2 compared to control hydrated OPC sample decreased by 43.6%, 26.7%, 21.3%, 6.5%, respectively.

Overall, less strength reduction was attained when higher proportion of OPC was used in the solidified/stabilized samples. This outcome can be associated with the growth in the amount of tricalcium silicate and dicalcium silicate in the specimens with higher OPC content which enhances the stabilization of CBA hardened matrices by the production of more calcium–silicate–hydrate (CSH) (Yin et al., 2007). Remarkably, all solidified samples at OPC/CBA ratios 0.5-2 exceeded the standard (Table 2.10) stipulated value of 0.414 MPa for safe disposal of solidified specimens at 28 days of capsulation matrices. Moreover, the solidified samples at OPC/CBA ratios 1, 1.5 and 2 achieved the equivalent strength mortar limit of 20 MPa at 3 days of air curing age. Except the solidified sample at OPC/CBA ratio of 0.5 that gained it at 14 days of air curing age.

Therefore, such high strength implies that solidified samples of OPC/CBA=1, 1.5, 2 have a great potential for sustainable application such as engineering fills, precast walls, pavement blocks and bricks.
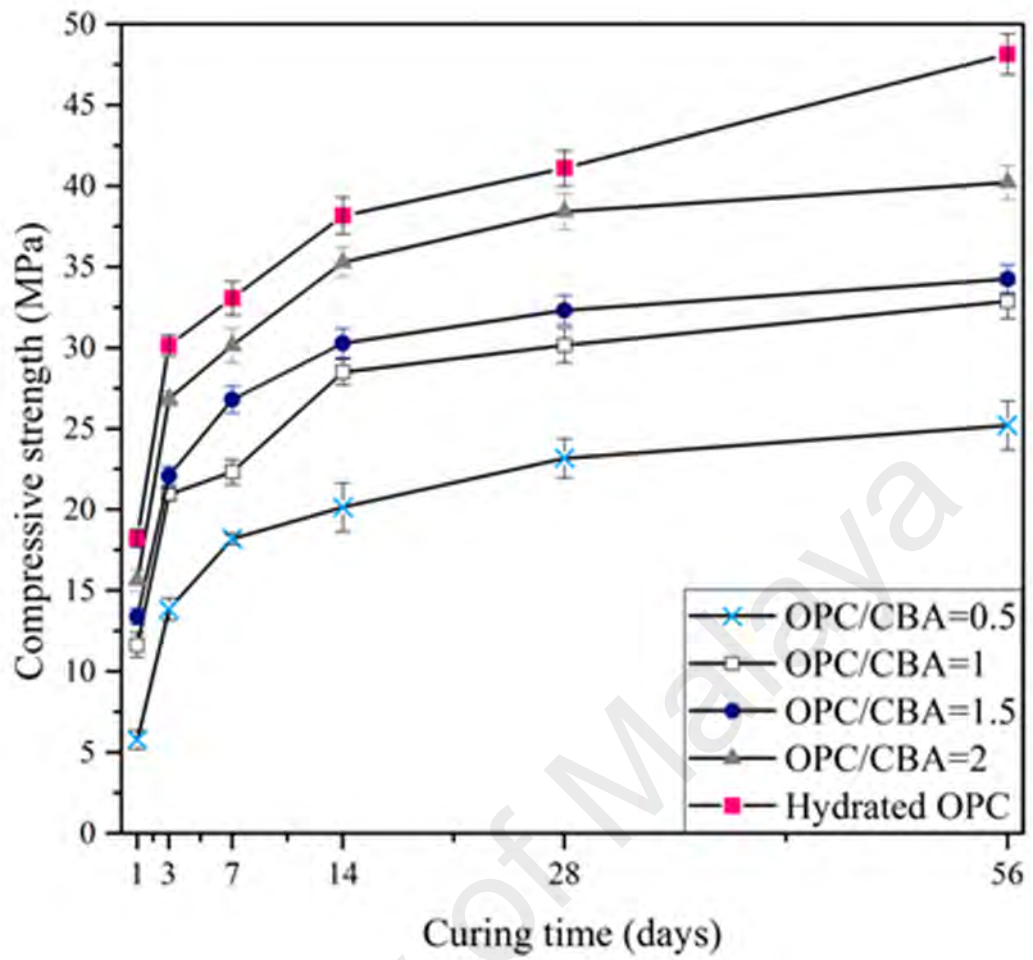
Figure 4.31: Compressive strength of solidified samples at OPC/CBA ratios

4.3.3   Permeable porosity of solidified samples

Figure 4.32 shows, the 28 days permeable porosity and density properties of the stabilized specimens at OPC/CBA ratios of 0.5-2. The bulk density of the solidified CBA was 1070, 1180, 1290 and 1420 kg/m^3 for solidified samples with OPC/CBA ratios of 0.5, 1, 1.5, and 2, respectively (Figure 4.32). The decrease in density is attributed to the porous structure of CBA. Further, the CBA particles do not roll over one another easily due their disordered particles shape, and thus the formation of extra porosity because of lack of proper compaction is possible. In contrast, the density of hardened samples with high cement proportion is increased due to better compaction and more hydration products which fill up the void spaces (Malviya & Chaudhary, 2006a).

Basically, permeable porosity is a measure of the ease liquid exchange through the matrix that shows mobility of leaching metals from the porous texture and total volume of capillary voids or pores was measured as porosity; pores decreases with increase in OPC proportions expressly at OPC/CBA ratios of 1.5 and 2 as shown in Figure 4.32. The contaminant heavy metals filled the cement pore voids and consequently results in reduction permeable pore (17%) in the solidified sample with OPC/CBA ratio of 2. Such low permeable porosity indicates reduction mobility in the solidified samples and slower transferring of contaminated metals from solidified sample to leaching waters. Higher permeable porosity of 40% was found when the solidified sample with higher mobility of metals at OPC/CBA ratio of 0.5 (Figure 4.32). This permeable porosity provides surface adsorption toward CBA incorporated in the cement. The porosity is an important factor that affects the strength of solidified waste. The porosity increases with increasing CBA contents of the solidified sample and resulted in lower strength. The solidified sample with higher pore volume under compression leads to decrease in effective cross section, a lateral tension maximizes around the pores and cause local failure in these areas and reduce the strength of the matrices.

Therefore, solidified samples at OPC/CBA ratios of 1.5 and 2 achieved the standard (Table 2.10) stipulated value of 15-25% porosity for safe disposal of solidified specimens at 28 days of capsulation matrices. Although, the solidified samples at OPC/CBA ratios of 0.5 and 1 achieved higher porosity with lower density categorized as lightweight mixtures but, the porosity value exceeded the standard specification.
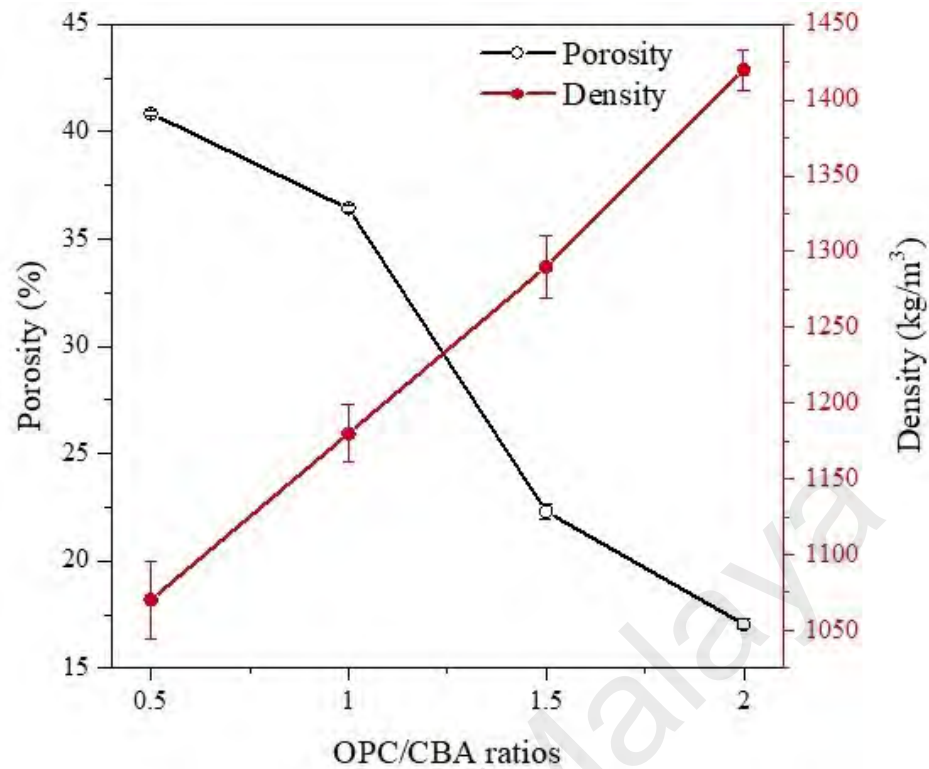
Figure 4.32: Porosity and density of solidifies samples at OPC/CBA ratios

### 4.3.4 Leachability of solidified samples

The leaching contaminated heavy metals concentrations at 3, 7, 14, 28 and 56 air curing days in the solidified samples was derived from crushed and whole block leachate methods and presented in Figure 4.33-Figure 4.37. All figures analyzed based on the white color that shows less leaching rate and more color which is presented high leaching rate (Figure 4.33 and Figure 4.37).

Generally, the values for all four metals measured in OPC treated crush and whole block leachates were either untraceable or significantly below the permitted leachability limits of the Malaysian Environmental Quality Orders (EQA, 1979). The untreated CBA contains high initial amounts Cu (2.66 mg/l) and lesser concentrations of Cd (0.071 mg/l), Ni (0.34mg/l), and Pb (0.20mg/l). Figure 4.33 and Figure 4.34 present CBL and WBL deionized water leachates, respectively. The leachability of selected contaminated metals in both leachates was primarily higher, but evidently diminished with longer age. Cd and

Ni concentrations were highest leached out from the solidified samples in CBL and WBL deionized water solutions, almost reaching the limitation of the value specified by the Malaysian standard as depicted with (Figure 4.33 and Figure 4.34).

The precipitated form of cadmium known as Cd $(OH)_2$ immobilized in most of the cement hydration system which has lower solvability compared to other metals (Conner, 1990). Cu and Pb is expressively immobilized by OPC hydration in CBL and WBL deionized water solution at 56 days (Figure 4.33 and Figure 4.34). The solidified sample at OPC/CBA ratios of 1.5 and 2 performed better immobilization of four metals (Cu, Cd, Ni and Pb) at all days. At higher OPC/CBA ratio more cement proportion is available to bind with the contaminants while reducing the interference effect of the heavy metal in the CBA.

Figure 4.35 and Figure 4.36 present CBL and WBL acetic acid leachates, respectively. CBL/WBL samples with acetic acid solutions present higher leachability than deionized water solutions. The leachability of selected contaminated metals in both leachates was primarily higher, but evidently diminished with longer age. Ni metals concentrations in crush block and whole block acetic acid solutions reaches significantly higher leachates than samples leachability in the CBL/WBL deionized water solutions and both leachates were below the restricted standard limits given in (Table 2.9). Leached Cu, Cd and Pb concentrations were expressively immobilized at OPC /CBA ratio of 2 at 56 days (Figure 4.35 and Figure 4.36). The leaching of four metals was higher in CBL solutions than WBL solutions. This is attributed to the higher surface area of the crushed sample (Zain et al., 2004). As shown in Figure 4.37, Cd was found as the highest leached metals in CBL samples of nitric acid solution. The concentration of four contaminated metals was lower in the deionized water leachates compared to nitric and acetic acidic leachates. Leached Cu and Pb concentrations were significantly immobilized at OPC /CBA ratio of 2 at 56 days (Figure 4.37).
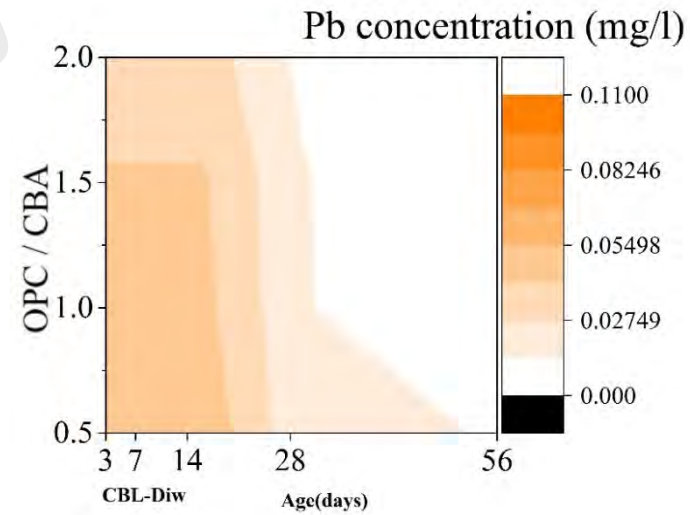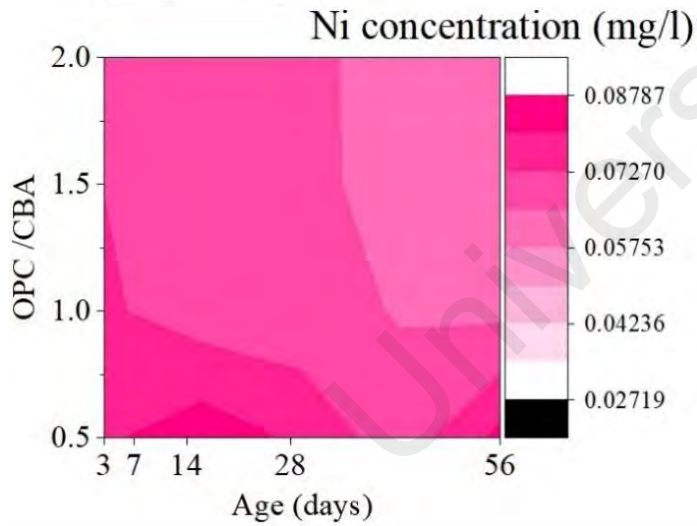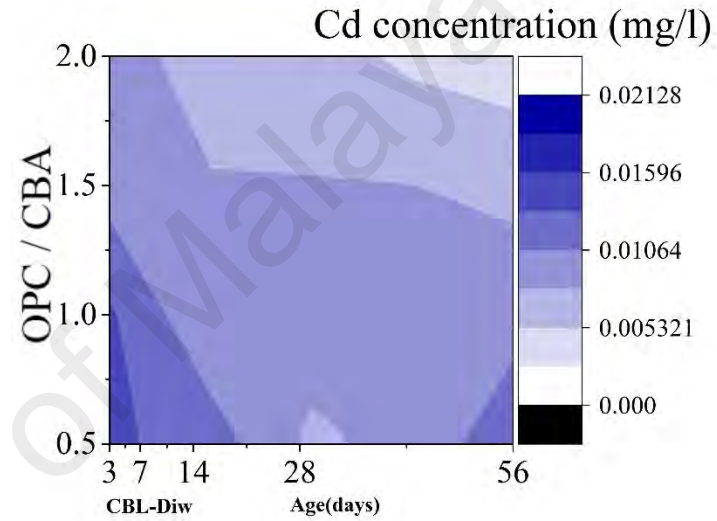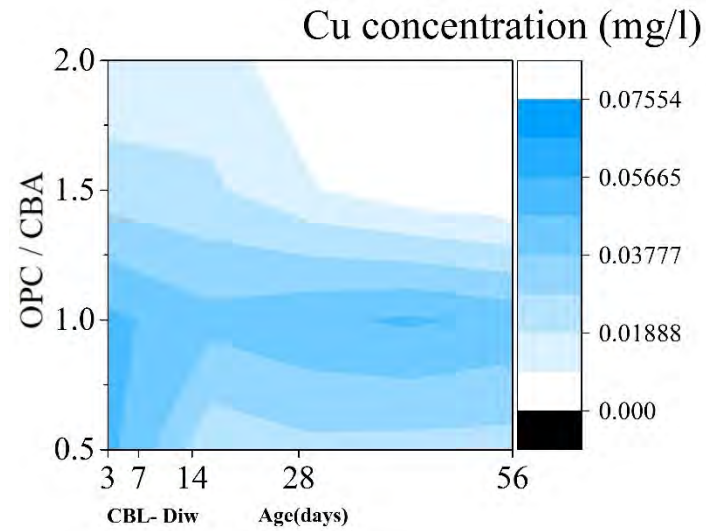
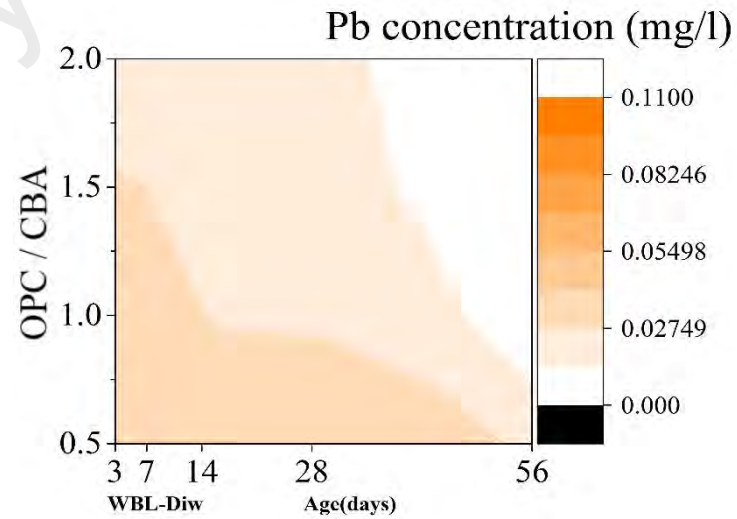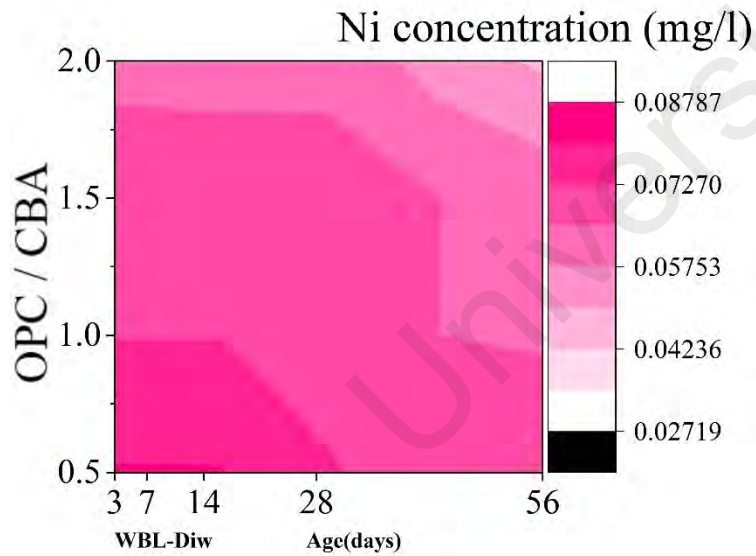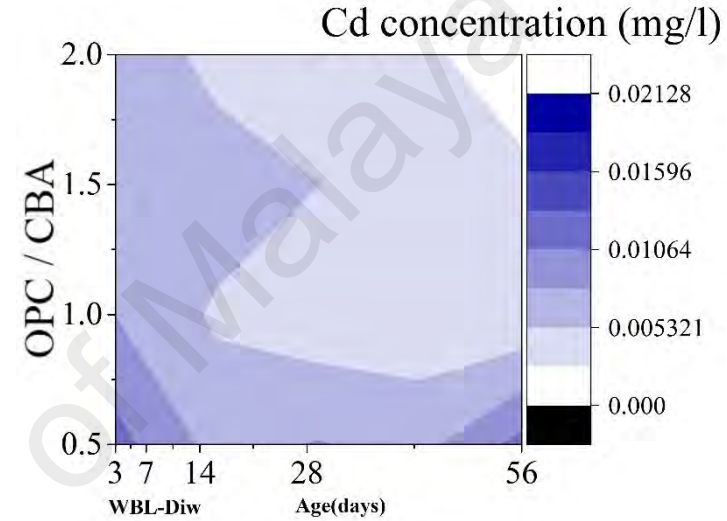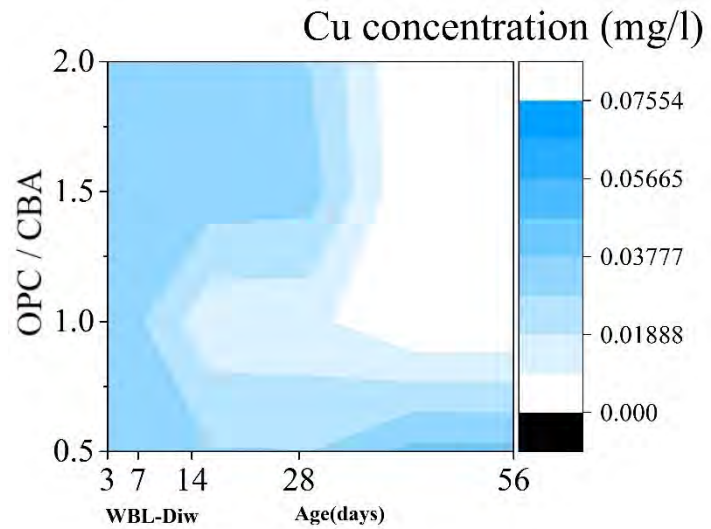**Figure 4.33: Metals leachability of CBL with deionized water solution**

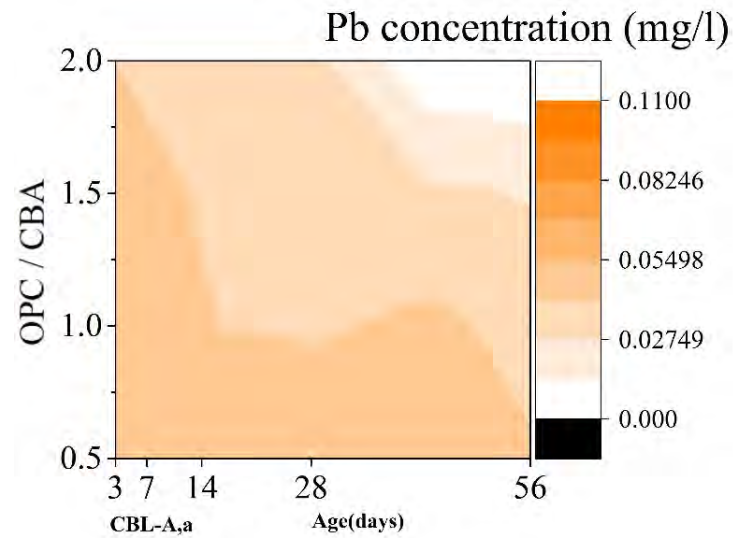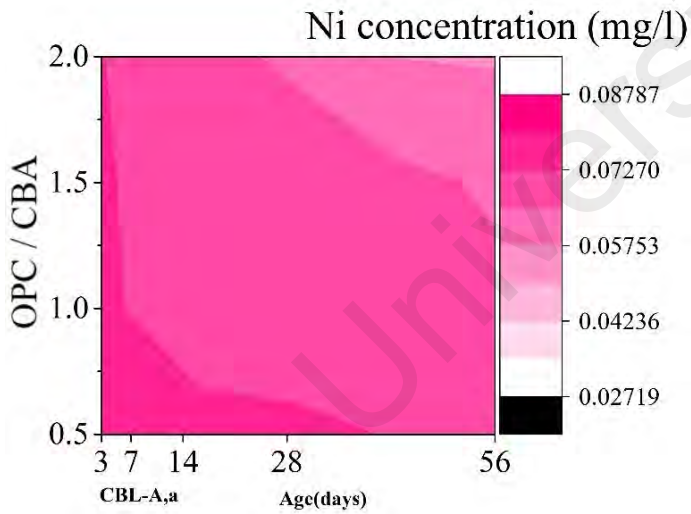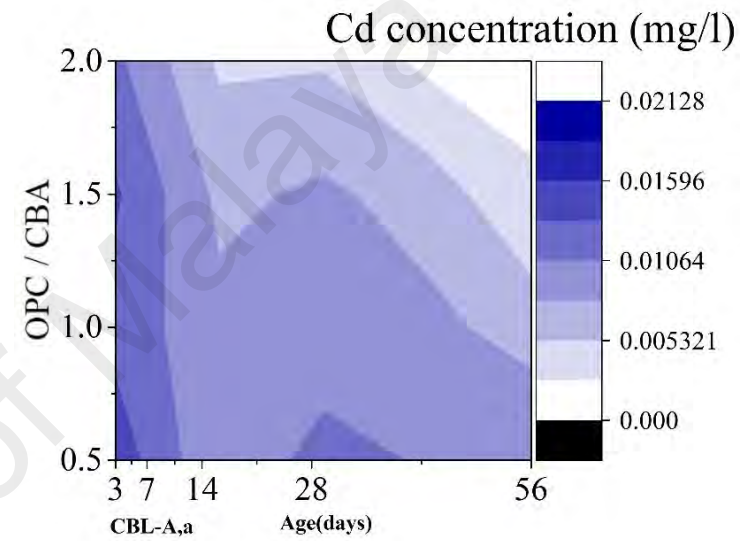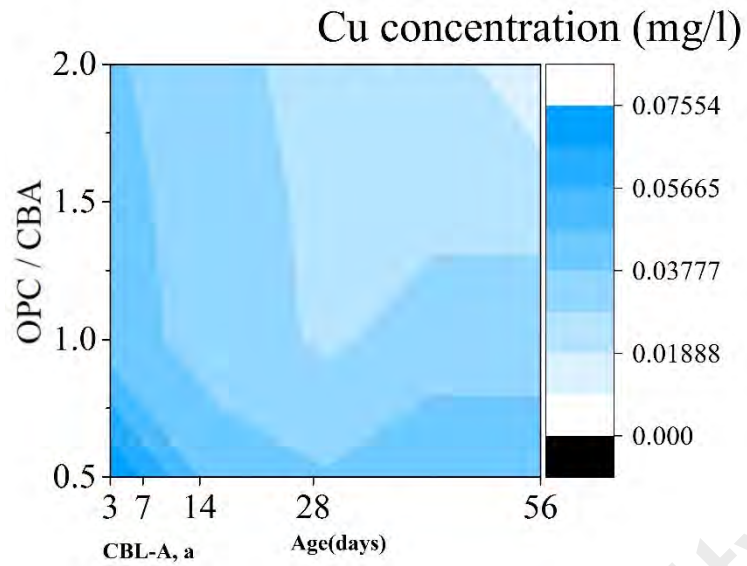**Figure 4.34: Metals leachability of WBL with deionized water solution**

Figure 4.35: Metals leachability of CBL with acetic acid solution
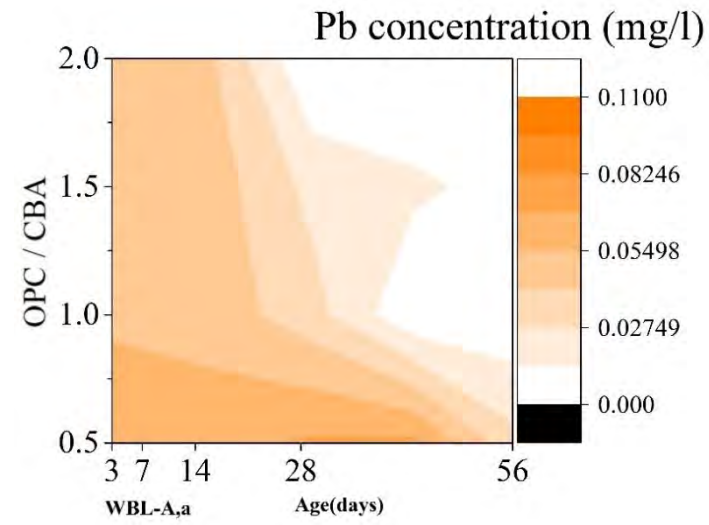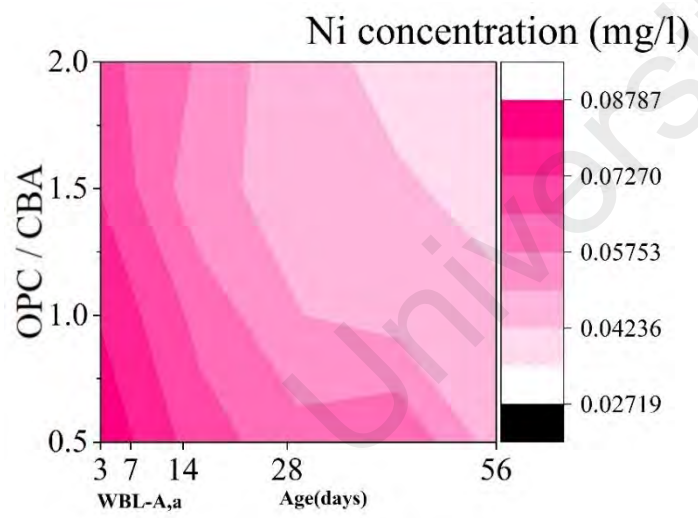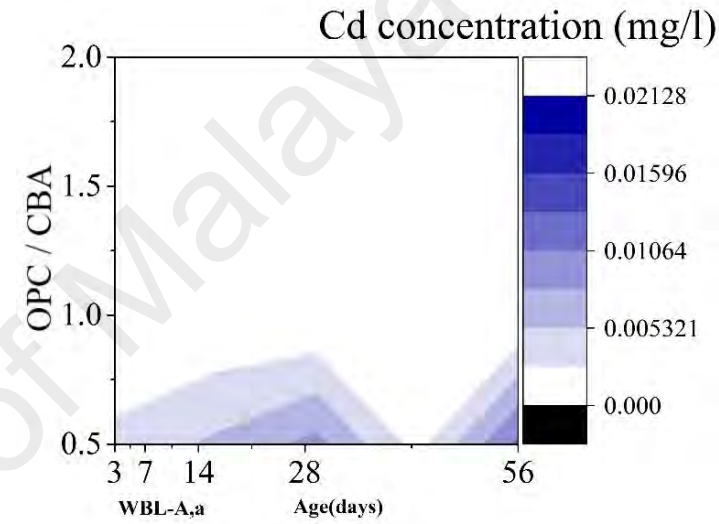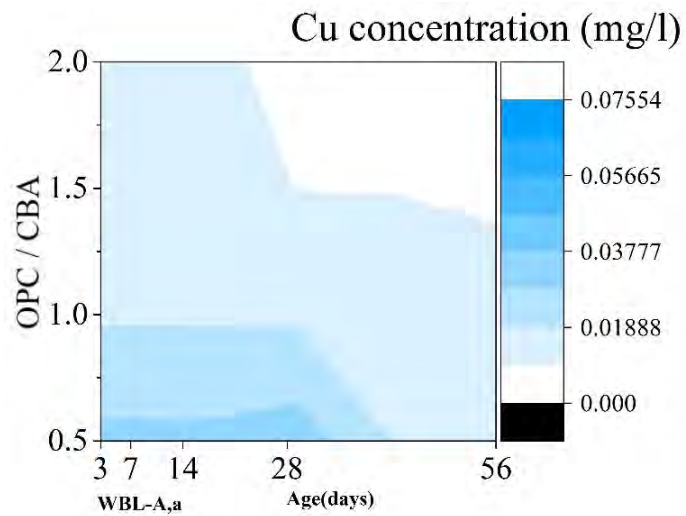
Figure 4.36: Metals leachability of WBL with acetic acid solution
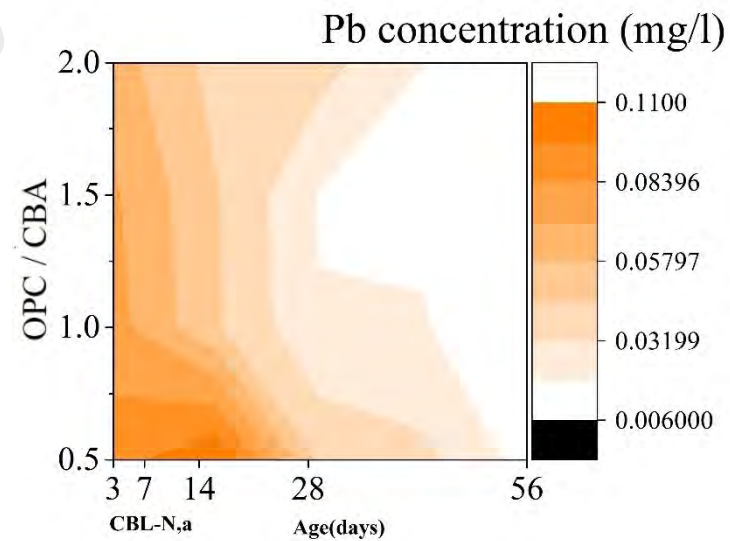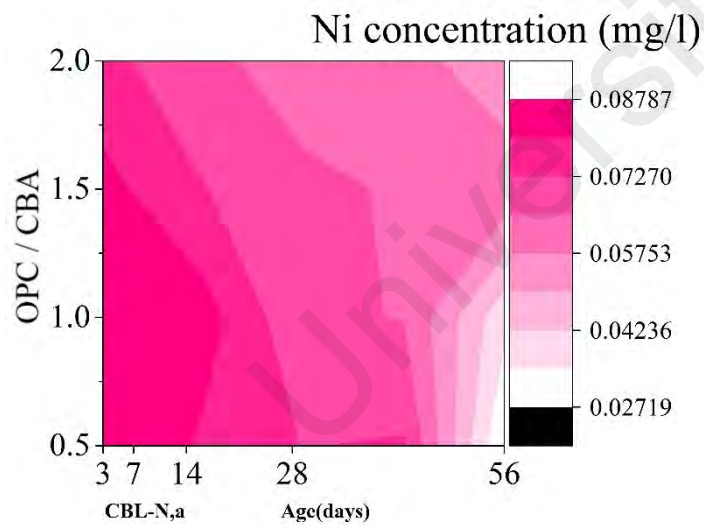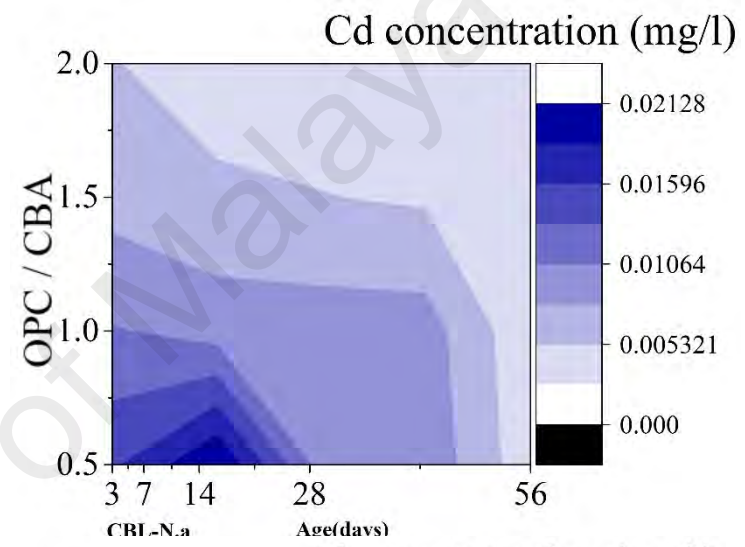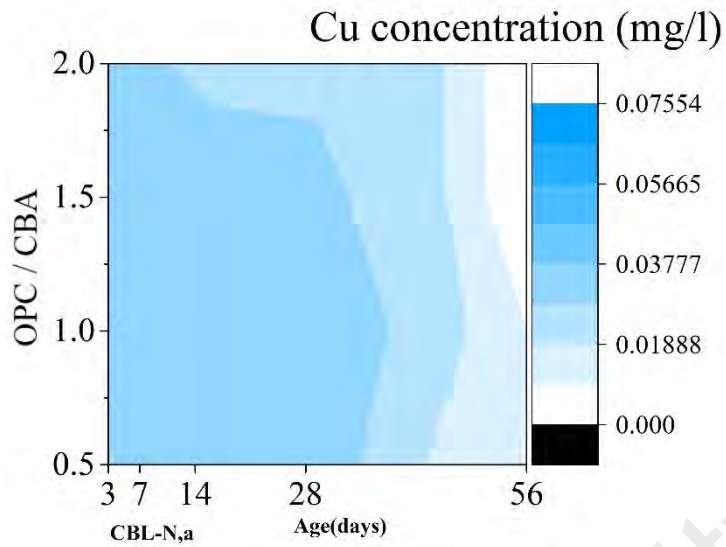
Figure 4.37: Metals leachability of CBL with nitric acid solution

Figure 4.38, Figure 4.39 and Figure 4.40, indicate the accumulated leaching percentage reduction of the selected four metals in a duration of 56 days for crush and whole block using different solutions of deionized water, acetic acid and nitric acid. The Cu ion reached the lowest leachability rate after stabilization at all solutions. As shown in Figure 4.38, the leachability of Cu ion is up to 9% and 6.61%, at OPC/CBA ratio of 1 and 0.5 in the CBL and WBL leachates respectively. The leachability of Cd ion, is up to 80%, and 65%, at OPC/CBA ratio of 0.5 in CBL and WBL leachates of deionized water solution, respectively (Figure 4.38). It is obvious that considerable reduction in leachability for copper and cadmium resulted in the crush block deionized water leachate at OPC/CBA ratio of 2. The leachability of Ni and Pb in WBL leachate of deionized water solution are highest at OPC/CBA ratio of 0.5 (Figure 4.38).

The superb reduction leachability of Cu, Cd, Ni and Pb ions are 1%, 1%, 66% and 37% at OPC/CBA ratio of 2 in the whole block acetic acid solution, respectively (Figure 4.39). However, the leachability of all metals is highest at OPC/CBA ratio of 0.5 after 56 days stabilization in all the whole block and crash block leachates using deionized water, acetic acid and nitric acid solutions. The leachability of Cu, Cd, Ni and Pb ions are 4%, 29%, 85% and 89% at OPC/CBA ratio of 2 in the crush block nitric acid solution, respectively (Figure 4.40).

Overall, the highest reduction of leachability for selected metals is at (OPC/CBA) ratio of 2 at 56 days. This shows that OPC based S/S technique can successfully provide safe disposal of CBA. Equations 4.1 and 4.2, show the highest to lowest immobilization rates of four metals for all solutions at (OPC/CBA) ratio of 2 as following:

Cu> Pb> Ni >Cd (Deionized water and acetic acid solutions)   (4.1)

Pb>Cu>Cd>Ni (Acetic acid solution)   (4.2)
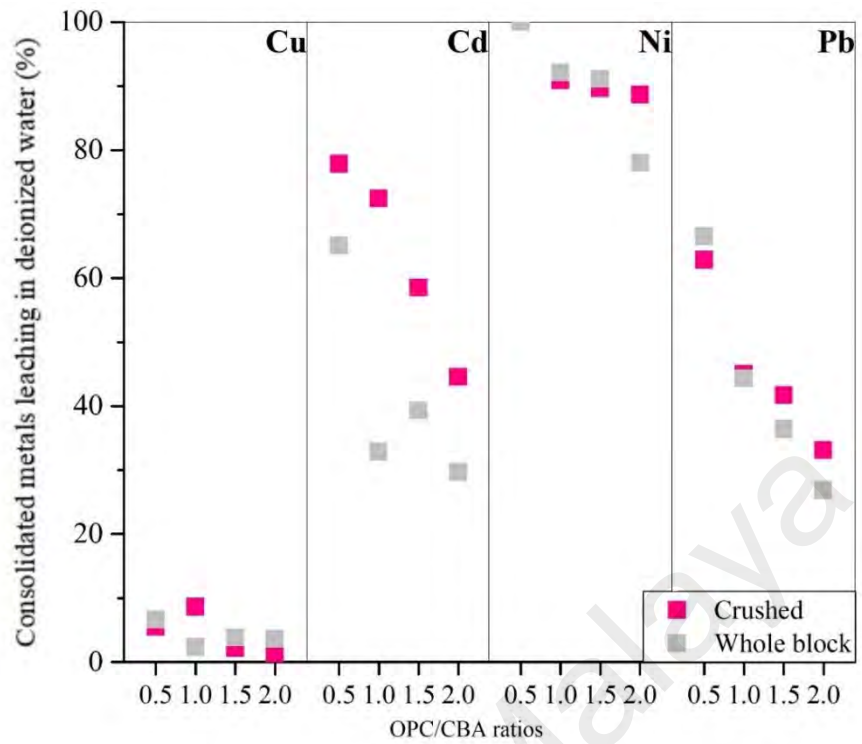
Figure 4.38: Leachability of metals in deionized water solution of crush and whole block
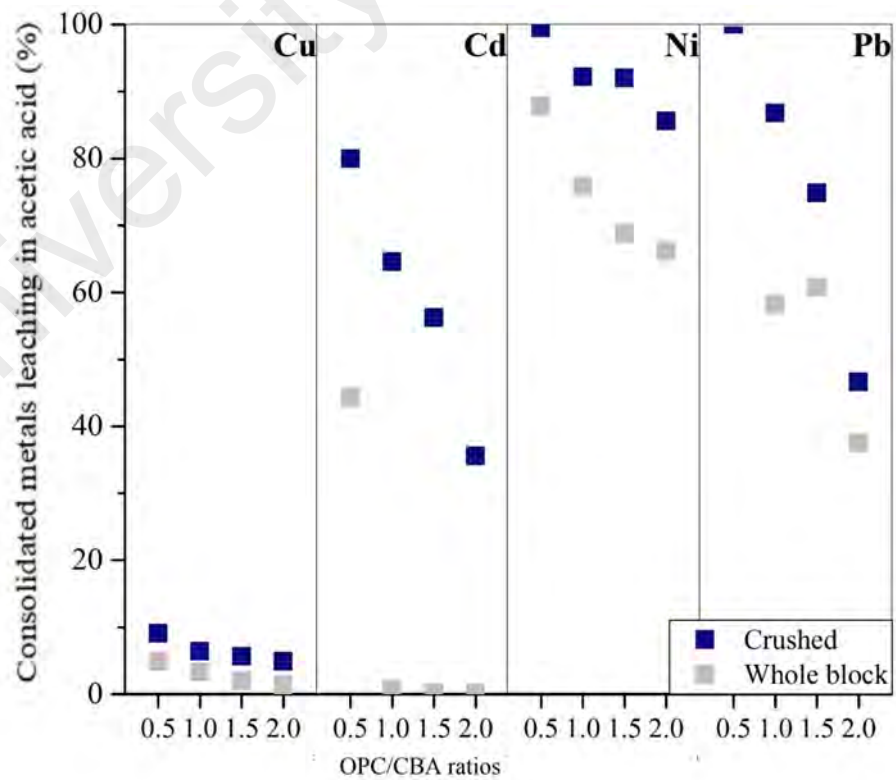
Figure 4.39: Leachability of metals in acetic acid solution of crush and whole block
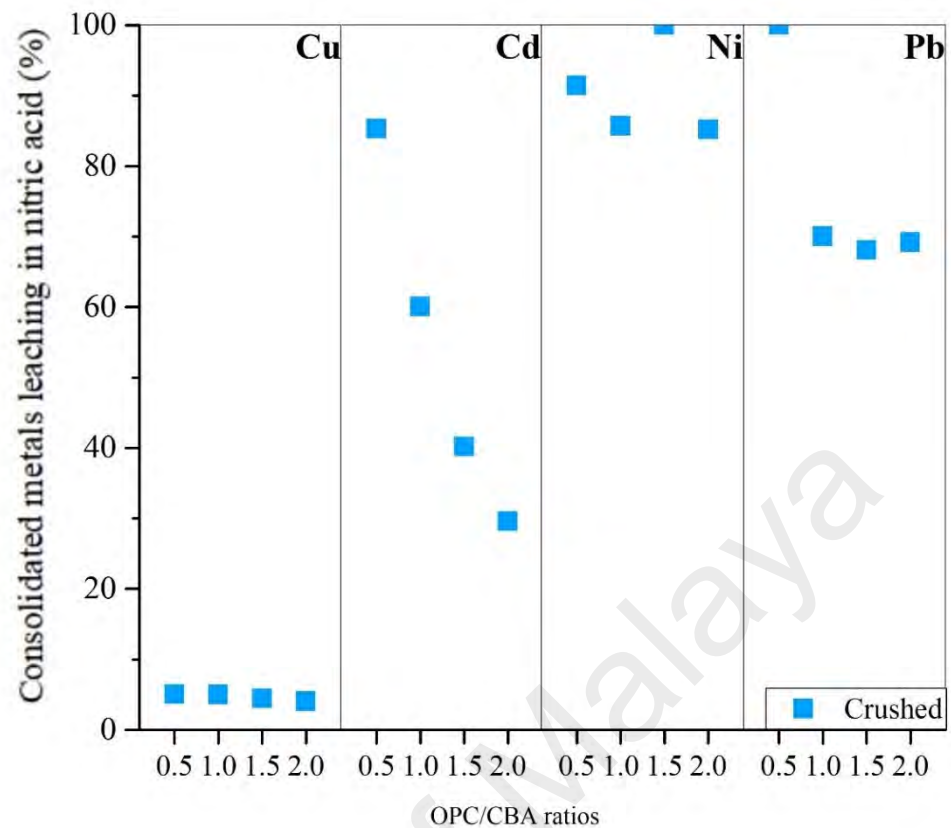
Figure 4.40: Leachability of metals in nitric acid solution of crush block

4.3.4.1 Alkalinities and pH of leachates

The pH value of solidified samples in both crushed and whole block leachates at all OPC/CBA ratios are presented in Figure 4.41-Figure 4.43. It was observed that the pH of the leachates in the crushed block deionized water was in the range of 12.30 to 12.97 (Figure 4.41), 11.32 to 12.50 in acetic acid (Figure 4.42) and 12.01 to 12.92 in nitric acid (Figure 4.43). The pH of the leachates was less alkaline in WBL samples in the range of 9.80 to 11.90 (deionized water) and 6.25 to 11.20 (acetic acid) at all OPC/CBA ratios. Higher alkaline of pH in the crush block leachates attributed to higher surface area in the crushed specimens that increase the fluidity of matrix (Zain et al., 2004). Basically, heavy metals leachability is measured by pH value of the solution. The diffusion of hydrogen ions H+ and acetate ions into the leached layer is resulted in acetic acid solution.

Free hydrogen ions can attack the cement edge at pH of 8.25, which caused the leaching of metals at the cement surface (Cheng, 2012).

The effect of OPC/CBA ratios on the change in alkalinity of the leachates was more tangible for the acetic acid solution where alkalinities of solidified samples at OPC/CBA ratios of 0.5 to 2.0 increased (Figure 4.42). On the other hand, the fluctuation in alkalinities of deionized water and nitric acid solutions were edgier at OPC/CBA ratios of 0.5 to 2.0 (Figure 4.41 and Figure 4.42). The specimens with higher OPC content at OPC/CBA ratio of 2 provide the most intense hydration reaction which resulted in higher alkalinity and less leachability (Yin et al., 2007). The study conducted by Valls and Vasquez (Valls & Vàzquez, 2000) supported this observation whereby alkalinity of the leachate could improve neutralization and decomposition of the heavy metal composites confinement in the waste. Therefore, all four metals (Cu, Cd, Ni and Pb) immobilized at OPC/CBA ratio of 2 which the pH is more alkaline.
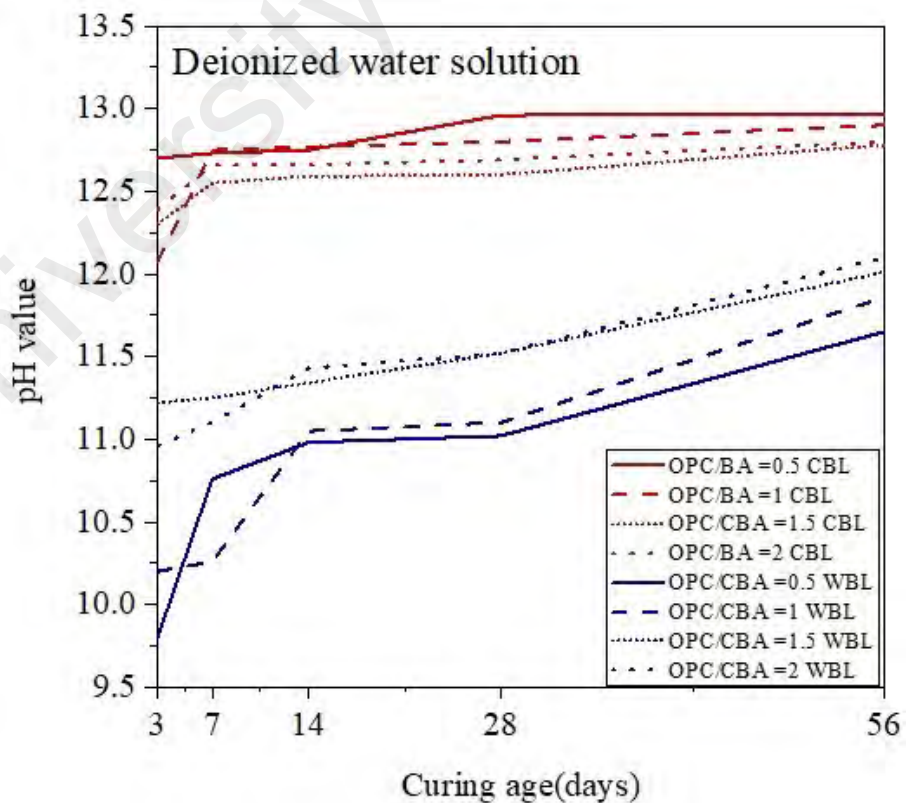
Figure 4.41: pH value of CBL and WBL in deionized water solution
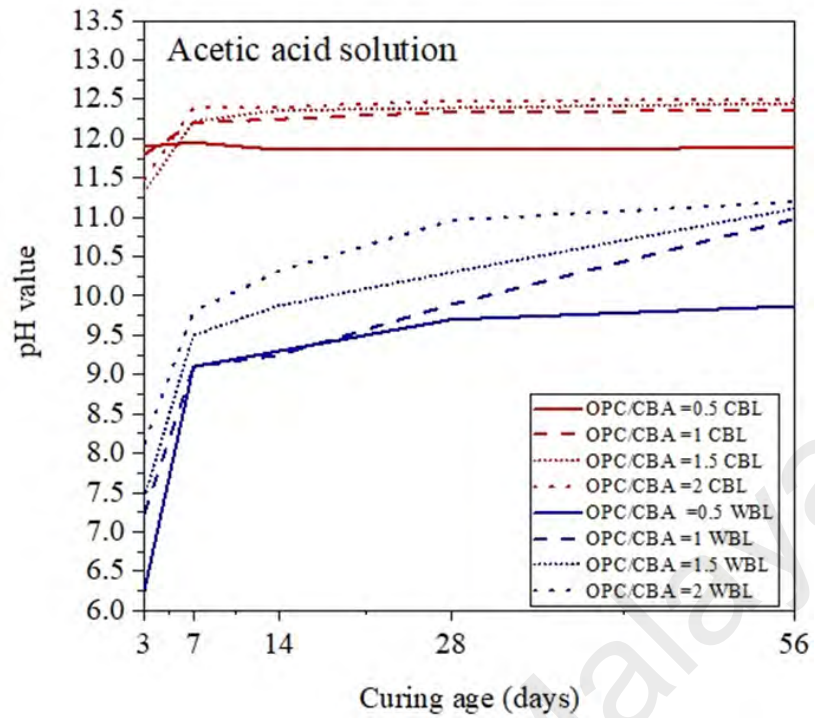
Figure 4.42: pH value of CBL and WBL in acetic acid solution
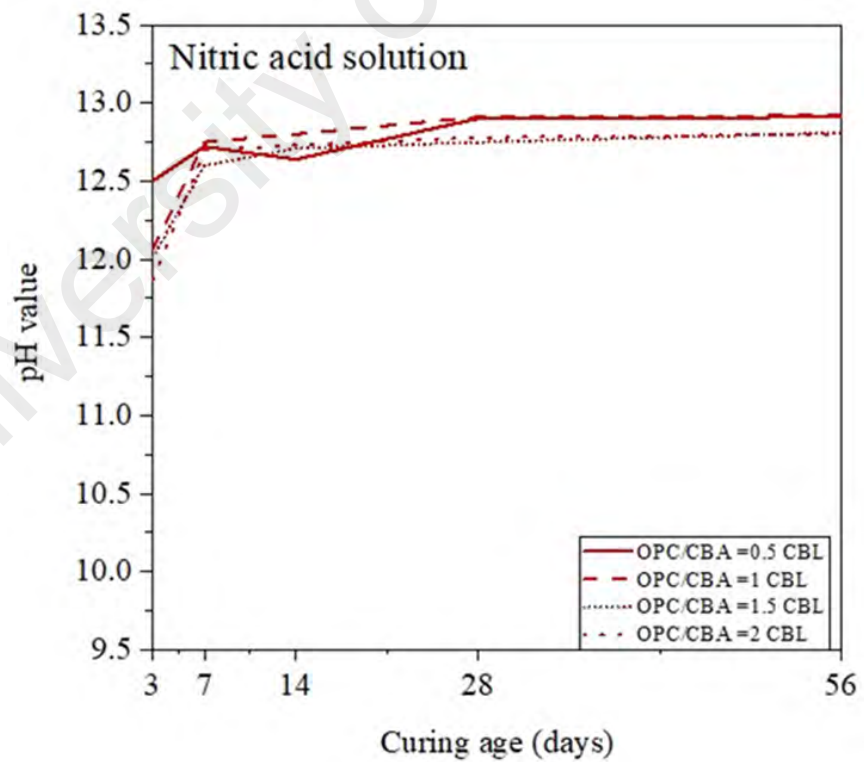
Figure 4.43: pH value of CBL and WBL in nitric acid solution

4.3.5   Microstructure analysis of solidified/ stabilized samples

The microstructure properties show the integrity of OPC-based stabilized/solidified samples. The strength and durability performances of solidified samples can be related by these microscopic views.

4.3.5.1 SEM analysis

The SEM micrographs present the solidified matrices strength and leachability performance in terms of permeable porosity, hydration products and physical properties. Figure 4.45 illustrates the micrograph of OPC-hydrated control sample. Figure 4.44-Figure 4.48 show the performance of the solidified sample at different OPC/CBA ratios through SEM imaging in two magnifications. They illustrate that CBA was substantially compressed and bounded to cement hydration products. The close-up micrograph of the hydrated OPC suggests that the control sample consists of the needle shape development of ettringite which places in the space between cement clinker and C-S-H gel (Figure 4.45). The OPC-hydrated surface was dense and interlinked with less air void spaces. The product formation of C-S-H gel was found in the hydrated OPC sample. Figure 4.44, shows that when the specimen contains higher amount of CBA, the pore size could increase to about 100µm due to the inherent porosity of CBA particles and the air void which was trapped between the agglomerated particles and the cement paste. The strength of specimens increased with higher OPC/CBA ratios due to higher OPC contents. This is in an agreement with the ICP results (Section 4.3.4). The surface structure of sample at OPC/CBA ratios of 1 and 1.5 are dense which resulted in higher strength property (Figure 4.46 and Figure 4.47). Figure 4.48 shows at higher OPC/CBA ratio of 2, specimen exhibited more homogenous texture. The higher strength of the OPC-based solidified sample is associated with the more homogenous surface of the hydrated cement product (C-S-H gel). The surface solidified sample at higher OPC-CBA ratio, due to the higher

contents of OPC, more compacted and interconnected CBA particles in the C-S-H product were formed. Furthermore, the vitreous fraction of CBA reacts with the hydration products, provides more gel and causes fewer air void space. Also, the heavy metals hydroxide is observed in filling between pore (Figure 4.48). As a result, solidified OPC samples exhibited ettringite and C-S-H as the main products of cement hydration. However, the glassy phases of CBA participate in cementitious reaction leads to reduction in porosity through the production of more cement hydration products, mainly C-S-H with higher surface area that traps the heavy metals.
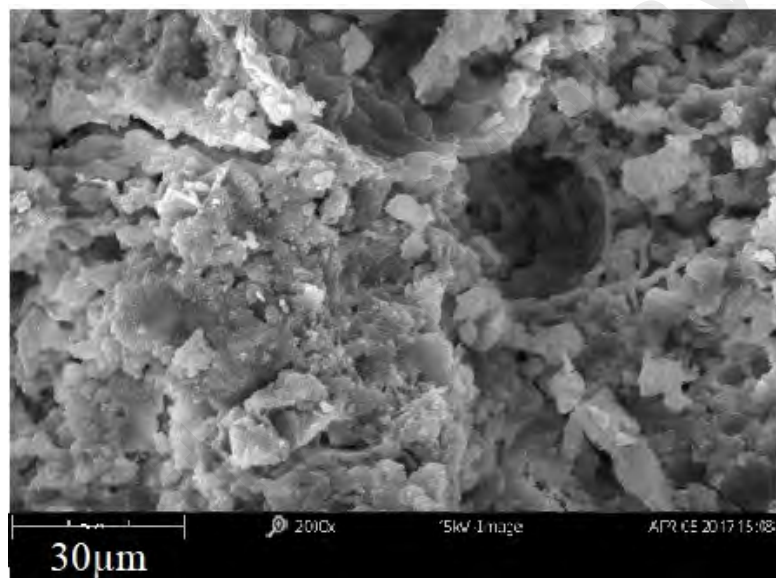
Figure 4.45: Morphology of OPC hydrated sample
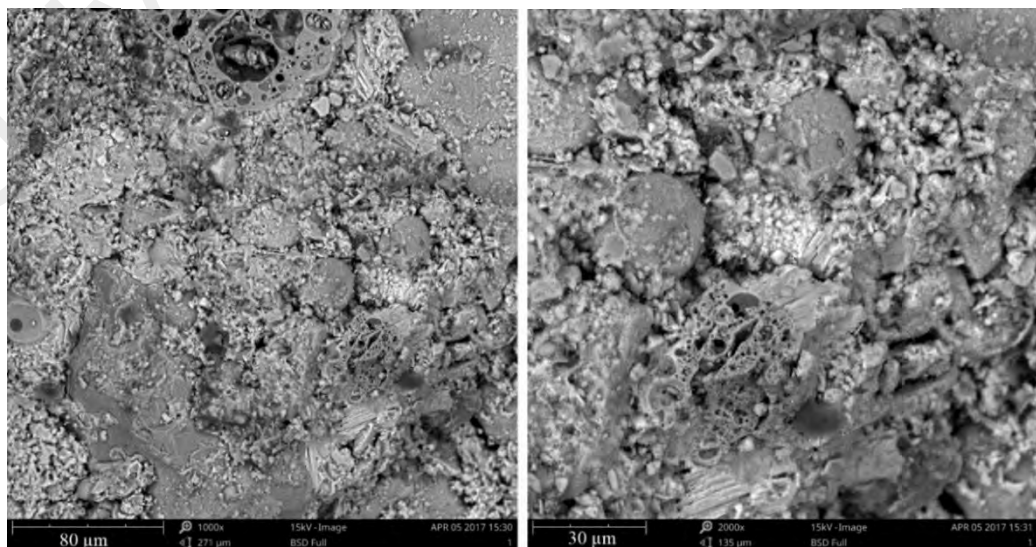
Figure 4.44: Morphology of solidified sample at OPC/CBA ratio of 0.5
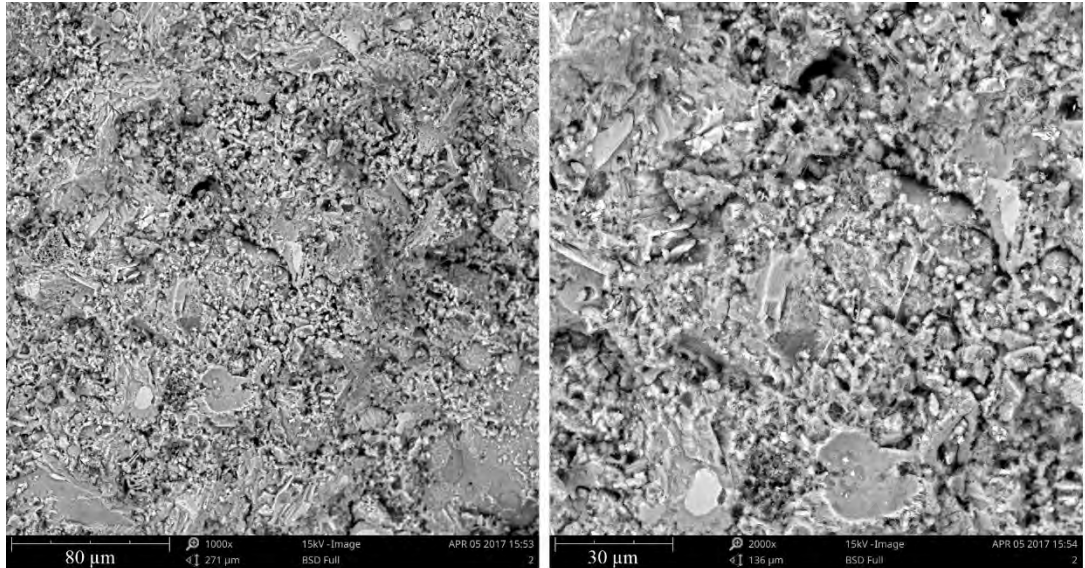
Figure 4.46: Morphology of solidified sample at OPC/CBA ratio of 1
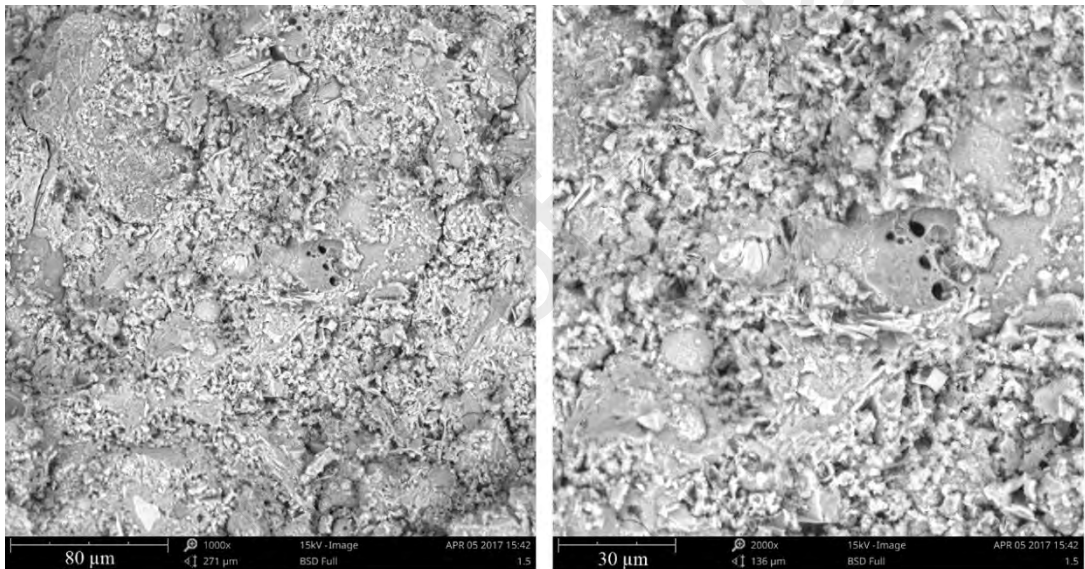
Figure 4.47: Morphology of solidified sample at OPC/CBA ratio of 1.5
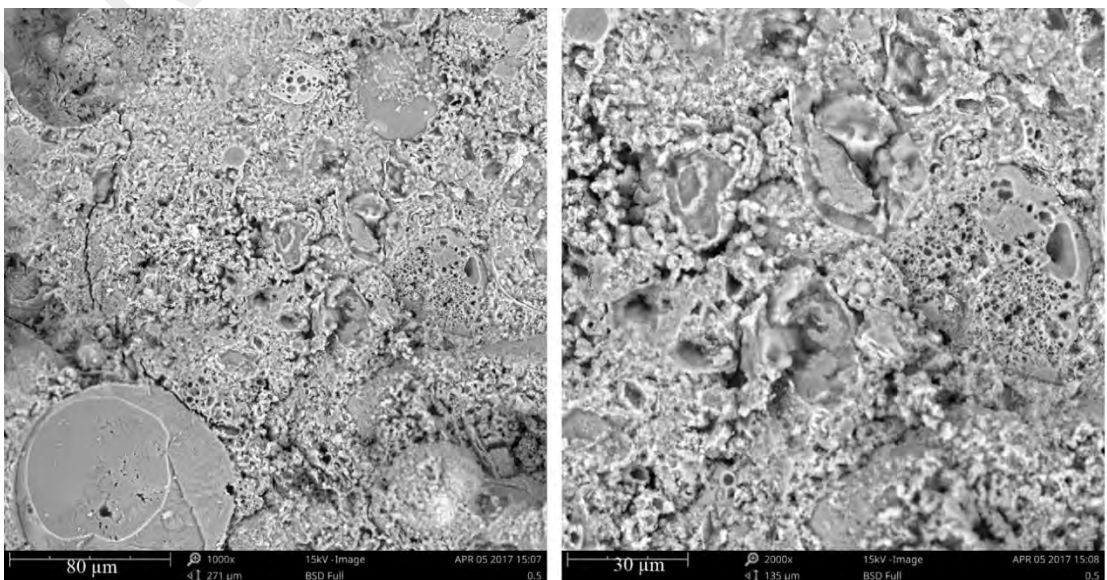
Figure 4.48: Morphology of solidified sample at OPC/CBA ratio of 2

4.3.5.2 XRD analysis

The changes in the crystalline structures of OPC-based solidified sample was determined by XRD at 28 air curing days (Figure 4.49). It is noticeable that, high OPC contents reduce the leachability of heavy metals with the existence of three significant peaks CSH, calcium carbonate, and portlandite (Katsioti et al., 2008; Malliou et al., 2007; Malviya & Chaudhary, 2006a). The change in the ion exchange as shown in Equation 4.3, the Me can be metals Cu, Cd, Ni and Pb resulted in the form of precipitated hydroxide heavy metals during the hydration of cement that showed a high treatment efficacy due to the low solubility of the precipitates. This result is in agreement with previous studies (Li et al., 2001) that showed the existence of heavy metals in the solidifies/stabilized matrices as metal hydrated phases or metal hydroxides precipitating on the surface of CSH gel (Yin et al., 2006). The C-S-H surface area with a high density of irregular hydrogen bonding, provide a strong potential for sorption of heavy metals. This conclusion agrees with the determined alkaline pH of leachate in section 4.3.4.1.

$$Me^{2+} + 2OH^- = Me(OH)_2 \qquad (4.3)$$

On the other hand, Equations 4.4 and 4.5 show that, the carbonation happens when C-S-H gel and $Ca(OH)_2$ react with CO_2 and produce calcite crystal (Nishikawa et al., 1992). Carbonation known as post-hydration process that reduced pH of pore liquid to about 8.3 where all available alkali metal hydroxides have reacted, which can combine in heavy metals (Nishikawa et al., 1992). The carbonation may cause reduction in permeable pores, in contrast the $CaCO_3$ precipitation in pore space may lead to increase in strength property (Kogbara, 2013). Moreover, the CBA comprised contaminated heavy metals that have increased the proneness to carbonation. The presence of CBA ions at carbonate phases through the solid solution reactions with calcite enhances the heavy metal fixation (Smith & Walton, 2011). In this mechanism, carbonation overcomes the retarding effects of

hydration which resulted in improved mechanical and chemical properties of the matrices (Lange et al., 1996). The permeable porosity was found to decrease with increase in OPC proportions (section 4.3.3). In fact, higher hydration causes higher amounts of dense C-S-H and lowers the remaining permeable porous (Malviya & Chaudhary, 2006a).

CBA includes a vitreous fraction that reacts with the hydration products of the cement, mainly portlandite, and forms a more interconnected cementitious gel and consequently fewer air voids. Therefore, the OPC based S/S technique could be viable to transform those metal composites into unsolvable metal hydroxides in high pH alkaline conditions by trapping them through lattice amalgamation into crystalline groups of the cement (Glasser, 1993; Lee et al., 2017).

$$\text{C-S-H} + CO_2 \rightarrow CaCO_3 + \text{silica} + H_2O \qquad (4.4)$$

$$Ca(OH)_2 + CO_2 \rightarrow CaCO_3 + H_2O \qquad (4.5)$$
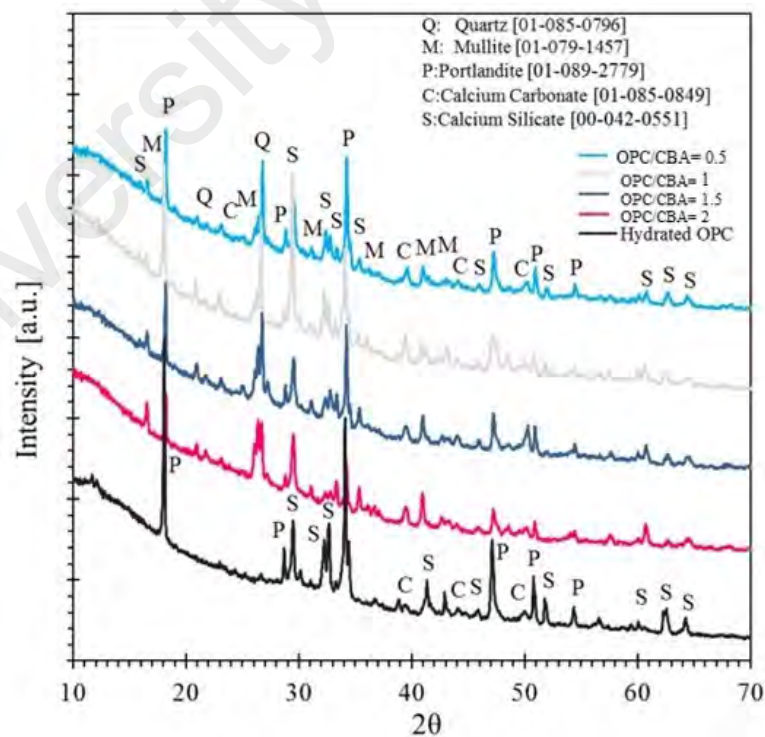
Figure 4.49: XRD analysis of hydrated OPC and solidified specimens at various OPC/CBA ratios

4.3.5.3 TGA analysis

The thermal gravimetric analysis of hydrated cement and OPC based solidified samples in the range of 0 °C -1000 °C, is shown in Figure 4.50. Thermal change associated weight loss contained decomposition of components. The OPC hydrated shows the result of decrease in weight peak at up to 300 °C represents hemihydrates hydration, syngenite, $K_2Ca(SO_4)$ $2.H_2O$ decompositions and dehydrated CSH and alumina (Figure 4.50). Also, its weight loss at about 400 to 500 ˚C and 500 to 800 ˚C might be related to decomposition of $Ca(OH)_2$ and $CaCO_3$, respectively (Kakali et al., 1998). The significant weight loss of all stabilized specimens corresponds to the water loss physically adsorbed or contained inside the pore structure which is up to about 150 °C. There is another weight loss which starts at about 400 to 450 °C which is attributed to the decomposition of the hydrated compounds mainly the CSH gel and calcium hydroxide and release of structural waters. The small weight loss at about 600 to 750°C implies the decomposition of calcite (Figure 4.50).

Moreover, the weight loss in thermograph of solidified samples at OPC/CBA ratios of 0.5-2 at temperature of 500 to 800 ˚C is attributed to $CaCO_3$ decarbonation by removal of CO_2 (Haq et al., 2014). This result agrees with those of XRD patterns. Furthered, the solidified sample at OPC/CBA ratio of 0.5 incorporated higher CBA contents showed higher thermal stability due to less weight loss which is mainly because of the less water content of the system and absorption by its porous structure.
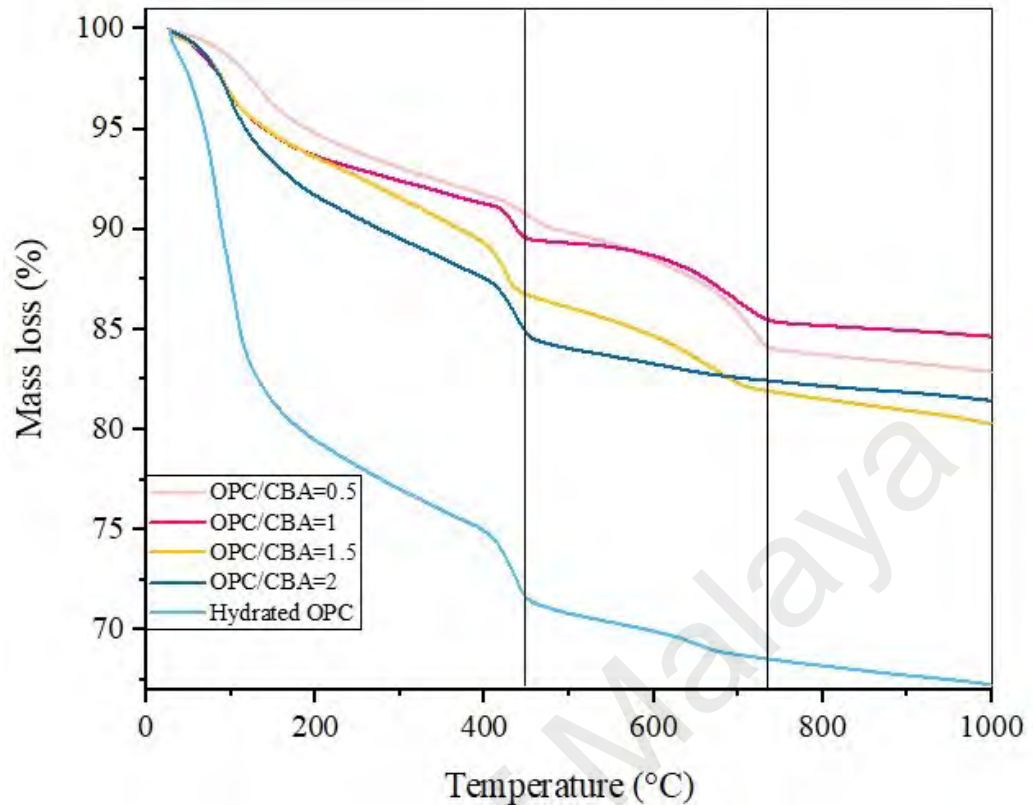
Figure 4.50: Thermograms patterns of hydrated OPC and solidified samples

4.3.6 Summary of OPC-based solidified/stabilized specimens

OPC based solidified samples salient points can be summarized as bellows:

(1) Fresh property of solidified samples: the initial and final setting time delayed up to the OPC/CBA ratios of mixtures =0.5 and 1 which cause retardation of effect of the OPC paste. CBA up-takes more mixing water in the mixtures, which leads to decrease in water content for hydration of the OPC mixtures. Therefore, at OPC/CBA ratios mixtures =1.5 and 2 the initial and final setting times reduced by up to 23% compared to hydrated OPC control mixture.

(2) Strength property of solidified samples, all solidified samples at OPC/CBA ratios of 0.5-2 exceeded the USEPA standard stipulated value of 0.414 MPa for safe disposal of solidified specimens at 28 days. Moreover, the solidified samples at OPC/CBA ratios = 1, 1.5 and 2 achieved the equivalent strength

mortar limit of 20 MPa at 3 days of air curing age. For the solidified sample at OPC/CBA ratio of 0.5, this strength was achieved at 14 days of air curing. The highest compressive strength at the 28-days, resulted from OPC/CBA ratio of 2. The combination of W/C of 0.55 and OPC/CBA of 2 resulted in the optimum strength of solidified sample of 40.2 MPa, slightly below the control sample 48.1 MPa at 56 days.

(3) solidified samples at OPC/CBA ratios of 1.5 and 2 achieved the USEPA standard stipulated value of 15-25% porosity for safe disposal of solidified specimens at 28 days. Although, the solidified samples at OPC/CBA ratios of 0.5 and 1 achieved higher porosity with lower density which are categorized as lightweight mixtures, the porosity value exceeded the USEPA standard specification. The higher CBA contents in solidified samples resulted in the increment of the permeable pore. The strength has opposition effect with porosity in solidified samples where, with the decrease in porosity at OPC/CBA ratio of 2 the strength increased. The ratio of OPC/CBA of 2 with the maximum strength peak depicts the occupation of contaminated metals ions in cement voids which causes reduction in porosity.

(4) Leachability of OPC- based solidified samples: four contaminated metals (Cu, Cd, Ni and Pb) were successfully immobilized at all ages. The concentration of selected contaminated metals was well below the untreated CBA Malaysian and EPA standard in all OPC/CBA ratios at 1, 3, 7, 14, 28 and 56 air curing ages. Cu and Pb ions in solidified samples leachates and Cd and Ni ions with more than 100% and 99% were immobilized, respectively. Solidified samples at (OPC/CBA) ratio of 2 for all analyzed metals showed minimum or zero metals leached values in semi-dynamic extract. The high treatment efficiency

may be credited to alkaline pH ranges (6.5-11.9) in which metal hydroxide exhibited minimal solubility.

(5) Micro-structural analysis of solidified samples: the OPC hydrated micrograph presents dense and interlinked C-S-H with a fewer void space and large surface areas for contaminant absorption.

- The SEM micrograph of solidified OPC exhibits the formation of CSH gel with voids which are occupied by heavy metals hydroxide that envelop the CBA disordered particles. The surface solidified sample at OPC/CBA ratio of 2 contains high contents of OPC, exhibited more compacted and interconnected main hydration product which is C-S-H. The micrograph of solidified sample at OPC/CBA ratio of 0.5 showing larger porosity on the surface composite.

- The XRD diffractograms indicate major crystals formed were CSH, calcium carbonate and portlandite. Diffractogram of stabilized sample at OPC/CBA ratio of 2 shows the C-S-H surface area with a high density of irregular hydrogen bonding, provide a strong potential for sorption of heavy metals and highest calcite crystal formation that decline the leachability of heavy metals. Therefore, the OPC based S/S technique could be viable to transform those metal composites into unsolvable metal hydroxides in high pH alkaline conditions by trapping them through lattice amalgamation into crystalline groups of the cement.

- TGA analysis corresponds to the water loss physically adsorbed or contained inside the pore structure, the decomposition of the hydrated compounds mainly the CSH gel and calcium hydroxide and decomposition of calcite at higher temperature. The solidified sample at OPC/CBA ratio of 0.5 incorporating higher CBA contents showed higher thermal stability due to less

weight loss which is mainly because of the less water content of the system and absorption by porous structure.

4.4   Production of paving block made of solidified specimens

Production of OPC based paving blocks incorporating total and partial replacement of sand with CBA were designed. Based on Table 4.6(A) six different OPC paving block based on various CBA/sand replacement were prepared. As shown in Figure 4.51 blocks are different in colors and porous structure due to variations in CBA contents. 8. It could be affected on geometrical stability of the pavement blocks. As shown in Figure 4.51 some of the blocks (more than 60% CBA replacement by silica sand) appear to be distorted, non-rectangular in shape. This due to increase porous structure of higher amount of CBA Ironically, the distortion appears to be less for higher CBA content, but most for the chosen of CBA content of 40% CBA and 60% silica sand were used in the paving block production with the particle size ranging between 4.75-0.075 mm with the aggregate grading being kept constant (Table 2.12). From Table 2.11, the main technological characterization of the paving blocks included compression, abrasion resistance, and water absorption at 28 and 56 curing ages tested in compliance to specifications in ASTM and Malaysian standards (ASTM, 2016; MS, 2003b). Dry shrinkage effects of the paving block were evaluated also for a period of 56 curing ages according to ASTM C 157-03 (ASTM, 2004). The properties of paving blocks are discussed in the following sections
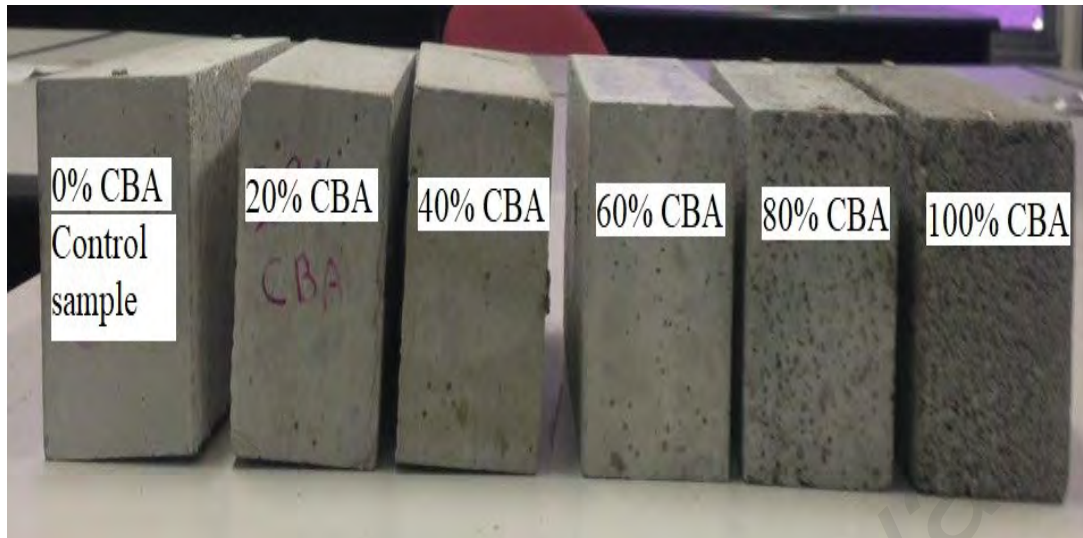
Figure 4.51: Production of paving blocks

4.4.1 Compressive strength

It can be observed from Figure 4.52, the compressive strength of mixture contains 40% CBA at constant W/C ratio of 0.55 was 55 MPa at 56 days. This surpassed the requirement of ASTM C936 standard of >50 MPa. It is also noticeable that the block contains 60% CBA at 28 days shows similar strength to that of the control sample. However, with increase in the CBA contents greater than 40%, the compressive strength decreases at 28 and 56 days. Compressive strength of the CBA mixtures improved in an analogous manner to that of control sample. Addition of CBA as fine aggregate in concrete resulted in lower compressive strength as compared to that of control concrete. With age, compressive strength of CBA concrete mixtures increased at a faster rate than that of the control concrete because of pozzolanic reaction. The pozzolanic reaction started after 28 days of curing which contributed significantly in improving the compressive strength of CBA concrete mixtures (Aggarwal et al., 2007; Singh & Siddique, 2014). Therefore, all blocks except the sample mixture containing 100% CBA achieved the strength requirement of paving block and brick values in accordance to the Malaysian standard (MS, 2003b) at 28 days.
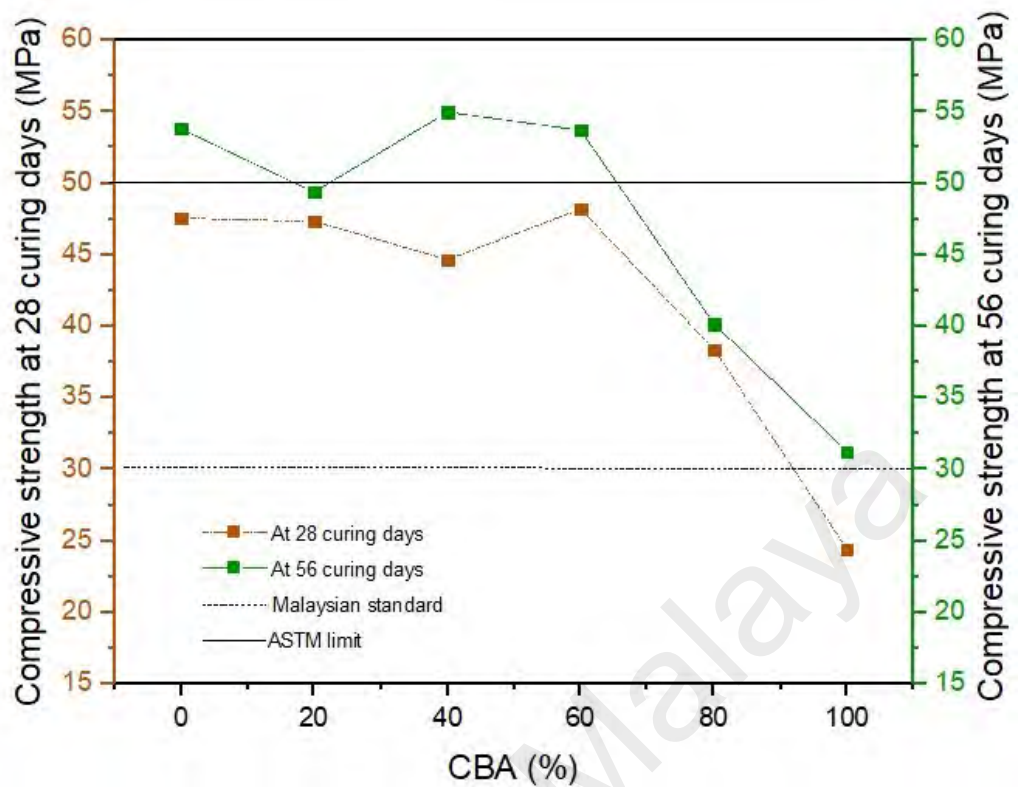
Figure 4.52: Compressive strength of CBA/ silica sand blocks at 28 and 56 curing days

4.4.2 Abrasion resistance

Abrasion resistance results of the paving block at 500 revolutions at 28 and 56 curing days are illustrated in Figure 4.53. The nature and action of abrasion based on surface abrasion occurred by sliding and scraping action of the sand used as an abrasive material. This action, in nature, is not compression. However, due to the sliding and scraping action of abrasive forces on the abrading surface, the total mass loss is calculated as abrasive resistance (Atiş & Çelik, 2002). As shown in Figure 4.53, the mixture containing 20% and 40% CBA substitution exhibits slightly lower wear surface losses than mixture containing 60-100% CBA replacement compared to control sample at 28 and 56 curing days. At 28 days of curing, total volume loss of block mixtures contains 20, 40, 60, 80 and 100%CBA was 2, 2.2, 4, 5.9, and 6.7 (cm^3) respectively, as compared to 1.10 (cm^3) for control sample. However, up to 40% mixture attained less than 3 cm^3 ASTM standard wear loss value at 28 curing ages (Table 2.11). At 56 days, total wear loss of the block

mixtures contains 20, 40, 60, 80 and 100%CBA was 1.90, 2.1, 3.3, 5.2, 6.3 (cm^3) respectively, as compared to 1 (cm^3) for conventional sample. The test results show that total wear loss for CBA mixtures reduced significantly with growth curing age which is in agreement with previous research (Singh & Siddique, 2015). The top surface of the mixture incorporating cement paste and higher disordered CBA particles affects the resistance to abrasion. CBA particles have extremely porous structure with disordered particles shape and are less firm compared to compressed and stiffer of silica sand. Consequently, the use of higher amount of CBA as substitution of sand in concrete block mixture influence the resistance to abrasion. CBA concrete mixtures present lower resistance to abrasion. Due to the porous microstructure of the CBA, it is more absorptive to moistness than control sample, as such its usage greater than 40% substitute of silica sand in concrete mixture results in decreasing abrasion resistance. In addition, all mixtures attained less than 8 cm^3 Malaysian paving blocks or bricks standard of wear loss value at 28 and 56 curing days (Table 2.11).
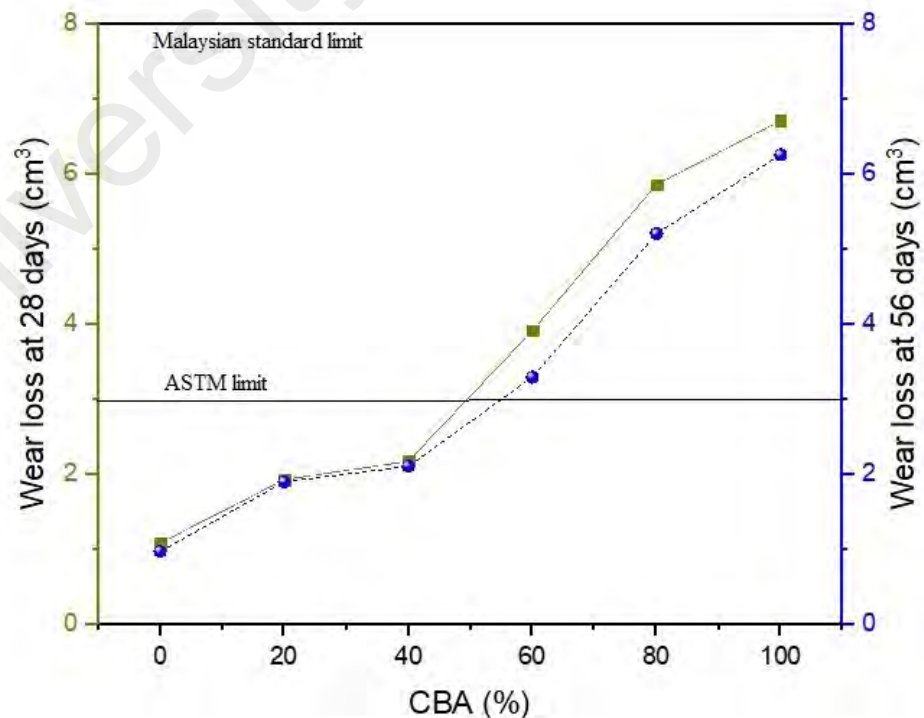
Figure 4.53: Wear loss of CBA/ silica sand paving blocks at 28 and 56 curing days

4.4.3 Water absorption

The results of water absorption of CBA paving block are illustrated in Figure 4.54. At 28 days of curing age, water absorption of paving concrete improved with growth in CBA content in mixtures. At 56 days, the water absorption of CBA mixtures was significantly comparable to control mixture. At 28 days, on incorporation of 20, 40, 60, 80 and 100% CBA as substitution of silica sand in concrete mixtures, water absorption was 3.44, 4.15, 4.32, 4.7, and 7.01%, respectively, as compared to 1.05% of control concrete (Figure 4.54). The outcomes verified that there is a link between the pore space and water absorption. At curing age of 28 days, the connectivity between the capillaries in the paste improved on incorporation of CBA in concrete (Singh & Siddique, 2013). The water absorption of CBA concrete mixtures slightly diminished with growth of curing days. Besides, the water absorption of mixture comprising 100% CBA slightly decreased from 7.01% to 7% at 28 and 56 days, respectively. Up to 80% CBA mixture concrete achieve the value of ASTM regulatory standard limit for water absorption paving block (Table 2.11).
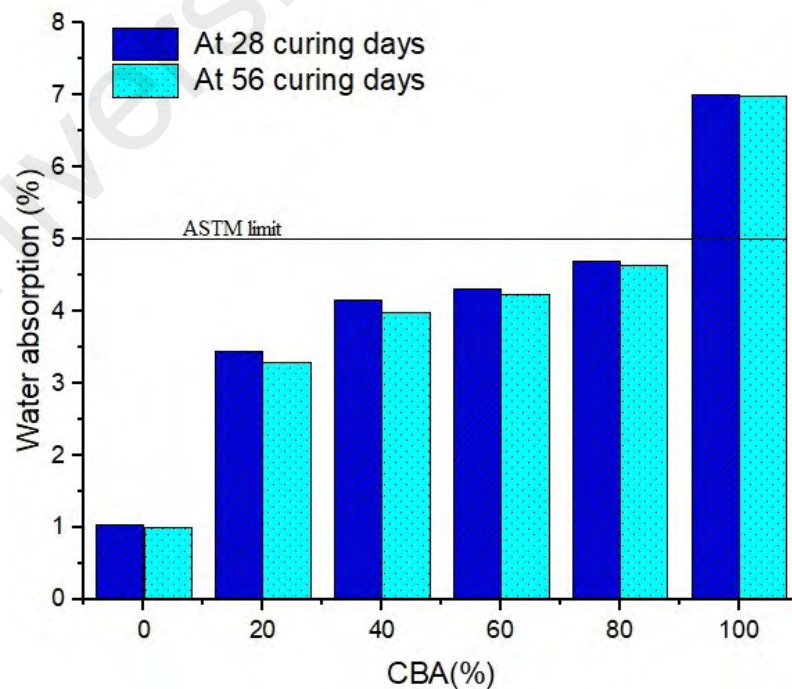
Figure 4.54: Water absorption of CBA/ silica sand paving blocks at 28 and 56 curing days

4.4.4 Drying shrinkage of paving blocks

As observed in Figure 4.55, drying shrinkage behavior of CBA block mixtures and control concrete in a period of 56 days. Shrinkage strains decreased with the increase in CBA content of paving blocks. This reduction might be attributed to pore texture of CBA. The amount of porous structure in mixtures increased with higher CBA proportion. It was founded that these pore spaces during drying of block slowly released the water and thus resulted in reduced drying shrinkage at fixed water/cement ratio of 0.55. This result is in agreement with previous research (Bai et al., 2005). It is observed that block containing CBA exhibited greater dimensional stability as compared to conventional sample. Higher porosity of the paving block contains 100% CBA caused greater reduction in drying shrinkage (Figure 4.55).
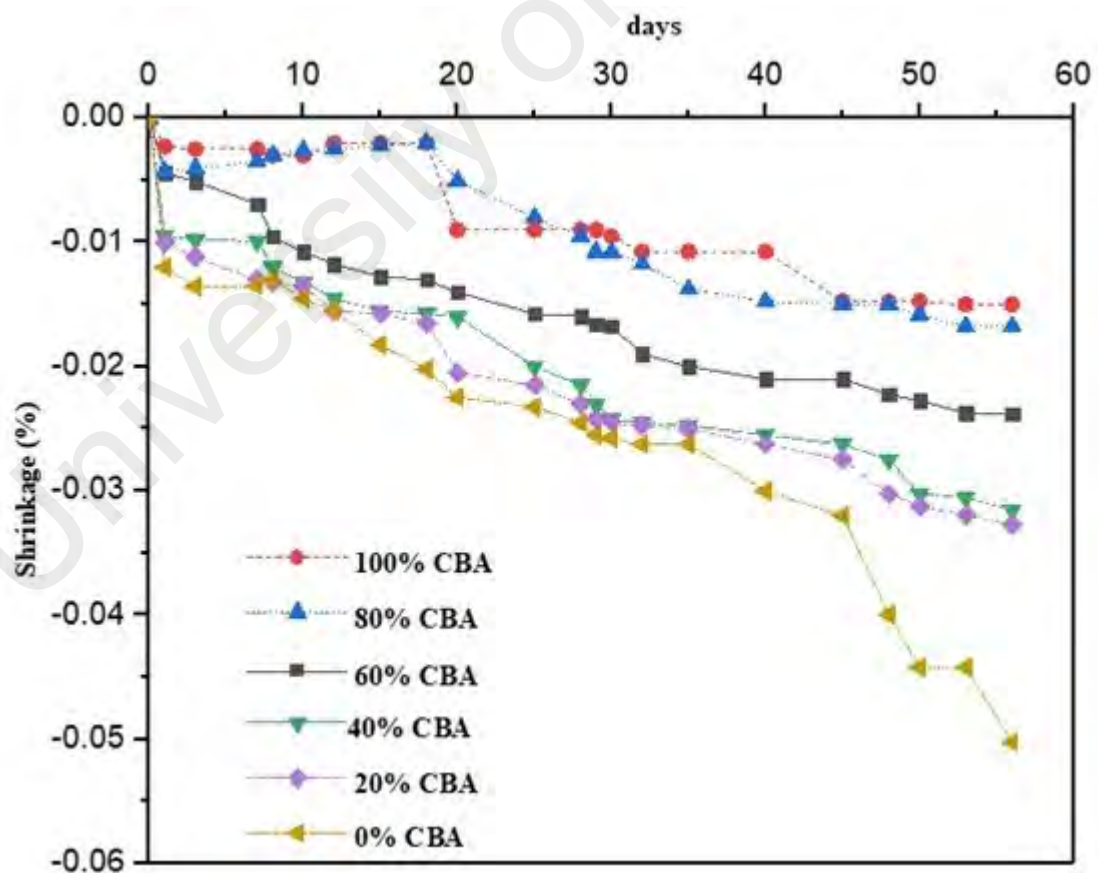
Figure 4.55: Drying shrinkage of CBA/ silica sand paving blocks

4.4.5   Summary of production of paving blocks containing CBA

The salient points of paving blocks parameters can be summarized as follows:

(1) Strength property: the compressive strength of mixture contains 40% CBA at constant W/C ratio of 0.55 achieved the specification paving block value compliance of ASTM C936. Moreover, all block mixtures except the block mixture containing 100% CBA achieved the strength requirement of paving block and brick values in accordance to the Malaysian standard (MS,2003).

(2) Abrasion resistance, up to 40% mixture attained less than 3 cm^3 ASTM standard wear loss value at 28 days. In addition, all mixtures attained less than 8 cm^3 Malaysian paving blocks and bricks standard of wear loss value at 28 and 56 days. The wear losses generally decreased with increase in the CBA content for constant W/C ratio of 0.55. The abrasive resistance of these CBA/ silica sand block increased with age.

(3) Water absorption and drying shrinkage properties of the paving blocks: with increase in the CBA content in the paving block, the water absorbed by porous structure increased. The water absorption of CBA concrete mixtures slightly reduced with increases of curing ages. Up to 80% CBA paving block mixture achieved the regulatory value of ASTM limit at 28 days. Shrinkage strains decreased with the increase in CBA content of paving blocks. This reduction might be attributed to pore texture of the CBA. It was founded that these pore spaces during drying of block slowly released the water and thus resulted in reduced drying shrinkage at fixed water/cement ratio of 0.55.

CHAPTER 5: CONCLUSIONS AND RECOMMENDATIONS

5.1   Conclusions

In this study, the potential of using CBA as fine aggregate with using ordinary Portland cement as a main binder with different water-cement ratios in mortar mixture were considered. The research explored the ideal design parameters of the CBA/sand combination, and water to cement ratio using the efficiency indicators of higher compressive strength property and better microstructure performance. Specific CBA is used throughout the experimental. Moreover, the results and conclusions are specific to this type of CBA and cannot necessarily be extrapolated to other CBAs. The S/S technique provides potential evidence in controlling three main post-treatment parameters of compressive strength, porosity and leachability of heavy metals. Moreover, the CBA paving blocks were fabricated to evaluate ways to utilize CBA as sustainable material building and construction for pedestrian pavement applications or wall partitions in the building prior to dispose it in landfill areas.

The following conclusions can be drawn from the current research:

1. The optimal parameters of OPC based mortar mixture using CBA/silica sand substitution as fine aggregate

    - The output data from flowability of samples shows an acceptable and practical degree for all the mortar mixture containing various CBA contents (0%-100%) and water/cement ratios of 0.2-0.55 having required value of between 10%-154%. The results show that there is a reactive fraction in CBA with pozzolanic features. The highest strength at 28 days was achieved by mixture containing 60% CBA (A4). Mortar mixture containing 40% CBA (A3) as fine aggregate substitution at 56

days achieved 2.1% higher compressive strength than the control mortar mixture. Therefore, the optimum mixture incorporating CBA was up to 40% and water/cement ratio of 0.55. As a result, the compressive strength of the Portland cement-based mortar mixtures at water to cement ratio 0.55 improves when the sand replacement with CBA is limited to below 40% of the total fine aggregate. However, a high-volume CBA replacement has a contrary outcome on the compressive strength of the final matrix. This reduction is attributed to the porous structure of CBA, which causes absorption of the mixing water as well as an increase in the total pore volume of the mortar. The reduction in compressive strength at higher CBA proportions and can be attributed to non-proper consolidation of CBA structure, which was partly compensated using superplasticizer. However, the mortar mixture with 100% CBA can be used as lightweight material mixture. Incorporation of superplasticizer enhances the mechanical properties of the CBA mortar mixture samples where water to cement ratio is above 0.3.

2. OPC based solidified/stabilized samples by using S/S technique

- The compressive strength values of the solidified/stabilized samples at OPC/CBA ratios of 0.5, 1, 1.5, 2 exceeded the minimum landfill disposal limit of 0.414 MPa at a disposal site in the US at 28 days. Although, the planned destination for treated solidified samples was landfill disposal, the high compressive strength values obtained (>20 MPa) showed that solidified samples are applicable in the production of paving blocks. The solidified samples at OPC/CBA ratio=2 were achieved higher compressive strength value. All selected heavy metals

concentrations (copper, cadmium, nickel and lead) were immobilized below the applicable Malaysian standard at all ages. The stabilized samples at OPC/CBA ratio of 2 with alkaline pH value reached the lowest leachability of heavy metals which provided adequate treatment. This result confirmed that, OPC/CBA ratio of 2 achieved the lowest permeable porosity limit of ASTM C936 at 28 days. Reduction in permeable pores showed the occupation of contaminant heavy metals with the cement in the pore voids. The predominant metals that were immobilized completely compared to the initial leaching of untreated CBA in the whole block leaching test were Cu, Pb and Cd. The Ni ion was immobilized more than 90% compared to initial leaching of untreated CBA in the crush block leaching test.

3. Micro-structural properties of mortar and solidified/stabilized samples

- The output data from microstructure analysis of the mortar samples shows that pozzolanic activity occurs slowly from 28 days and thereafter CBA particles started to react with calcium hydroxide resulting in the formation of CSH gel. When the CBA substitution level was increased from 40 to 100%, compact CSH gel structure was somewhat less uniform than that of control mixture. Pore volumes of samples with more than 40% CBA exhibited increase in meso and macro pore volumes. TGA analysis showed that the amount of CSH gel formed increases with the silica sand replacement by CBA. This is due to the pozzolanic activity of CBA, which reacts with the calcium hydroxide from cement hydration to give more CSH gels in the system.

- The output data from microstructure of the solidified/stabilized samples major crystals formed were CSH, calcium carbonate and portlandite.

The existence of heavy metals in the S/S matrices as metal hydrated phases or metal hydroxides precipitating on the surface of the CSH gel. Carbonation overcomes the retarding effects of hydration which leads to improve mechanical and chemical bonding properties of the solidified/stabilized samples. The Cu, Cd, Ni, and Pb had precipitated to produce hydroxide of $Cu(OH)_2$, $Cd(OH)_2$, $Ni(OH)_2$, and $Pb(OH)_2$ through the cement hydration that offers a high treatment efficacy because of the low solubility of the precipitates. The result of TGA analysis showed that, active pozzolanic reaction has occurred in solidified/stabilized samples with substantial mass loss of all the specimens corresponds to the water loss physically adsorbed or contained inside the pore structure. There are weight losses which are attributed to the decomposition of the hydrated compounds mainly the CSH gel, calcium hydroxide, calcite and release of structural waters. As a conclusion, the solidification/stabilization of CBA containing heavy metals with Portland cement is effective by the immobilization of the heavy metals to reduce toxicity and acceptable compressive strength to produce paving blocks prior to dispose in landfill areas.

4. Production of paving blocks containing CBA

- The capability of 40% CBA substitution with sand can be utilized to fabricate paving blocks, in compliance with the requirements of interlocking pavement blocks of ASTM C936, in terms of compressive strength, abrasion value and water absorption. Besides, all CBA/ silica sand paving blocks met the requirements of the Malaysian standard (MS,2003) for blocks or bricks. The degree of shrinkage of CBA/ silica sand paving blocks decreased with increase in the CBA content. For

higher CBA contents in paving blocks, the higher porosity of the composite resulted in retention of moisture which contributed to release of water during drying and reduced the shrinkage and consequently decrease the compressive strength.

5.2   Recommendations for future study

The current research has explored the inclusion of CBA as fine aggregate in mortar mixture and certain aspects of S/S technique to fabricate the interlocking paving block. The optimal CBA mortar mixture parameters were designed and the immobilization and encapsulation of solidified/stabilized samples with regards to heavy metals were investigated. However, further investigations need to be investigated towards using CBA in mortar or concrete mixtures and the solidification and stabilization of CBA. Following are recommendations for future studies:

1. The immobilization of heavy metals concentration might work better by using supplementary cementation materials such as fly ash, blast furnace slag and rice husk ash.

2. Further research is needed to investigate the effect of reduction of water to cement ratios such as 0.2-0.4 of the solidified/stabilized cement paste on the three main parameters (strength, porosity and leachability) of S/S technique.

3.   The CBA comprises organic contents such as volatile and Polychlorinated biphenyls. Evaluation of their chemical bonding with cement hydration can be explored.

4. A remark on stiffness of CBA should be measured to ascertain sound serviceability performance of CBA concrete, can be explored for structural engineering such as precast wall.

REFERENCES

Abo-El-Enein, S. A., El-kady, G., El-Sokkary, T. M., & Gharieb, M. (2015). Physico-mechanical properties of composite cement pastes containing silica fume and fly ash. *HBRC Journal, 11*(1), 7-15.

Abubakar, A. U., & Baharudin, K. S. (2012). Potential use of Malaysian thermal power plants coal bottom ash in construction. *International Journal of Sustainable Construction Engineering and Technology, 3*(2), 25-37.

ACAA. (2016). *Coal Combustion Products (CCPs) production and use.* Retrieved from American Coal Ash Association.USA.:

Aggarwal, P., Aggarwal, Y., & Gupta, S. (2007). Effect of bottom ash as replacement of fine aggregates in concrete. *Asian journal of civil engineering, 8*(1), 49-62.

Aggarwal, Y., & Siddique, R. (2014). Microstructure and properties of concrete using bottom ash and waste foundry sand as partial replacement of fine aggregates. *Construction and Building Materials, 54*, 210-223.

Ahmaruzzaman, M. (2010). A review on the utilization of fly ash. *Progress in Energy and Combustion Science, 36*(3), 327-363.

Anastasiadou, K., Christopoulos, K., Mousios, E., & Gidarakos, E. (2012). Solidification/stabilization of fly and bottom ash from medical waste incineration facility. *Journal of Hazardous Materials, 207–208*, 165-170.

Andrade, L. B., Rocha, J. C., & Cheriaf, M. (2007). Evaluation of concrete incorporating bottom ash as a natural aggregates replacement. *Waste Management, 27*(9), 1190-1199.

Andrade, L. B., Rocha, J. C., & Cheriaf, M. (2009). Influence of coal bottom ash as fine aggregate on fresh properties of concrete. *Construction and Building Materials, 23*(2), 609-614.

Aramraks, T. (2006). *Experimental study of concrete mix with bottom ash as fine aggregate in Thailand.* Paper presented at the Symposium on infrastructure development and the environment.

Arumugam, K., Ilangovan, R., & Manohar, J. D. (2011). A study on characterization and use of Pond Ash as fine aggregate in Concrete. *International journal of civil and structural engineering, 2*(2), 466.

ASTM. (1997). American Standard Test Method for bleeding *C 232-09, .* ASTM International,: West Conshohocken, USA.

ASTM. (2004). American Standard Test Method for Length Change of Hardened Hydraulic-Cement Mortar and Concrete. *C 157-03, .* ASTM International, : West Conshohocken, USA.

ASTM. (2005a). American Standard Test Method for Compressive Strength of Hydraulic Cement Mortars. *C109 / C109M - 16a,* (pp. (pp. 76-81):). ASTM international,: West Conshohocken, USA.

ASTM. (2005b). American Standard Test Method for Density, Absorption, and Voids in Hardened Concrete Cement, Lime, Gypsum *ASTM C642,* (pp. (pp. 321-322).). ASTM International, : West Conshohocken, USA.

ASTM. (2005c). Standard Test Methods for Time of Setting of Hydraulic Cement by Vicat Needle Cement; Lime; Gypsum (pp. 179-185): ASTM International.

ASTM. (2014a). American Standard Test Method for Relative Density(Specific Gravity) and Absorption of Fine Aggregate *C128-15,* . ASTM international,: West Conshohocken, USA.

ASTM. (2014b). American Standard Test Method for Total Evaporable Moisture Content of Aggregate by Drying *C566 - 13,* . ASTM international,: West Conshohocken, USA.

ASTM. (2015). American Standard Test Method forApparent Porosity, Water Absorption, Apparent Specific Gravity, and Bulk Density of Burned Refractory Brick and Shapes by Boiling Water. *C20,* . ASTM international,: West Conshohocken, USA.

ASTM. (2016). American Standard Test Method for Solid Concrete Interlocking Paving Units *C936,* . ASTM international,: West Conshohocken, USA.

ASTM. (2013). American Standard Test Method for Flow of Hydraulic Cement Mortar *C1437-13,* . ASTM international,: West Conshohocken, USA.

Atiş, C. D., & Çelik, O. N. (2002). Relation between abrasion resistance and flexural strength of high volume fly ash concrete. *Materials and Structures, 35*(4), 257-260.

Aughenbaugh, K. L. (2013). Fly ash-based geopolymers: identifying reactive glassy phases in potential raw materials.

Bai, Y., & Basheer, P. A. M. (2003). Influence of furnace bottom ash on properties of concrete. *Proceedings of the Institution of Civil Engineers - Structures and Buildings, 156*(1), 85-92.

Bai, Y., Darcy, F., & Basheer, P. A. M. (2005). Strength and drying shrinkage properties of concrete containing furnace bottom ash as fine aggregate. *Construction and Building Materials, 19*(9), 691-697.

Bajare, D., Bumanis, G., & Upeniece, L. (2013). Coal Combustion Bottom Ash as Microfiller with Pozzolanic Properties for Traditional Concrete. *Procedia Engineering, 57*, 149-158.

Bone, B., Barnard, L., Boardman, D., Carey, P., Hills, C., Jones, H., . . . Tyrer, M. (2004). Review of scientific literature on the use of stabilisation/solidification for the

treatment of contaminated soil, solid waste and sludges. *UK Environment Agency Science Report SC980003/SR2, Bristol.*

BSI. (1983). Biritish Standard Institution for Determination of Particle Size Distribution of fine aggregate *BS 812: part 103*. Biritish Standard Institution: UK,London.

BSI. (1993). Biritish Standard Institution for Determination of Aggeregate Abrasion Value (AAV) *812 Part 113,* . Biritish Standard Institution: UK,London.

Cachim, P., Velosa, A. L., & Ferraz, E. (2014). Substitution materials for sustainable concrete production in Portugal. *KSCE Journal of Civil Engineering, 18*(1), 60-66.

Cerbo, A. A. V., Ballesteros, F., Chen, T. C., & Lu, M.-C. (2017). Solidification/stabilization of fly ash from city refuse incinerator facility and heavy metal sludge with cement additives. *Environmental Science and Pollution Research, 24*(2), 1748-1756.

Chen, Q. Y., Tyrer, M., Hills, C. D., Yang, X. M., & Carey, P. (2009). Immobilisation of heavy metal in cement-based solidification/stabilisation: A review. *Waste Management, 29*(1), 390-403.

Cheng, A. (2012). Effect of incinerator bottom ash properties on mechanical and pore size of blended cement mortars. *Materials & Design (1980-2015), 36*, 859-864.

Cheriaf, M., Rocha, J. C., & Péra, J. (1999). Pozzolanic properties of pulverized coal combustion bottom ash. *Cement and Concrete Research, 29*(9), 1387-1391.

Choi, W. H., Lee, S. R., & Park, J. Y. (2009). Cement based solidification/stabilization of arsenic-contaminated mine tailings. *Waste Management, 29*(5), 1766-1771.

Chun, L. B., Sung, K. J., Sang, K. T., & Chae, S. (2008). *A study on the fundamental properties of concrete incorporating pond-ash in Korea.* Paper presented at the The 3rd ACF international conference-ACF/VCA.

Conner, J. R. (1990). ChemicalFixation and Solidificationof Hazardous Wastes. *Van Nostrand Reinhold, New York, 692*, f5.

Conner, J. R., Wilson, D., & Clarke, A. (1994). Chemical stabilization of contaminated soils. *Hazardous Waste Site Soil Remediation: Theory and Application of Innovative Technologies*, 128-130.

Coz, A., Andrés, A., Soriano, S., & Irabien, Á. (2004). Environmental behaviour of stabilised foundry sludge. *Journal of Hazardous Materials, 109*(1–3), 95-104.

Cyr, M., & Ludmann, C. (2006). Low risk meat and bone meal (MBM) bottom ash in mortars as sand replacement. *Cement and Concrete Research, 36*(3), 469-480.

Du, Y.-J., Wei, M.-L., Reddy, K. R., Liu, Z.-P., & Jin, F. (2014). Effect of acid rain pH on leaching behavior of cement stabilized lead-contaminated soil. *Journal of Hazardous Materials, 271*, 131-140.

Environmental Quality Act (Sewage and Industrial Effluents);, P. U. (A) 12/1979. C.F.R. (1979).

Erdem, M., & Özverdi, A. (2011). Environmental risk assessment and stabilization/solidification of zinc extraction residue: II. Stabilization/solidification. *Hydrometallurgy, 105*(3–4), 270-276.

Fatta, D., Papadopoulos, A., Stefanakis, N., Loizidou, M., & Savvides, C. (2004). An Alternative Method for the Treatment of Waste Produced at a Dye and a Metal-Plating Industry Using Natural and/or Waste Materials. *Waste Management & Research, 22*(4), 234-239.

Fuessle, R. W., & Taylor, M. A. (2004). Long-term solidification/stabilization and toxicity characteristic leaching procedure for an electric arc furnace dust. *Journal of Environmental Engineering, 130*(5), 492-498.

Ganjian, E., Jalull, G., & Sadeghi-Pouya, H. (2015). Using waste materials and by-products to produce concrete paving blocks. *Construction and Building Materials, 77*, 270-275.

Ghafoori, N., & Bucholc, J. (1996). Investigation of Lignite-Based Bottom Ash for Structural Concrete. *Journal of Materials in Civil Engineering, 8*(3), 128-137.

Ghafoori, N., & Bucholc, J. (1997). Properties of high-calcium dry bottom ash concrete. *ACI Materials Journal, 94*(2), 90-101.

Ghafoori, N., & Cai, Y. (1998). Laboratory-Made Roller Compacted Concretes Containing Dry Bottom Ash: Part II—Long-Term Durability. *Materials Journal, 95*(3).

Ghafoori, N., & Mathis, R. (1998). Prediction of freezing and thawing durability of concrete paving blocks. *Journal of materials in civil engineering, 10*(1), 45-51.

Ghafoori, N., & Sukandar, B. M. (1995). Abrasion Resistance of Concrete Block Pavers. *Materials Journal, 92*(1).

Gildeh, H. K., Saeedi, M., Eshtehardian, E., & Taheriattar, R. (2013). Solidification/Stabilization of Sludge Waste from Thermal Power Plants Using Portland Cement. *Journal of Frontiers in Construction Engineering Mar, 2*(1), 10-16.

Glasser, F. (1993). Chemistry of cement-solidified waste forms. *Chemistry and microstructure of solidified waste forms*, 1-39.

Goodarzi, F. (2006). Characteristics and composition of fly ash from Canadian coal-fired power plants. *Fuel, 85*(10), 1418-1427.

Hale, B., Evans, L., & Lambert, R. (2012). Effects of cement or lime on Cd, Co, Cu, Ni, Pb, Sb and Zn mobility in field-contaminated and aged soils. *Journal of Hazardous Materials, 199–200*, 119-127.

Halim, C. E., Amal, R., Beydoun, D., Scott, J. A., & Low, G. (2003). Evaluating the applicability of a modified toxicity characteristic leaching procedure (TCLP) for the classification of cementitious wastes containing lead and cadmium. *Journal of Hazardous Materials, 103*(1–2), 125-140.

Halim, C. E., Amal, R., Beydoun, D., Scott, J. A., & Low, G. (2004). Implications of the structure of cementitious wastes containing Pb(II), Cd(II), As(V), and Cr(VI) on the leaching of metals. *Cement and Concrete Research, 34*(7), 1093-1102.

Han, M.-C., Han, D., & Shin, J.-K. (2015). Use of bottom ash and stone dust to make lightweight aggregate. *Construction and Building Materials, 99*, 192-199.

Haq, E., Kunjalukkal Padmanabhan, S., & Licciulli, A. (2014). Synthesis and characteristics of fly ash and bottom ash based geopolymers–A comparative study. *Ceramics International, 40*(2), 2965-2971.

Harbottle, M. J., Al-Tabbaa, A., & Evans, C. W. (2007). A comparison of the technical sustainability of in situ stabilisation/solidification with disposal to landfill. *Journal of Hazardous Materials, 141*(2), 430-440.

Humpola, B. (1996). *Some Aspects of Concrete Block Pavement CBP Quality".* Paper presented at the The Fifth International Conference on Concrete Block Paving, Tel-Aviv, Israel.

Hunce, S. Y., Akgul, D., Demir, G., & Mertoglu, B. (2012). Solidification/stabilization of landfill leachate concentrate using different aggregate materials. *Waste Management, 32*(7), 1394-1400.

Hussain, K., Choktaweekarn, P., Saengsoy, W., Srichan, T., & Tangtermsirikul, S. (2013). Effect of cement types, mineral admixtures, and bottom ash on the curing sensitivity of concrete. *International Journal of Minerals, Metallurgy, and Materials, 20*(1), 94-105.

Jaturapitakkul, C. a. C., R. (2003). Development of Bottom Ash as Pozzolanic Material. *Journal of Materials in Civil Engineering, 15*(1), 48-53.

Jayaranjan, M. L. D., van Hullebusch, E. D., & Annachhatre, A. P. (2014). Reuse options for coal fired power plant bottom ash and fly ash. *Reviews in Environmental Science and Bio/Technology, 13*(4), 467-486.

John, U. E., Jefferson, I., Boardman, D. I., Ghataora, G. S., & Hills, C. D. (2011). Leaching evaluation of cement stabilisation / solidification treated kaolin clay. *Engineering Geology, 123*(4), 315-323.

Kakali, G., Tsivilis, S., & Tsialtas, A. (1998). Hydration of Ordinary Portland Cements Made from Raw Mix Containing Transition Element Oxides 11Communicated by F. Massazza. *Cement and Concrete Research, 28*(3), 335-340.

Kanadasan, J., & Razak, H. A. (2014). Mix design for self-compacting palm oil clinker concrete based on particle packing. *Materials & Design (1980-2015), 56*, 9-19.

Katsioti, M., Katsiotis, N., Rouni, G., Bakirtzis, D., & Loizidou, M. (2008). The effect of bentonite/cement mortar for the stabilization/solidification of sewage sludge containing heavy metals. *Cement and Concrete Composites, 30*(10), 1013-1019.

Khan, R. A., & Ganesh, A. (2016). The effect of coal bottom ash (CBA) on mechanical and durability characteristics of concrete. *Journal of Building Materials and Structures, 3*(1), 31-42.

Kim, H. K., & Lee, H. K. (2011). Use of power plant bottom ash as fine and coarse aggregates in high-strength concrete. *Construction and Building Materials, 25*(2), 1115-1122.

Kogbara, R. B. (2013). A review of the mechanical and leaching performance of stabilized/solidified contaminated soils. *Environmental Reviews, 22*(1), 66-86.

Kogbara, R. B., Al-Tabbaa, A., Yi, Y., & Stegemann, J. A. (2012). pH-dependent leaching behaviour and other performance properties of cement-treated mixed contaminated soil. *Journal of Environmental Sciences, 24*(9), 1630-1638.

Kou, S.-C., & Poon, C.-S. (2009). Properties of concrete prepared with crushed fine stone, furnace bottom ash and fine recycled aggregate as fine aggregates. *Construction and Building Materials, 23*(8), 2877-2886.

Kurama, H., & Kaya, M. (2008). Usage of coal combustion bottom ash in concrete mixture. *Construction and Building Materials, 22*(9), 1922-1928.

Lange, L. C., Hills, C. D., & Poole, A. B. (1996). Preliminary Investigation into the Effects of Carbonation on Cement-Solidified Hazardous Wastes. *Environmental Science & Technology, 30*(1), 25-30.

Lee, D. J. (2004). Solidification /Stabilization Mechanisms of Calcite on Solidified Waste Forms. Ph.D, University of New South Wales, Australia.

Lee, H., Yu, G., Choi, Y., Jho, E. H., & Nam, K. (2017). Long-term leaching prediction of constituents in coal bottom ash used as a structural fill material. *Journal of Soils and Sediments*, 1-10.

Li, X. D., Poon, C. S., Sun, H., Lo, I. M. C., & Kirk, D. W. (2001). Heavy metal speciation and leaching behaviors in cement based solidified/stabilized waste materials. *Journal of Hazardous Materials, 82*(3), 215-230.

Malliou, O., Katsioti, M., Georgiadis, A., & Katsiri, A. (2007). Properties of stabilized/solidified admixtures of cement and sewage sludge. *Cement and Concrete Composites, 29*(1), 55-61.

Malviya, R., & Chaudhary, R. (2006a). Factors affecting hazardous waste solidification/stabilization: A review. *Journal of Hazardous Materials, 137*(1), 267-276.

Malviya, R., & Chaudhary, R. (2006b). Leaching behavior and immobilization of heavy metals in solidified/stabilized products. *Journal of Hazardous Materials, 137*(1), 207-217.

Marto, A., Kassim, K. A., Makhtar, A. M., Wei, L. F., & Lim, Y. S. (2010). Engineering characteristics of Tanjung Bin coal ash. *Electronic Journal of Geotechnical Engineering, 15*, 1117-1129.

Mehta, P. K., & Monteiro, P. J. M. (2006). Concrete–Microstructure, Properties, and Materials,. *PJM , United States: McGrawHill*, 85-86.

Menéndez, E., Álvaro, A. M., Hernández, M. T., & Parra, J. L. (2014). New methodology for assessing the environmental burden of cement mortars with partial replacement of coal bottom ash and fly ash. *Journal of Environmental Management, 133*, 275-283.

MESV. (2014). Malaysia Electricity Supply & Voltage (MESV). http://www.malaysiatrulyasia.com/tourism/electricity_suppl.htm

Michelle Christine, M. (2008). The determination of heavy metals in coal ash (Bachelor research,University Malaysia Sarawak).Retrieved from

Minocha, A. K., Jain, N., & Verma, C. L. (2003). Effect of organic materials on the solidification of heavy metal sludge. *Construction and Building Materials, 17*(2), 77-81.

MS. (2003a). Malaysian Standard,Ordinary Portland Cement specification and rapid hardening. *522: PART 1* Department Of Standards Malaysia,: Malaysia.

MS. (2003b). Malaysian Standard,specification for concrete paving block and brick. Department Of Standards Malaysia,: Malaysia.

Nishigaki, M. (2000). Producing permeable blocks and pavement bricks from molten slag. *Waste Management, 20*(2–3), 185-192.

Nishikawa, T., Suzuki, K., Ito, S., Sato, K., & Takebe, T. (1992). Decomposition of synthesized ettringite by carbonation. *Cement and Concrete Research, 22*(1), 6-14.

Oka, Y., & Embi, M. R. (2007). Coal-Fired Boiler Plant History for Malaysian Projects. In K. Cen, Y. Chi, & F. Wang (Eds.), *Challenges of Power Engineering and Environment: Proceedings of the International Conference on Power Engineering 2007* (pp. 197-203). Berlin, Heidelberg: Springer Berlin Heidelberg.

Panda, B. C., & Ghosh, A. K. (2002). Structural behavior of concrete block paving. II: Concrete blocks. *Journal of transportation Engineering, 128*(2), 130-135.

Paria, S., & Yuet, P. K. (2006). Solidification–stabilization of organic and inorganic contaminants using portland cement: a literature review. *Environmental Reviews, 14*(4), 217-255.

Polettini , Pomi R., & Valente M. (2004). Remediation of a Heavy Metal-Contaminated Soil by Means of Agglomeration. *Journal of Environmental Science and Health, Part A, 39*(4), 999-1010.

Poon, C. S. (2002). Use of recycled aggregates in molded concrete bricks and blocks. *Construction and Building Materials, 16*(5), 281-289.

Poon, C. S., & Chan, D. (2006). Paving blocks made with recycled concrete aggregate and crushed clay brick. *Construction and Building Materials, 20*(8), 569-577.

Pratt, C. (2003). Guide to design construction and maintenance of concrete block permeable pavements. http://www.paving.org.uk/commercial/permeable.php

Rafieizonooz, M., Mirza, J., Salim, M. R., Hussin, M. W., & Khankhaje, E. (2016). Investigation of coal bottom ash and fly ash in concrete as replacement for sand and cement. *Construction and Building Materials, 116*, 15-24.

Raju, R., Paul, M. M., & Aboobacker, K. (2014). Strength performance of concrete using bottom ash as fine aggregate. *International Journal of Research in Engineering & Technology, 2*(9), 111-122.

Ramzi, N. I. R., Shahidan, S., Maarof, M. Z., & Ali, N. (2016). *Physical and Chemical Properties of Coal Bottom Ash (CBA) from Tanjung Bin Power Plant.* Paper presented at the IOP Conference Series: Materials Science and Engineering.

Ranjbar, N., Behnia, A., Alsubari, B., Moradi Birgani, P., & Jumaat, M. Z. (2016a). Durability and mechanical properties of self-compacting concrete incorporating palm oil fuel ash. *Journal of Cleaner Production, 112, Part 1*, 723-730.

Ranjbar, N., & Kuenzel, C. (2017a). Cenospheres: A review. *Fuel, 207*, 1-12.

Ranjbar, N., & Kuenzel, C. (2017b). Influence of preheating of fly ash precursors to produce geopolymers. *Journal of the American Ceramic Society*, 1-10.

Ranjbar, N., Mehrali, M., Behnia, A., Alengaram, U. J., & Jumaat, M. Z. (2014). Compressive strength and microstructural analysis of fly ash/palm oil fuel ash based geopolymer mortar. *Materials & Design, 59*, 532-539.

Ranjbar, N., Mehrali, M., Behnia, A., Pordsari, A. J., Mehrali, M., Alengaram, U. J., & Jumaat, M. Z. (2016b). A comprehensive study of the polypropylene fiber reinforced fly ash based geopolymer. *PloS one, 11*(1), e0147546.

Raut, S. P., Ralegaonkar, R. V., & Mandavgane, S. A. (2011). Development of sustainable construction material using industrial and agricultural solid waste: A review of waste-create bricks. *Construction and Building Materials, 25*(10), 4037-4042.

Reijnders, L. (2005). Disposal, uses and treatments of combustion ashes: a review. *Resources, Conservation and Recycling, 43*(3), 313-336.

Roy, D., Scheetz, B., & Spence, R. (1992). The chemistry of cementitious systems for waste management: The Penn state experience. *Chapter, 3*, 83-101.

Rozumová, L., Motyka, O., Čabanová, K., & Seidlerová, J. (2015). Stabilization of waste bottom ash generated from hazardous waste incinerators. *Journal of Environmental Chemical Engineering, 3*(1), 1-9.

Safiuddin, M., & Hearn, N. (2005). Comparison of ASTM saturation techniques for measuring the permeable porosity of concrete. *Cement and Concrete Research, 35*(5), 1008-1013.

Sani, M. S. H. M., Muftah, F., & Muda, Z. (2011). The properties of special concrete using washed bottom ash (WBA) as partial sand replacement. *International Journal of Sustainable Construction Engineering and Technology, 1*(2), 65-76.

Santos, C. R. d., Filho, J. R. d. A., Tubino, R. M. C., & Schneider, I. A. H. (2013). Use of Coal Waste as Fine Aggregates in Concrete Paving Blocks. *Geomaterials, Vol.03No.02*, 6.

Shaaban, M. G. (1993). *Stabilization and Solidification (S/S) of Hazardous Wastes, Evaluation of Cement-Based Method.* Retrieved from Universiti Kebangsaan Malaysia, Bangi:

Shi, C. (2004). Hydraulic cement systems for stabilization/solidification. *Stabilization and solidification of hazardous, radioactive, and mixed wastes. Editado por RD Spence y C. Shi*, 49-77.

Silva, M. A. R., Mater, L., Souza-Sierra, M. M., Corrêa, A. X. R., Sperb, R., & Radetski, C. M. (2007). Small hazardous waste generators in developing countries: use of stabilization/solidification process as an economic tool for metal wastewater treatment and appropriate sludge disposal. *Journal of Hazardous Materials, 147*(3), 986-990.

Singh, M., & Siddique, R. (2013). Effect of coal bottom ash as partial replacement of sand on properties of concrete. *Resources, Conservation and Recycling, 72*, 20-32.

Singh, M., & Siddique, R. (2014). Strength properties and micro-structural properties of concrete containing coal bottom ash as partial replacement of fine aggregate. *Construction and Building Materials, 50*, 246-256.

Singh, M., & Siddique, R. (2015). Properties of concrete containing high volumes of coal bottom ash as fine aggregate. *Journal of Cleaner Production, 91*, 269-278.

Singh, M., & Siddique, R. (2016). Effect of coal bottom ash as partial replacement of sand on workability and strength properties of concrete. *Journal of Cleaner Production, 112*, 620-630.

Singh, P. R., & Shah, N. (2017). Impact of Coal Combustion Fly Ash used as a Binder in Pavement.

Smith, R. W., & Walton, J. C. (2011). The Effects of Calcite Solid Solution Formation on the Transient Release of Radionuclides from Concrete Barriers. *MRS Proceedings, 212*.

Sokol, E. V., Maksimova, N. V., Volkova, N. I., Nigmatulina, E. N., & Frenkel, A. E. (2000). Hollow silicate microspheres from fly ashes of the Chelyabinsk brown coals (South Urals, Russia). *Fuel Processing Technology, 67*(1), 35-52.

Sollars, C. J., & Perry, R. (1989). Cement-based Stabilization of Wastes: Practical and Theoretical Considerations. *Water and Environment Journal, 3*(2), 125-134.

Spence, R. D., & Shi, C. (2004). *Stabilization and solidification of hazardous, radioactive, and mixed wastes*: CRC press.

Sri Bala Kameswari, K., Bhole, A., & Paramasivam, R. (2001). Evaluation of solidification/stabilization (S/S) process for the disposal of arsenic-bearing sludges in landfill sites. *Environmental engineering science, 18*(3), 167-176.

Stegemann, J. A., & Zhou, Q. (2009). Screening tests for assessing treatability of inorganic industrial wastes by stabilisation/solidification with cement. *Journal of Hazardous Materials, 161*(1), 300-306.

Susie, S. (2008). The determination of heavy metals in coal ash(Bachelor research,University Malaysia Sarawak).Retrieved from

Tiwari, M., Sahu, S. K., Bhangare, R. C., Ajmal, P. Y., & Pandit, G. G. (2014). Elemental characterization of coal, fly ash, and bottom ash using an energy dispersive X-ray fluorescence technique. *Applied Radiation and Isotopes, 90*, 53-57.

Topçu, I. B., & Bilir, T. (2010). Effect of Bottom Ash as Fine Aggregate on Shrinkage Cracking of Mortars. *ACI Materials Journal, 107*(1).

Torkittikul, P., Nochaiya, T., Wongkeo, W., & Chaipanich, A. (2015). Utilization of coal bottom ash to improve thermal insulation of construction material. *Journal of Material Cycles and Waste Management*, 1-13.

USEPA. (1986). United States Environmental Protection Agency, Handbook for Stabilization/Solidification of Hazardous Wastes. . H. W. E. R. Laboratory, Trans., Cincinnati, Ohio: U.S. : USA.

USEPA. (1993). United States Environmental Protection Agency, Technical resource document: solidification/stabilization and its application to waste materials *STP1123* (Vol. EPA/530/R-93/012,). H. W. E. R. Laboratory, Trans., Cincinnati, Ohio: U.S. : USA.

USEPA. (1994a). United States Environmental Protection Agency, synthetic precipitation leaching procedure. *Method 1312:* (Vol. SW-846). H. W. E. R. Laboratory, Trans., Cincinnati, Ohio: U.S. : USA.

USEPA. (1994b). United States Environmental Protection Agency, Test Methods for Evaluating Waste, Physical/Chemical. *Method 1311:* (Vol. SW-846). H. W. E. R. Laboratory, Trans., Cincinnati, Ohio: U.S. : USA.

USEPA. (2000). United States Environmental Protection Agency, Solidification/stabilization use at superfund sites (Vol. EPA-542-R-00-010,2000., pp. p.7). H. W. E. R. Laboratory, Trans., Cincinnati, Ohio: U.S. : USA.

Valls, S., & Vàzquez, E. (2000). Stabilisation and solidification of sewage sludges with Portland cement. *Cement and Concrete Research, 30*(10), 1671-1678.

Vassilev, S. V., Menendez, R., Diaz-Somoano, M., & Martinez-Tarazona, M. R. (2004). Phase-mineral and chemical composition of coal fly ashes as a basis for their multicomponent utilization. 2. Characterization of ceramic cenosphere and salt concentrates. *Fuel, 83*(4), 585-603.

Vassilev, S. V., & Vassileva, C. G. (1996). Mineralogy of combustion wastes from coal-fired power stations. *Fuel Processing Technology, 47*(3), 261-280.

Viana, C. E., Dias, D. P., Holanda, J. N. F. d., & Paranhos, R. P. d. R. (2009). The use of submerged-arc welding flux slag as raw material for the fabrication of multiple-use mortars and bricks. *Soldagem & Inspeção, 14*, 257-262.

Vinai, R., Lawane, A., Minane, J. R., & Amadou, A. (2013). Coal combustion residues valorisation: Research and development on compressed brick production. *Construction and Building Materials, 40*, 1088-1096.

Yin, C.-Y., Ghazaly Shaaban, M., & Bin Mahmud, H. (2007). Chemical stabilization of scrap metal yard contaminated soil using ordinary portland cement: Strength and leachability aspects. *Building and Environment, 42*(2), 794-802.

Yin, C.-Y., Mahmud, H. B., & Shaaban, M. G. (2006). Stabilization/solidification of lead-contaminated soil using cement and rice husk ash. *Journal of Hazardous Materials, 137*(3), 1758-1764.

Yuksel, I., & Genç, A. (2007). Properties of concrete containing nonground ash and slag as fine aggregate. *ACI materials journal, 104*(4), 397.

Zain, M. F. M., Islam, M. N., Radin, S. S., & Yap, S. G. (2004). Cement-based solidification for the safe disposal of blasted copper slag. *Cement and Concrete Composites, 26*(7), 845-851.

Zhang, J., Liu, J., Li, C., Jin, Y., Nie, Y., & Li, J. (2009). Comparison of the fixation effects of heavy metals by cement rotary kiln co-processing and cement based solidification/stabilization. *Journal of Hazardous Materials, 165*(1–3), 1179-1185.

Zhang, L. (2013). Production of bricks from waste materials – A review. *Construction and Building Materials, 47*, 643-655.

LIST OF PUBLICATIONS AND PAPERS PRESENTED

1. S.S.G. Hashemi, H.B. Mahmud, M.A. Ashraf, Performance of green roofs with respect to water quality and reduction of energy consumption in tropics: a review, Renewable and Sustainable Energy Reviews, 52 (2015) 669-679, **Impact Factor: 8.05 (Q1).**

2. S.S.G. Hashemi, H.B. Mahmud, J.N.Y. Djobo, C.G. Tan, B.C. Ang, N. Ranjbar, Microstructural characterization and mechanical properties of bottom ash mortar, Cleaner Production, **Impact Factor: 5.71 (Q1).**

3. S.S.G. Hashemi, H.B. Mahmud, C.G. Tan, B.C. Ang, N. Ranjbar, the safe disposal of Coal Bottom Ash by Solidification/Stabilization technique, Construction and Building Material, **Impact Factor: 4.03 (Q1).**